Development of Lipid based Nanoparticles for Melanoma Treatment

by

Li Chen

A dissertation submitted to the Graduate Faculty of
Auburn University
in partial fulfillment of the
requirements for the Degree of
Doctor of Philosophy

Auburn, Alabama
May 9, 2015

Keywords: Nanoparticles, Lipid coated Nanoparticles, Liposome, Microemulsion, Melanoma, Cancer Treatment

Approved by

William R. Ravis, Co-chair, Professor, Drug Discovery and Development
Jayachandra Babu Ramapuram, Co-chair,
Associate Professor, Drug Discovery and Development
Daniel L. Parsons, Professor, Drug Discovery and Development
Robert D. Arnold, Associate Professor, Drug Discovery and Development

Abstract

Melanoma is the most malignant skin cancer with high mortality. Currently, it can be treated multiple ways, such as chemotherapy, immunotherapy and targeted therapy. However, patients under these therapies usually have low response rates due to inefficient drug delivery and multidrug resistance. Nanoparticles are a promising technology for delivering one or two agents to the cellular level. Among these, lipid based nanoparticles attract more attention due to its easy preparation and modification, biocompatibility, enhanced permeability and retention (EPR) effects and reduced toxicity. This dissertation focuses on the lipid based nanoparticles delivery system for leukemia and melanoma treatment.

We prepared micelles with an oxidized phospholipid, 1-palmitoyl-2-azelaoyl-sn-glycero-3-phosphocholine (PazPC), via both electrostatic and hydrophobic interaction for delivery of Doxorubicin (DOX) and Idarubicin (IDA). *In vitro* uptake and cytotoxicity were evaluated on leukemia P388 and its resistant subline P388/ADR. The drug-loaded PazPC micelles enhanced drug uptake and exhibited higher cytotoxicity in both leukemia P388 and its resistance subline P388/ADR in comparison to free drugs.

Both zolendronic acid and Polyinosinic acid-polycytidylic acid [poly (I:C)] showed potent anticancer activity in melanoma treatment. However, high preferential accumulation of zolendronic acid within bone and poor intracellular delivery of poly (I:C) limited their uses in chemo-immunotherapy. Cationic lipid-coated calcium phosphate nanoparticles (LCP) were developed to enable intracellular co-delivery of zoledronic acid and poly (I: C). The co-delivery

system demonstrated significantly enhanced and synergistic activity both in vitro in melanoma cell line B16BL6 and in vivo in melanoma-bearing mice.

Genistein, a soy flavone, is a well-known anti-oxidant and has been reported to be effective in preventing UV induced skin damage and melanoma. However, intradermal delivery of genistein is inefficient due to its low permeability as well as its low solubility. We reported microemulsions for enhanced transdermal delivery of genistein, *in vitro*. The optimized formulation consisted of 2% (w/w) genistein, 18% (w/w) oleic acid, 60% (w/w) cremophor EL/ethanol (5:11), and 20% (w/w) water and it exhibited small particle size and highest skin permeation rate based on various formulation factors optimization.

Finally, to achieve co-delivery of Doxorubicin (DOX) and ceramide using a liposomal system in B16BL6 melanoma cell lines for synergistic cytotoxic effects, different types of ceramides (C_6-ceramide, C_8-ceramide and C_8-glucosylceramide) and lipids (DOTAP, DPPC, DSPE and DSPC) were screened to optimize the formulation. The optimum liposome formulation provided a mean diameter 150 nm with a narrow size distribution (poly-dispersity index, 0.09) and a positive zeta potential (+34mv) with 92% DOX recovery. DOX and C_8-Ceramide loaded DOTAP liposomes exhibited a significantly higher anti-tumor activity in melanoma cell line B16BL6 in comparison with liposomes made with other lipids such as DSPC, and a combination of DSPC and DSPE ($P < 0.05$). Co-delivery of DOX and C_8-ceramide with DOTAP lipids based liposome demonstrated 9 folds higher cytotoxicity in the B16BL6 melanoma cell line as compared to DOX alone.

Acknowledgments

I would like to express my deepest gratitude to Dr. Weili Yan for his support, guidance, and for providing me with this great opportunity for doing research. I want to offer my special thanks to Dr. William Ravis and Dr. Jayachandra Ramapuram for their excellent guidance, caring, and support in and out of laboratories. Thanks for serving as my mentors after Dr. Weili Yan left the department. It meant a lot to me, and only thanks are not enough from me to appreciate what they have done in my life. Without their generous support, I can't imagine how I could have handled it.

I am especially thankful for my dissertation committee members, Dr. Daniel Parsons, Dr. Robert Arnold, and Dr. Valery Petrenko for their substantial efforts and suggestions for my research and dissertation. I thank Dr. Petrenko for providing valuable ideas in my research projects and letting me use facilities in his laboratory. I would like to extend my special thanks to Dr. Satyanarayana Pondugula for serving as an outside reader of my dissertation at this monent. Thanks also go to Dr. Yongzhong Wang for his wonderful insights and help in my professional and personal life.

I would like to thank Dr. Vishnu Suppiramaniam, Dr. Randall Clark, and Dr. David Riese for their support in many ways. I also would like to thank all the faculty members, staff and fellow students in the Department of Drug Discovery and Development for their support and help. I specially like to thank Jennifer Johnston, Denise Nims, and Kandi Dawson for their generous help whenever needed. I would like to thank Dr. Bruce Smith and other AURIC

committee members for providing me with an AURIC fellowship. I would also like to extend my appreciations to my laboratory mates, Kasturi, Dr. Deng, Mohammad, Philip, and Haley. They all are really amazing and make me feel very comfortable and enjoyable while working in the laboratory. I thank all the friends' help and accompanies during my stay in Auburn. Special thanks go to Sharmila for considering me as a family member and I really appreciate it.

I am grateful to my parents who always give me unconditional support and love. Their continuous motivation and encouragement make me complete my doctoral program smoothly and successfully. Finally I want to give special thanks and appreciation to my brother. Without his caring and support, I would have not pursued doctoral study in United States on my own. Thanks for pushing me to get stared and keep moving. He is always on my side whenever I am in need of help. Thank you all!

Table of Contents

List of Figures

List of Tables

List of Abbreviations

HSPC	Hydrogenated Soy PhosphatidylCholine
EPC	Egg PhosphatidylCholine
mPEG-DSPE (2000)	MethoxypolyEthyleneGly-col-Distearoyl Phosphatidyl-Ethanolamine
CaP	Calcium Phosphate
LCP	Lipid-coated Calcium Phosphate Nanoparticles
Poly (I:C)	Polyinosinic Acid-Polycytidylic Acid
ZOL	Zoledronic Acid
PBS	Phosphate-Buffered Saline
C_6-Ceramide	N-hexanoyl-D-erythro-sphingosine
C_8-Ceramide	N-Octanoyl-D-erythro-sphingosine
C_8-Glucosylceramide	D-Glucosyl-β1-Octanoyl-D-erythro-sphingosine
DOX	Doxorubicin
PEG	PolyEthylene Glycol

1. Introduction to Lipid based Drug Delivery Systems for Melanoma Treatment

1.1 Abstract

Melanoma is one of the most aggressive forms of malignancy and the treatment options are limited. Although it only accounts for a very small proportion of skin cancer incidence, it leads to the vast majority of skin cancer deaths. Melanoma can be surgically removed if detected in early stages with up to a 99% survival rate. However, metastatic melanoma can only be treated by other therapies, such as chemotherapy, immunotherapy and the combination of these and targeted therapy. These treatments still show low patient response rate and high adverse effects even though they have enhanced efficacy in the beginning, but develop resistance gradually.

There is an urgent need for the development of efficient melanoma treatment methods. Nanoparticle based delivery systems have been studied extensively for their application in the diagnosis and treatment of melanoma. Nanoparticles can deliver drug candidates with a wide range of solubilities and improve blood circulation time by avoiding the reticulo-endothelial system. Nanoparticles could enhance tumor cell uptake with minimized toxicity. Moreover, delivering two or more drugs simultaneously for combinational therapies can be achieved with nanoparticles. In this review, the progress of using different lipid based delivery systems including solid lipid nanoparticles, nanoemulsions, and liposomes for melanoma treatment are presented. They can be utilized either for single drug delivery or multiple agents delivery such as chemotherapeutic drugs, siRNA, DNA and targeting antibodies.

1.2 Melanoma

The skin is the largest organ protecting the body from foreign injury and infections, maintaining fluid retention and controlling and adjusting body temperature (1, 2). The skin can be affected by many ailments, the severe one is cancer. They are three main types of skin cancer: basal cell carcinoma, squamous cell carcinoma and melanoma. Melanoma, originating from melanocytes, is the most aggressive type of skin cancer (3). Although melanoma accounts for only a very small proportion of skin cancer incidence, it leads to the vast majority of skin cancer mortality. There were more than 2 million new cases of skin cancer in USA in 2012 and melanoma only accounts for 3.75% (75,000) of skin cancer cases. The incidence of melanoma is increasing faster than that of all preventable cancers, except lung cancer, and is becoming more severe in the caucasians (4, 5).

Treatment of melanoma is largely dependent on the stage of the disease. Surgery provides the best prevention procedure for patients with early-stage melanoma. An early-stage melanoma that has not metastasized to other organs can be removed by surgery with high survival rates (6). The cure rate for those patients with removable melanoma is 97%−99.8%. The standard excision size was usually considered to be around 0.5 cm with 0.2 cm margin, which is acceptable for margin-controlled surgery (7). However, metastatic melanoma is a highly aggressive malignant skin cancer that is notoriously difficult to be treated through surgical removal. It could only be treated by other therapies, such as chemotherapy, immunotherapy, the combination of the two and targeted therapy (8-11). Traditional chemotherapy is still the most conventional therapy for melanoma treatment. Common chemotherapeutic agents typically include dacarbazine, cisplatin, vinblastine and temozolomide, which interfere with cell division leading to cell death. Dacarbazine, approved for first-line treatment of wild-type melanomas, is

one of the commonly used drugs in melanoma treatment. No other drugs or combinational therapies are superior to dacarbazine (12).

Combination of two or more of these drugs is one of the main strategies to prevent the development of multidrug resistance in tumors. Dacarbazine is co-administered with cisplatin and vinblastine, and this combination is known as the CVD regimen for the treatment of cancer (14). Trametinib, a MEK inhibitor, and dabrafenib, a BRAF inhibitor, were the first-ever approved combination therapy, but did not show significant improvement in melanoma treatment.

Intracellular signaling pathways play a key role in the carcinogenesis of melanoma. The mitogen-activated protein kinase (MAPK)/ERK (extracellular signal-regulated kinase) and phosphoinositide 3-kinase (PI3K) are the major pathways in the development and progression of melanoma. Also, the PI3K/protein kinase B (Akt) pathway has been shown to facilitate the development of melanoma in a synergistic manner with MAPK/ERK pathway (15). Some inhibitors have been developed based on these cellular mechanisms to treat melanoma. Inhibition of both pathways was found to show synergistic effects in the treatment of melanoma. Nanoparticles loading with two siRNAs targeting the oncogene v-Raf murine sarcoma viral oncogene homolog B1 (BRAF) and Akt Pathways exhibit significantly increased cytotoxicity in 1250Lu human melanoma cell line (16-17). Ipilimumab, an anti-cytotoxic T lymphocyte antigen 4 antibody that enhances T-cell activity in the tumor, and selective BRAF inhibitors, such as vemurafenib that blocks tumor cell proliferation in patients with activating BRAF mutations, are two promising therapies. Ipilimumab is the first and vemurafenib is the second drugs shown to improve patient survival rate (18). However, acquired drug resistance to these agents is a major issue in the treatment of melanoma. The majority of patients will develop drug resistance despite

the high initial response to vemurafenib (80%). The occurrence of the resistance could be attributed to multiple factors, such as overexpression of P-gp, altered drug targets and the dysregulation of intracellular signaling pathways (19, 20).

Traditional therapies including surgery, chemotherapy and radiotherapy are ineffective in metastatic melanoma treatment and are usually associated with severe adverse effects. However, melanoma is highly immunogenic, which provides the rationale to develop immunotherapies for its treatment. Immunotherapy could boost immune response of patients with melanoma, also it can help clear cancer cells, especially cells which are impaired or killed by chemotherapy agents (21). Thus, the combination of immunotherapy and chemotherapy could produce synergistic effects. Meanwhile, the survival cancer cells after chemotherapy will contribute to development of drug resistance. The immunotherapeutic drugs that are effective in melanoma treatment are interferon (IFN)-alpha, ipilimumab, and interleukin (IL)-2. IL-2 plasmid loaded in nanoparticle with low molecular weight polyethylenimine and folate inhibit tumor growth and prolong survival rate of melanoma bearing mice (22, 23).

Unfortunately, most of these treatment outcomes are not satisfactory and response rate of patients are very low. The median survival time of patients with metastasized melanoma is only 6-10 months, and the 5-year survival rate is less than 20%. Several approaches improve current melanoma therapeutics: identification of protein targets causing the disease, development of novel agents, determination of optimal therapeutic combinations, and effective delivery of agents into tumor cells. Moreover, promising effects from combination therapies of conventional drugs are difficult to obtain in clinical trials. It may be due to the diverse pharmacokinetic profiles of drugs in patients. The development of multi-drug resistance (MDR) is one of the major reasons for the low efficiency of these therapies. Unfortunately, the mechanisms for acquired drug

resistance in melanoma have been shown to be diverse (24, 25). Therefore, this situation makes it urgent to design and develop novel nanoparticle based drug delivery systems for melanoma treatment. In recent years nanotechnology based delivery systems have been studied extensively and demonstrated to have many advantages for melanoma treatment including the ability to target the drugs to tumors, reduced side effects and drug resistance.

Nanoparticle-based drug delivery systems are superior to conventional drug delivery in the following three aspects. First, nanoparticles protect encapsulated drugs from degradation in the body, especially biotechnology-based drugs. Second, the nanoparticle delivery system could significantly change the pharmacokinetic profile of drugs. Because of the targetable nature, nanoparticles provide increased drug accumulation at the cancer site, which leads to improved efficacy and decreased side effects. Also, the enhanced permeability and retention (EPR) effect caused by the leakiness of tumor vasculature as well as poor lymphatic drainage could result in drug accumulation in the tumors (26). Third, nanoparticles make it easy to deliver multiple agents in the common platform so that chemotherapy, immunotherapy can be combined to achieve potent effects against melanoma tumors. Furthermore, nanoparticles can be designed to have multiple functions, such as therapeutics and diagnostics called theranostics (27-29). Various nanotechnology based drug delivery platforms for melanoma include liposomes, dendrimers, polymersomes, carbon-based nanoparticles, nanoemulsions and protein-based nanoparticles (30-39). Among these, polymeric nanoparticles usually have poor physical stability and relatively high toxicity from the use of polymers. Lipid based drug delivery systems have some advantages over other particulate carrier systems such as good physical stability, controlled release and excellent biocompatibility. Among these, lipid based nanoparticles are usually biodegradable,

biocompatible with low side effects, and have relatively high physical stability. A brief review on the use of lipids based nanoparticle delivery system for melanoma is presented here.

1.3 Lipid based Nanoparticle Delivery Systems

Lipid based nanoparticle delivery systems focusing on melanoma treatment can be classified into solid lipid nanoparticles (SLNs), nanoemulsions and liposomes. Niosomes and polymerosomes that are related to liposomes make a minor role in melanoma delivery systems.

1.3.1 Solid Lipid Nanoparticles

Solid lipid nanoparticles have been used increasingly since the early 1990s as an alternative delivery system to liposomes, nanoemulsions, and polymeric nanoparticles. Solid lipid nanoparticles are made from crystalline solid lipids with particle size under the submicron range (50-1000 nm). Currently, there are three main methods for SLNs preparation: homogenization, solvent emulsification/evaporation and emulsification at high temperature (40, 41). There are many distinct advantages that differentiate SLNs from liposomes: SLNs generally provide good physical stability and prolonged and modulated drug release due to the solid state of the lipids used in the formulation, avoidance of organic solvents in the formulation and ease of large-scale production and commercialization. Also, SLNs can protect encapsulated agents from degradation and have better passive targeting ability for drugs (42). Nanostructured lipid carriers (NLC) composed of a solid lipid matrix with a certain content of a liquid lipid phase are another generation of SLNs (43).

Solid lipid nanoparticles containing docetaxel were prepared with compritol, precirol, and hydrogenated soy phosphatidylcholine using the microemusion and probe sonication method. The docetaxel loaded solid lipid nanoparticles showed increased cytotoxicity (2-fold) in

the malignant melanoma (A-375) cell line compared with Taxotere® (TXT) (44). Cholesteryl butyrate SLNs inhibited human umbilical vein endothelial cells' adhesiveness to cancer human melanoma cell line (45). Huang et. al., prepared different camptothecin loaded SLNs, NLCs and lipid emulsion and compared their cytotoxicity toward a melanoma cell line with the free drug group (46). Camptothecin loaded SLNs made of precirol exhibited 3-fold higher cytotoxicity towards the melanoma cell line compared with the free control group, while NLCs and lipid emulsion had comparable cytotoxicity with the control, which may be due to the excellent endocytotic activity of SLNs. Etoposide has poor solubility and associated low bioavailability. However, the SLNs made with the solid lipid trimyristin, tripalmitin, and tristearin and compritol ATO 888 provided an accumulative effect in the highly perfused organ, suggesting targeting effect toward metastasized tumors. Improvement in the tumoricidal activity and survival rate was found in the B16F10 mouse melanoma model. This study substantiates the application of nanoparticles for improved therapeutic activity of etoposide (47).

1.3.2 Nanoemulsion

Nanoemulsion is a heterogeneous system composed of emulsifying agent and oil suspended in water with mean particle diameters usually of 50-200 nm based on the components and preparation method. Emulsifying agents are surfactants that can reduce interfacial tension between two immiscible liquid phases by preferentially adsorbing at their interfaces (48, 49). There are two types of nanoemulsion: water-in-oil and oil-in-water, the formation depends on the emulsifying agent used. Nanoemulsions are commonly prepared from Generally Recognized as Safe (GRAS) grade excipients approved by the United States Food and Drug Administration (US-FDA) (50). Nanoemulsions are easily produced in large quantities by high shear stress or a mechanical extrusion process. Nanoemulsion based drug delivery systems offer several

advantages. These include greater physical stability, and increased surface to volume ratios containing the drug that enhances the drug bioavailability (51, 52). They serve not only as excellent vehicles for drug encapsulation, but could also alleviate the hypersensitivity associated with surfactants such as ethoxylated castor oil (Cremophor®EL) (53). Because of the nanometer oil droplet size, they can easily be targeted to the tumor tissue using targeting ligands on their surface or by passive accumulations.

Dacarbazine is approved for the first line treatment of malignant melanoma. It is usually administered intravenously, but different dosing and administration methods are warranted in certain therapeutic situations which are accompanied by significant side effects. Nanoemulsions containing dacarbazine showed a 10-fold greater reduction of tumor size compared to the suspension preparation of dacarbazine. During drug cessation period dacarbazine nanoemulsion showed 5-fold greater efficacy (73% versus 14%) in preventing tumor growth compared with dacarbazine suspension (54).

A cholesterol-rich lipid nanoemulsion (LDE) was used as a vehicle to target etoposide for melanoma. LDE was prepared using cholesteryl oleate, egg phosphatidylcholine, triolein and cholesterol. The efficacy of LDE-etoposide oleate or commercial etoposide was evaluated in melanoma-bearing mice. LDE drastically reduced the drug toxicity, as the maximum tolerated dose was approximately five-fold greater than for commercial etoposide. LDE-etoposide oleate accumulated at four-fold higher concentrations in the tumor compared with the surrounding normal cells, and remained in the bloodstream longer than commercial etoposide. The tumor growth inhibition rate and survival were greater in animals treated with LDE-etoposide oleate compared with commercial etoposide. The incorporation of etoposide oleate into LDE resulted in markedly reduced toxicity and superior antitumoral activity (55).

Kretzer and coworkers studied the combination of etoposide (ETP) with paclitaxel in cholesterol-rich lipid (LDE-PTX) nanoemulsions in comparison to administrating etoposide and paclitaxel directly. The results indicated that B16F10 melanoma bearing mice treated with LDE-PTX+ETP had much less metastases than mice treated with PTX+ETP (30% versus 82%). LDE-PTX+ETP reduced cellular density, and blood vessels and increase collagen fibers in tumor tissues, which is absent in the PTX+ETP group (56).

1.3.3 Liposomes

Liposomes were introduced in 1961 and was the first nanoparticle used in medicine. The concept of using a liposome as a selective drug delivery system for the skin was described initially in 1980 (57). A liposome is a nanoscopic or microscopic structure that contains an aqueous core for hydrophilic drugs and hydrophobic drugs can be contained in the lipid bilayer, which provides a broader choice of drugs for encapsulation. Homogeneous nanosized liposomes can be achieved by filtering through polycarbonate membranes with different sizes. Furthermore, specific ligands against tumor antigens can be attached to the liposome surface so that the nanoparticles can target cancer cells specifically (58, 59).

There are certain factors affecting drug loaded liposome efficacy in cancer treatment. The size of liposome vesicles plays a crucial role. Vesicles less than 100 nm have reduced uptake into liver tissue, while vesicles >100 nm are quickly cleared by the reticulo-endothelial system (RES). Furthermore, surface modification of liposomes with polyethylene glycol (PEG) can result in prolonged circulation by the liposome escaping from RES. Heating and light can also be used to facilitate nanovesicle contents release in the body rather than through nanoparticle degradation alone (60, 61). Liposomes have been investigated extensively in melanoma research. Several liposomes based anticancer drugs are either on the market or in clinical trials. Some

examples are doxorubicin liposomes and camptothecin liposomes. Many chemotherapeutic drugs, antibodies and siRNAs have been encapsulated in liposomes to enhance treatment efficacy for melanoma treatment (62-64).

Niosome is a relatively new drug delivery system. It presents a similar bilayer structure as liposome, but the bilayer in niosome is composed of non-ionic surfactant rather the phospholipids in the liposomes. Most aqueous solution of surfactants can form micelles automatically, however some surfactants can form bilayer vesicles called niosomes (25). Therefore, niosomes generally have some advantages over conventional liposomes such as increased penetrating ability, physicochemical stability and reduced toxicity. Niosomes can accommodate drugs with a wide range of solubilities due to the structure containing hydrophobic and hydrophilic parts. The hydrophilic drugs within the space were enclosed in the vesicle, the hydrophobic drugs were embedded in the bilayer. The particle size of niosome is usually 100 nm to 2 μm (66).

The first niosomes were formulated with cholesterol and single-chain surfactants such as polyglycerol monoakyl ethers and polyoxylate analogs and another non-ionic surfactant for further stabilization. Positively charged molecules such as stearylamine and cetylpyridinium choloride were added to prevent the aggregation of niosome. There are three major types of niosomes: multi lamellar vesicles (MLV), large unilamellar vesicles (LUV) and small unilamellar vesicels (SUV). They can be unilamellar or multilamellar depending on the preparation method. Current preparation methods are: the ether injection method, thin film hydration method, remote loading, reverse-phase evaporation technique, sonication, the bubble method and multiple membrane extrusion method.

The advantages of niosomes include high patient compliance due to the water-based delivery system rather than conventional oil based delivery system, wide range of solubilities, flexibility and ability to release drugs in a controlled manner (67, 68). They have been developed for multiple uses in cancer treatments such as drug targeting, peptide and anti-neoplastic drugs delivery and immune response related studies. Niosome have been widely studied in drug delivery and targeting. These have been employed for dermal and transdermal delivery, ocular and oral delivery, pulmonary, parenteral delivery and gene delivery (69-74).

Fang et al. showed enhanced skin permeation of enoxacin encapsulated in niosomes compared with liposomes of enoxacin (75). Also, tretinoin stability was better in noisome than it was incorporated into liposomes. Niosomes demonstrated prolonged circulation time, drug release, and increased drug permeation and retention in skin (76). A novel niosomal system made of alpha, omega-hexadecyl-bis-(1-aza-18-crown-6), Span 80, and cholesterol (2:5:2 molar ratio) was formulated as a topical delivery system for 5-fluorouracil (5-FU). The drug loaded niosome provided 8- and 4-fold increased drug permeation compared with aqueous drug solution and mixture of blank niosome and free drug solution (77). Overall, niosomes have great potential in melanoma treatment due to their superiority, such as higher stability and cost-effectiveness in comparison with liposomes.

1.3.3.1 Chemotherapy

Liposome delivery system has been widely used in traditional chemotherapeutic agents' delivery for melanoma treatment (78-81). Among these, liposomal doxorubicin (Doxil®) is widely used for various cancers treatment. Liposomal doxorubicin prolongs blood circulation and decreases cardiovascular related toxicity when compared with free doxorubicin in cancer

treatment (82-84). However, phase II trials oDoxil in melanoma patients were discontinued because of low activity (85). Pegylated phosphatidyl ethanolamine liposomal cisplatin with a particle size of approximately 100 nm had a higher cytotoxicity than free cisplatin, and provided 3.6 fold higher level of intra-tumoral drug concentration for 72 h than the free drug (86). Vincristine encapsulated liposomes formulation was investigated and showed an extended drug circulation time and the potential for enhanced tumor targeting and anti-tumor activity. The safety and activity of vincristine liposome were evaluated in patients with metastatic melanoma and had good tolerance and promising antitumor activity (87). Four types of synthetic glucocorticoids were loaded into long-circulating liposome and the in vitro results suggested that all drug loaded liposomes had strong cytotoxic effects on B16F10 melanoma cells (88).

1.3.3.2 Immunotherapy

Endogenous sphingolipids such as ceramides play an important role as mediators of the intracellular signaling molecules involved in cell differentiation, cell cycle arrest and apoptosis through the PI3K/Akt pathway (89, 90). However, due to hydrophobicity of ceramides, the bioavailability is low and limits its use in the systemic delivery for cancer treatment (91). Liposomes can incorporate ceramides in their lipid core and provide a better delivery method to overcome this limitation. Intravenous administration of both pegylated and non-pegylated liposomal ceramide showed improved pharmacokinetics and resulted in inhibition of breast tumors in mice (92). Intracellular delivery of ceramides via liposomes increased apoptosis in the MDA435/LCC6 human breast cancer and J774 mouse macrophage cell lines (93). Sorafenib and liposomal ceramide synergistically inhibited melanoma cell growth through mitogen-activated protein kinase and phosphatidylinositol 3-kinase signaling. In a co-delivery system, cell

apoptosis was increased two-fold and cellular proliferation decreased by 25% compared with agent delivered alone, suggesting an additive effect between ceramide and sorafenib (94).

Gene therapy has become a promising strategy for the treatment of various inheritable or acquired diseases (95-97). However, nucleic acids are rapidly degraded by nucleases in the body and result in poor cellular uptake, so that the development of safe and efficient gene carriers is critical for the success of gene therapy (98). Viral vectors (DNA and RNA) have been developed for gene delivery. But they are usually associated with immunogenicity, high toxicity and production cost. Viral integration can induce severe immune response which may cause harm to normal tissues and interrupt normal gene expression. Non-viral vectors, such as cationic lipids and polymers, have been developed to efficiently deliver gene products (99).

Liposomes, especially positively charged ones, provide an alternative in which nucleic acids are protected and delivered into targeted cells without limitations along with viral vectors. Cationic polymers and nanoparticles are frequently used for gene delivery, because the positive charges of these delivery systems can interact with negative charges on nucleic acids. Moreover, cell membranes are known to have negative charges which enable them to attract cationic nanoparticles (100). Cationic liposomes also have other common advantages of nanoparticles such as protection of genes from degradation in the body, and passive targeting because of their EPR effects. However, liposomes with positive charges are known to show higher associated cell toxicity than neutral or negative liposomes. Strategies, such as surface modifications by pegylation (101) and targeting ligand conjugation (102) have been used to overcome or minimize this side effect. A number of investigations demonstrate that liposomes are capable of delivering different nucleic acids and show promising anti-melanoma effects.

Cationic liposomes loaded with interferon-beta (IFNβ) genes were formulated to study their mechanisms of action and anti-tumor effects in mouse B16F1 melanoma cells in vitro and in vivo. A liposome based IFNβ formulation exhibited 5.5-fold reductions in subcutaneous melanoma lesions in mice and higher infiltration of natural killer (NK) cells compared with phosphate buffered saline. The data confirms that cationic liposome-mediated IFNβ could induce cell death and increase production of NK cells to tumors (103).

Human leukocyte antigen (HLA)-B7/β-2 macroglobulin plasmid DNA/lipid complex, also known as Allovectin-7® loaded liposome have an extremely safe toxicity profile with low toxicities (104). mRNAs instead of DNA loaded liposomes have been developed for melanoma treatment. The mRNAs delivery skips the transcription procedure, which is necessary in DNA delivery. MART1 mRNA in liposome formulations with L-histidine-(N, N-di-n-hexadecylamine) ethylamide (HDHE) and cholesterol prevent murine B16 melanoma cell growth and metastasis (105). Polyinosinic-polycytidylic acid (PIC), synthetic dsRNA, is well known to react with Toll-like receptor 3 and then stimulate innate immune response. PIC liposomes could directly suppress the growth of B16F10 melanoma *in vitro* in a dose-dependent manner. The mechanism can be explained by the enhanced immune response due to the maturation of dendritic cells and TRP-2-specific IFN-gamma-producing cells in the lymph nodes as well as spleen (106). BAX mRNA is a proapoptotic gene and inhibits the growth of various types of tumors. The BAX mRNA gene was loaded in cationic liposomes composed of 1, 2-dioleoyl-3-trimethylammonium-propane and 1, 2-dioleoyl-sn-glycero-3-phosphoethanolamine and human melanoma treated with liposomes were 36.7% smaller than saline control after 10 days' treatment (107).

It is well known that liposomes are preferentially accumulated in tumors cells due to their EPR effect. Tumor cells have leaky vasculature while normal cells lack this property, which

gives a priority for nanoparticles based delivery system to be passively accumulated in tumor cells rather than normal cells (108). In addition to passive targeting, specific antigens have been conjugated on the surface of liposomes for targeting tumor cells. Many specific proteins are found on melanoma cells surfaces, which could distinguish them from normal cells in patients (109,110). Therefore, melanoma cells can be targeted specifically through various antibodies and ligands which can recognize proteins specifically expressed on melanoma cells. Folic acid and transferrin are two common molecules expressed highly in tumor cells. GD_2 was originally identified as an antigen from a melanoma cell line and found to be expressed on 65% of melanoma cells (111). GD_2 modification of the oncogene c-Myc loaded liposome had increased blood circulation time, inhibition of tumor growth and survival rate in human melanoma cell lines (NG, MZ2-MEL). This suggested that inhibition of tumor growth via GD_2 targeting could provide an effective approach for the treatment of melanoma (112). Finally, several external physical energy sources have been utilized to prepare targeting liposome, such as ultrasound, magnetics and electrics (113, 114).

1.3.3.3 Combinational Therapies

Complicated tumor microenvironment and signaling pathways involved in cancer cell growth and metastasis are the major factors which make the development of an efficient cancer treatment very challenging (115). Single chemotherapeutics always showed low survival rate and melanoma tumor cells developed resistance toward the drug, so chemotherapy is usually performed with a combination of two or more agents. Targeting two or more specific sites simultaneously or sequentially is expected to show maximal efficacy (116). As combinational drugs inhibit tumor growth under different mechanisms such as proliferation, angiogenesis, and metastasis, this provides a novel idea for treatment of melanoma. Different drug combinations in

clinical trials involve the co-administration of two or more anticancer drugs, the co-administration of multidrug resistance (MDR) modulators with anticancer drugs, and the co-administration of anticancer drugs and gene regulating drugs. This may also lead to addidative or possibly effects (117, 118).

Nanoparticles such as liposomes or microemulsions provide visible options for simultaneous delivery of two or more drugs. Liposomes presented a good co-delivery strategy for loading hydrophobic and hydrophilic molecules simultaneously for decreasing drug resistance and toxicity, thus improving patient compliance (119). Liposomes co-delivering 4-S-cystaminyl-phenol (4-S-CAP) and magnetite particles resulted in 17% tumor regression in mice. Combination of a vascular-disruptive drug, combretastatin A4 phosphate, and an anticancer drug, doxorubicin, in encapsulated liposomes produced 2-fold higher inhibition of B16-F10 tumor growth than single therapy (120). Treatment of doxorubicin-loaded liposomes along with cyclophosphamide obtained a 1.5-fold higher inhibitory effect on pulmonary metastatic B16BL6 melanoma-bearing mice compared with drug solutions. However, treatment with combined chemotherapy is also associated with higher toxicities as more cytotoxic drugs are introduced. The combination of high dose DXR-SL and cyclophosphamide caused significant decreases in lung weight indicating increased toxicity (121). Co-delivering paclitaxel and etoposide in a cholesterol-rich nanoemulsion showed strong tumor growth inhibition and reduced tumor metastases (119). A cross-linked multilamellar liposome co-delivering doxorubicin and paclitaxel exhibited enhanced encapsulation efficiency (approximately 90%) and a 2.5-fold increased therapeutic effect in the treatment of melanoma-bearing mice compared with delivering drug solution. Also, a synergistic function in inhibiting tumor growth was found in the co-delivery of doxorubicin and paclitaxel (122).

Chemo-immunotherapy using cytotoxic drugs and immune stimulators could increase efficacy in the treatment of cancers. Moreover, some chemotherapeutics bring synergistic function with certain cytokines. The anticancer drugs can not only kill cells directly, but also could adjust the immune response, and activated immune response would cause more cell apoptosis. Meanwhile, the induction of immune response from the cytokines inhibits tumor cell growth to a greater degree, which provides support for direct cell killing capabilities of chemotherapeutic drugs (123, 124). Significantly enhanced tumor growth inhibition (4-fold) and a 30 day prolongation in survival time were found in melanoma-bearing mice treated by anionic liposomes co-delivering paclitaxel and adenoviral vector expressing IL-12 compared with delivery of paclitaxel alone within liposomes (125).

Gene therapy is becoming more popular in cancer treatment over the past several decades due to the deep understanding of the relationship between gene and cancer development. MDR is a major obstacle to the successful treatment of cancer (126, 127). There are two major advantages of co-delivering a small molecule anticancer drug and siRNA including a decrease in drug efflux and an increase in cell apoptosis. The use of nanoparticles co-delivering small interfering RNA (siRNA) and small molecule anticancer drugs in cancer treatment has been reported in many studies. A co-delivery system of siRNA and small anticancer drugs has three major advantages: overcoming drug resistance, synergistic apoptotic effect, and reduced toxicities. All these characteristics could enhance anti-tumor effects in cancer treatment (128, 129).

Many nanoparticle delivery systems such as liposomes (130), polymer micelles (131) and dentrimers (132) have been developed for gene delivery. Nanoparticles are taken up by cells via two major pathways: endocytosis and micropinocytosis pathways (133). Doxorubicin was co-

administrated with different siRNAs, such as MVP siRNA, ASCL 1 siRNA in triblock co-polymeric system, and nanorods. They were tested in a human carcinoid cell line (in vitro) and HeLa cells (*in vitro* and *in vivo*) and co-delivery of siRNA and anticancer drugs significantly decreased drug efflux and increased cell apoptosis, causing enhanced anti-tumor effects (134). The efficacy of combined chemotherapy containing cisplatin, vinblastine and dacarbazine (CVD) and biotherapy using interleukin-2 and interferon-alpha was tested in patients with melanoma. The biochemotherapy treated group had a longer median survival period compared with only CVD treated groups, which was 13 and 9 months, respectively (135).

1.4 Conclusion

Nanoparticle based drug delivery systems can provide a major contribution in cancer treatment. They can encapsulate drugs having a wide range of solubility with significantly enhanced cell cytotoxicity. Meanwhile, it offers many other advantages: protection from degradation, increased circulation time, controlled release of drugs at tumor sites, and potent targeting efficiency. Among these, liposome, nanoemulsion and SLNs exhibited great potential in melanoma treatment. The passive accumulation and active targeting could significantly decrease adverse side effects usually associated with chemotherapeutic agents. Liposomes can be applied in melanoma diagnosis and theranostics.

However, it is still challenging to develop formulations for effective delivery of therapeutic agents to treat melanoma. Many patients develop multidrug resistance. Combinational therapies, such as multiple agents and immuno-chemotherapy, are promising strategies to overcome MDR. However, most reports showed that separate administrations of different agents are necessary in these combination therapies. Formulation and co-delivery two or more agents in one system in melanoma treatment is generally complicated. While there are

obvious advantages of co-delivery systems for tumors, limited information is available on nanoparticle based co-delivery systems for melanoma treatment.

Therefore, the objective of this dissertation research was to develop lipid based nanoparticle delivery systems for melanoma treatment. This dissertation is presented in six chapters. In Chapter 1, a brief review of various lipid based drug delivery systems for tumor targeting with a special emphasis on melanoma tumors was presented. The application of liposomes in chemotherapy, immunotherapy and their combination, and various co-delivery systems were presented.

Chapter 2 provides a compilation of data generated on oxidized phospholipid based micelles for the delivery of drugs to leukemia cell lines. A novel pH sensitive oxidized phospholipid-based micellar formulation with potential use in delivering anthracycline anti-cancer drugs (doxorubicin and idarubicin) was developed. This formulation provides a novel strategy for increasing the therapeutic index and overcoming multidrug resistance for leukemia treatment.

Chapter 3 presents data on a co-delivery system containing zoledronic acid and a double-strand RNA as a nanoparticle system. This formulation combines agents for chemotherapy and immunotherapy for effective treatment of melanoma. The formulation consists of a cationic lipid (DOTAP) coated CaP nanoparticle for simultaneous delivery of zoledronic acid and polyinosinic acid-polycytidylic acid (a synthetic double-stranded RNA). The cytotoxicity of the formulations was evaluated in B16BL6 melanoma cell line and melanoma tumor bearing mice.

Chapter 4 consists of data on genistein microemulsion formulation optimization for prevention and treatment of melanoma. Microemulsions were optimized through pseudo-ternary

phase diagrams and these formulations were further optimized for better human skin permeation and retention.

Chapter 5 presents data on a liposome based co-delivery system containing ceramide and doxorubicin. A liposome formulation is utilized for delivering doxorubicin for treating various types of cancers, but to our knowledge very limited data has been reported on a co-delivery system for melanoma treatment. A liposome formulation for co-delivering doxorubicin and ceramide for additive or synergistic cytotoxicity in a melanoma cell line was optimized.

Chapter 6 presents a comprehensive summary and conclusions on the data pertaining to each project presented in this dissertation. The author's opinion and perspective on future directions based on this work is provided.

1.5 Reference

1. Ryman-Rasmussen JP, Riviere JE, Monteiro-Riviere NA. Penetration of intact skin by quantum dots with diverse physicochemical properties. Toxicol Sci. 2006; 91(1):159-65.
2. Foletto MC, Haas SE. Cutaneous melanoma: new advances in treatment. An Bras Dermatol. 2014; 89(2):301-10.
3. Eigentler TK, Mugge LO， Bembenek A, Garbe C. Cutaneous melanoma. Onkologie. 2007; 13(8):745-757.
4. Chen J, Shao R, Zhang XD, Chen C. Applications of nanotechnology for melanomatreatment, diagnosis, and theranostics. Int J Nanomedicine. 2013; 8: 2677-88.
5. Geller AC, Cantor M, Miller DR, et al. The Environmental Protection Agency's National SunWise School Program: sun protection education in US schools (1999-2000). J Am Acad Dermatol. 2002; 46(5):683-9.
6. Mukaiya M, Hirata K, Tarumi K, et al. Surgical treatment for recurrent tumors of primary

malignant melanoma of the esophagus: a case report and review of the literature. Hepatogastroenterology. 1999; 46(25):295-8.

7. Garbe C, Eigentler TK. Diagnosis and treatment of cutaneous melanoma: state of the art 2006. Melanoma Res. 2007; 17(2):117-27.

8. Matos AM, Francisco AP. Targets, structures, and recent approaches in malignant melanoma chemotherapy. Chem Med Chem. 2013; 8(11):1751-65.

9. Hao MZ, Zhou WY, Du XL, et al. Novel anti-melanoma treatment: focus on immunotherapy. Chin J Cancer. 2014 5; 33(9):458-65.

10. Yushak M, Kluger HM, Sznol M. Advances in the Systemic Treatment of Metastatic Melanoma. Oncology (Williston Park). 2013, 15; 27(5).

11. Leiter U, Meier F, Garbe, C. Targeted therapies for melanoma.2014; 65(7): 600-606.

12. Anderson CM, Buzaid AC, Legha SS. Systemic treatments for advanced cutaneous melanoma. Oncology (Williston Park). 1995; 9(11):1149-58;

13. Khan KH, Goody RB, Hameed H, et al. Metastatic melanoma: a regional review and future directions. 2012; 98(5):575-80.

14. Hofmann MA, Hauschild A, Mohr P, et al. Prospective evaluation of supportive care with or without CVD chemotherapy as a second-line treatment in advanced melanoma by patient's choice: a multi-center Dermatologic Cooperative Oncology Group trial. Melanoma Res. 2011; 21(6):516-23.

15. Evans MS, Madhunapantula SV, Robertson GP, Drabick JJ. Current and future trials of targeted therapies in cutaneous melanoma. Adv Exp Med Biol. 2013; 779:223-55.

16. Lopez Bergami P, Fitchman B, Ronai Z. Understanding signaling cascades in melanoma. Photochem Photobiol. 2008; 84(2):289-306.

17. Tran MA1, Gowda R, Sharma A, et al. Targeting V600EB-Raf and Akt3 using nanoliposomal-small interfering RNA inhibits cutaneous melanocytic lesion development. Cancer Res. 2008; 68(18):7638-49.

18. Burgeiro A, Mollinedo F, Oliveira PJ. Ipilimumab and vemurafenib: two different routes for targeting melanoma. Curr Cancer Drug Targets. 2013; 13(8):879-94.

19. Agostinelli E, Condello M, Tempera G, et al. The combined treatment with chloroquine and the enzymatic oxidation products of spermine overcomesmultidrug resistance of melanoma M14 ADR2 cells: a new therapeutic approach. Int J Oncol. 2014; 45(3):1109-22.

20. Kanwar JR, Singh N, Kanwar RK. Role of nanomedicine in reversing drug resistance Mediated by ATP binding cassette transporters and P-glycoprotein in melanoma. Nanomedicine (Lond). 2011; 6(4):701-14.

21. Recchia F, Candeloro G, Necozione S, et al. Multicenter phase II study of Chemoimmunotherapy in the treatment of metastatic melanoma. Anticancer Drugs. 2008; 19(2):201-7.

22. Kirkwood JM. Studies of interferons in the therapy of melanoma. Semin Oncol. 1991; 18 (5 Suppl 7):83-90.

23. Atkins MB, Kunkel L, Sznol M, Rosenberg SA. High-dose recombinant interleukin-2 therapy in patients with metastatic melanoma: long-term survival update. Cancer J Sci Am. 2000; 6 Suppl 1:S11-4.

24. La Porta CA. Mechanism of drug sensitivity and resistance in melanoma. Curr Cancer Drug Targets. 2009; 9(3):391-7.

25. Berger W , Elbling L; Micksche M. Chemoresistance of human malignant melanoma: Cellular and molecular aspects .Onkologie.1998; 21(2):105-110

26. Ballarín-González B, Ebbesen MF, Howard KA. Polycation-based nanoparticles for RNAi-mediated cancer treatment. Cancer Lett. 2014 28; 352(1):66-80.

27. Gabizon A, Catane R, Uziely B, et al. Prolonged circulation time and enhanced accumulation in malignant exudates of doxorubicin encapsulated inpolyethylene-glycol coated liposomes. Cancer Res. 1994; 15; 54(4):987-92.

28. Kim MJ, Lee JY, Nehrbass U, et al. Detection of melanoma using antibody-conjugated quantum dots in a coculture model for high-throughput screening system. Analyst. 2012; 21; 137(6):1440-5.

29. Fraix A, Kandoth N, Manet I, et al. An engineered nanoplatform for bimodal anticancer phototherapy with dual-color fluorescence detection of sensitizers. Chem Commun (Camb). 2013 18; 49(40):4459-61.

30. Zamboni WC, Gervais AC, Egorin MJ, et al. Systemic and tumor disposition of platinum after administration of cisplatin or STEALTH liposomal-cisplatinformulations (SPI-077 and SPI-077 B103) in a preclinical tumor model of melanoma. Cancer Chemother Pharmacol. 2004; 53(4):329-36.

31. Silverman JA, Reynolds L, Deitcher SR. Pharmacokinetics and pharmacodynamics of vincristine sulfate liposome injection (VSLI) in adults with acutelymphoblastic leukemia. J Clin Pharmacol. 2013; 53(11):1139-45.

32. Yu KF, Zhang WQ, Luo LM, et al. The antitumor activity of a doxorubicin loaded, iRGD-modified sterically-stabilized liposome on B16-F10melanoma cells: in vitro and in vivo evaluation. Int J Nanomedicine. 2013; 8: 2473-85.

33. Zhu S, Hong M, Tang G, et al. Partly PEGylated polyamidoamine dendrimer for tumor-selective targeting of doxorubicin: the effects ofPEGylation degree and drug conjugation style.Biomaterials. 2010; 31(6):1360-71.

34. Malik N, Evagorou EG, Duncan R. Dendrimer-platinate: a novel approach to cancer chemotherapy. Anticancer Drugs. 1999; 10(8):767-76.

35. Cline EN, Li MH, Choi SK, et al. Paclitaxel conjugated PAMAM dendrimers adversely affect microtubule structure through two independentmodes of action. Biomacromolecules. 2013; 14(3):654-64.

36. Kim HO, Kim E, An Y, et al. A biodegradable polymersome containing Bcl-xL siRNA and doxorubicin as a dual delivery vehicle for asynergistic anticancer effect. Macromol Biosci. 2013; 13(6):745-54.

37. Li S, Byrne B, Welsh J, Palmer AF. Self-assembled poly (butadiene)-b-poly (ethylene oxide) polymersomes as paclitaxel carriers. Biotechnol Prog. 2007; 23(1):278-85.

38. Chaudhuri P, Soni S, Sengupta S. Single-walled carbon nanotube-conjugated chemotherapy exhibits increased therapeutic index in melanoma. Nanotechnology. 2010; 21(2):025102.

39. Hawkins MJ, Soon-Shiong P, Desai N. Protein nanoparticles as drug carriers in clinical medicine. Adv Drug Deliv Rev. 2008; 60(8):876-85.

40. Mehnert W, Mäder K. Solid lipid nanoparticles: production, characterization and applications. Adv Drug Deliv Rev. 2001; 47(2-3):165-96.

41. Wong HL, Bendayan R, Rauth AM, et al. Chemotherapy with anticancer drugs encapsulated in solid lipid nanoparticles. Adv Drug Deliv Rev. 2007; 59(6):491-504.

42. Harms M; Muller-Goymann, CC. Solid lipid nanoparticles for drug delivery.J Drug Deliv. 2011; 21(1): 89-99

43. Weber S, Zimmer A, Pardeike J. Solid Lipid Nanoparticles (SLN) and Nanostructured Lipid Carriers (NLC) for pulmonary application: a review of the state of the art. Eur J Pharm Biopharm. 2014; 86(1):7-22.

44. Mosallaei N, Jaafari MR, Hanafi-Bojd MY, et al. Docetaxel-loaded solid lipid nanoparticles: preparation, characterization, in vitro, and in vivo evaluations. J Pharm Sci. 2013; 102(6):1994-2004.

45. Dianzani C, Cavalli R, Zara GP, et al. Cholesteryl butyrate solid lipid nanoparticles inhibit adhesion of human neutrophils to endothelial cells. Br J Pharmacol. 2006; 148(5):648-56.

46. Huang ZR, Hua SC, Yang YL, Fang JY. Development and evaluation of lipid nanoparticles for camptothecin delivery: a comparison of solid lipidnanoparticles, nanostructured lipid carriers, and lipid emulsion. Acta Pharmacol Sin. 2008; 29(9):1094-102.

47. Athawale RB, Jain DS, Singh KK, Gude RP. Etoposide loaded solid lipid nanoparticles for curtailing B16F10 melanoma colonization in lung. Biomed Pharmacother. 2014; 68(2):231-40.

48. Maali A, Mosavian, MTH. Preparation and Application of Nanoemulsions in the Last Decade (2000-2010) .J Dis Sci Tech. 2013; 34(1):92-105.

49. Lu Y, Qi J, Wu W. Absorption, disposition and pharmacokinetics of nanoemulsions. Curr Drug Metab. 2012; 13(4):396-417.

50. Pawar KR, Babu RJ. Lipid materials for topical and transdermal delivery of nanoemulsions. Crit Rev Ther Drug Carrier Syst. 2014; 31(5):429-58.

51. Souto EB, Nayak AP, Murthy RS. Lipid nanoemulsions for anti-cancer drug therapy. 2011; 66(7):473-8.

52. Thanos CG, Liu Z, Reineke J, Edwards E, Mathiowitz E. Improving relative bioavailability of dicumarol by reducing particle size and adding the adhesive poly(fumaric-co-sebacic) anhydride. Pharm Res. 2003; 20(7):1093-100.

53. Gelderblom H, Verweij J, Nooter K, Sparreboom A. Cremophor EL: the drawbacks and advantages of vehicle selection for drug formulation. Eur J Cancer. 2001; 37(13):1590-8.

54. Tagne JB, Kakumanu S, Nicolosi RJ. Nanoemulsion preparations of the anticancer drug dacarbazine significantly increase its efficacy in a xenograftmouse melanoma model. Mol Pharm. 2008; 5(6):1055-63.

55. Lo Prete AC, Maria DA, Rodrigues DG, et al. Evaluation in melanoma-bearing mice of an etoposide derivative associated to a cholesterol-rich nanoemulsion. J Pharm Pharmacol. 2006; 58(6):801-8.

56. Kretzer IF, Maria DA, Maranhão RC. Targeting in combined cancer chemotherapy: tumor growth inhibition in mice by association of paclitaxel and etoposide with a cholesterol-rich nanoemulsion. Cell Oncol (Dordr). 2012; 35(6):451-60.

57. Moghimi SM, Patel HM. Current progress and future prospects of liposomes in dermal drug delivery. J Microencapsul. 1993; 10(2):155-62.

58. Dua JS, Rana AC, Bhandari AK. Liposome: methods of preparation and application. IJPSR. 2012:3(2):14-20.

59. Langner M, Kral TE. Liposome-based drug delivery systems. Pol J Pharmacol .1999; 51 (3): 211-222.

60. De Jong WH, Borm PJ. Drug delivery and nanoparticles: applications and hazards. Int J Nanomedicine. 2008; 3(2):133-49.

61. Cai L, Wang X, Wang W, et al. Peptide ligand and PEG-mediated long-circulating liposome targeted to FGFR overexpressing tumor in vivo. Int J Nanomedicine. 2012; 7: 4499-510.

62. Hu Q, Bally MB, Madden TD.Subcellular trafficking of antisense oligonucleotides and and down-regulation of bcl-2 gene expression in humanmelanoma cells using a fusogenic liposome delivery system. Nucleic Acids Res. 2002; 30(16):3632-41.

63. Daoud SS, Fetouh MI, Giovanella BC. Antitumor effect of liposome-incorporated camptothecin in human malignant xenografts. Anticancer Drugs. 1995; 6(1):83-93.

64. Jérôme V, Graser A, Müller R, et al. Cytotoxic T lymphocytes responding to low doseTRP2 antigen are induced against B16 melanoma by liposome-encapsulated TRP2 peptide and CpG DNA adjuvant. J Immunother. 2006; 29(3):294-305.

65. Kong M, Park H, Feng C, et al. Construction of hyaluronic acid noisome as functional transdermal nanocarrier for tumor therapy. Carbohydr Polym. 2013; 94(1):634-41.

66. Makeshwar KB, Wasankar SR. Niosome: a Novel Drug Delivery System. Asian J Pharm Res. 2013; 3 (1): 16-20.

67. Azeem A, Anwer MK, Talegaonkar S. Niosomes in sustained and targeted drug delivery: some recent advances. J Drug Target. 2009; 17(9):671-89.

68. Marianecci C, Di Marzio L, Rinaldi F, et al. Niosomes from 80s to present: the state of the art. Adv Colloid Interface Sci. 2014; 205:187-206.

69. Sinico C, Fadda AM. Vesicular carriers for dermal drug delivery. Expert Opin Drug Deliv. 2009; 6(8):813-25.

70. Paolino D, Muzzalupo R, Ricciardi A, et al. In vitro and in vivo evaluation of Bola-surfactant containing niosomes for transdermal delivery. Biomed Microdevices. 2007; 9(4):421-33.

71. Jain S, Singh P, Mishra V, Vyas SP. Mannosylated niosomes as adjuvant-carrier system for oral genetic immunization against hepatitis B. Immunol Lett. 2005; 101(1):41-9.

72. Mukherjee B, Patra B, Layek B, Mukherjee A. Sustained release of acyclovir from nano-liposomes and nano-niosomes: an in vitro study. Int J Nanomedicine. 2007; 2(2):213-25.

73. Bragagni M, Mennini N, Ghelardini C, Mura P. Development and characterization of niosomal formulations of doxorubicin aimed at brain targeting. J Pharm Pharm Sci. 2012; 15(1):184-96.

74. Marianecci C, Paolino D, Celia C, et al. Non-ionic surfactant vesicles in pulmonary glucocorticoid delivery: characterization and interaction with human lung fibroblasts. J Control Release. 2010; 147(1):127-35.

75. Manconi M, Sinico C, Valenti D, et al. Niosomes as carriers for tretinoin. III. A study into the in vitro cutaneous delivery of vesicle-incorporatedtretinoin. Int J Pharm. 2006; 311(1-2):11-9.

76. Shahiwala A, Misra A.Studies in topical application of niosomally entrapped Nimesulide. J Pharm Pharm Sci. 2002; 5(3):220-5.

77. Paolino D, Cosco D, Muzzalupo R, et al. Innovative bola-surfactant niosomes as topical delivery systems of 5-fluorouracil for the treatment of skincancer. Int J Pharm. 2008; 353(1-2): 233-42.

78. Siddikuzzaman, Grace VM.Anti-Metastatic Study of Liposome-Encapsulated All trans Retinoic Acid (ATRA) in B16F10 Melanoma Cells-Implanted C57BL/6 Mice. Cancer Invest. 2014 Oct 14.

79. Liu GX, Fang GQ, Xu W. Dual targeting biomimetic liposomes for paclitaxel/DNA combination cancer treatment. Int J Mol Sci. 2014; 15(9):15287-303.

80. Matsumoto K, Saida T, Mizuno M, Yoshida J. Cationic liposome-mediated human interferon-beta (HuIFN beta) gene therapy for patients with advanced melanoma. J Gene Med. 2006; 8(3): 372-373.

81. Zhou WZ, Kaneda Y, Huang S, et al. Protective immunization against melanoma by gp100 DNA-HVJ-liposome vaccine. Gene Ther. 1999; 6(10):1768-73.

82. Zakaria S, Gamal-Eldeen AM, El-Daly SM, Saleh S. Synergistic apoptotic effect of Doxil and aminolevulinic acid-based photodynamic therapy on human breastadenocarcinoma cells. Photodiagnosis Photodyn Ther. 2014; 11(2):227-38.

83. Batist G, Ramakrishnan G, Rao CS, et al. Reduced cardiotoxicity and preserved antitumor efficacy of liposome-encapsulated doxorubicin and cyclophosphamide compared with conventional doxorubicin and cyclophosphamide in a randomized, multicenter trial of metastatic breast cancer. J Clin Oncol. 2001; 19(5):1444-54.

84. Zhao C, Feng Q, Dou Z, et al. Local targeted therapy of liver metastasis from colon cancer by galactosylated liposome encapsulated with doxorubicin. PLoS One. 2013; 8(9):e73860.

85. Smylie MG, Wong R, Mihalcioiu C, et al. A phase II, open label, monotherapy study of liposomal doxorubicin in patients with metastatic malignant melanoma. Invest New Drugs. 2007; 25(2):155-9.

86. Hwang TL, Lee WR, Hua SC, Fang JY. Cisplatin encapsulated in phosphatidylethanolamine liposomes enhances the in vitro cytotoxicity and in vivo intratumor drug accumulation against melanomas. J Dermatol Sci. 2007; 46(1):11-20.

87. Bedikian AY, Papadopoulos NE, Kim KB, et al. A pilot study with vincristine sulfate liposome infusion in patients with metastatic melanoma. Melanoma Res. 2008; 18(6):400-4.

88. Banciu M, Metselaar JM, Schiffelers RM, Storm G. Liposomal glucocorticoids as tumor-targeted anti-angiogenic nanomedicine in B16 melanoma-bearing mice.J Steroid Biochem Mol Biol. 2008;111(1-2):101-10.

89. Oskouian B, Saba JD. Cancer treatment strategies targeting sphingolipid metabolism. Adv Exp Med Biol. 2010; 688:185-205.

90. Davaille J, Li L, Mallat A, Lotersztajn S. Sphingosine 1-phosphate triggers both apoptotic and survival signals for human hepatic myofibroblasts. J Biol Chem. 2002; 277(40):37323-30.

91. Fonseca NA, Gomes-da-Silva LC, Moura V, et al. Simultaneous active intracellular delivery of doxorubicin and C6-ceramide shifts the additive/antagonistic drug interaction of non-encapsulated combination. J Control Release. 2014 Oct 10.

92. Heakal Y, Kester M. Nanoliposomal short-chain ceramide inhibits agonist-dependent translocation of neurotensin receptor 1 to structured membrane microdomains in breast cancer cells. Mol Cancer Res. 2009; 7(5):724-34.

93. Shabbits JA, Mayer LD. Intracellular delivery of ceramide lipids via liposomes enhances apoptosis in vitro. Biochim Biophys Acta. 2003; 1612(1):98-106.

94. Tran MA, Smith CD, Kester M, Robertson GP. Combining nanoliposomal ceramide with sorafenib synergistically inhibits melanoma and breast cancer cell survival to decrease tumor development. Clin Cancer Res. 2008;14(11):3571-81.

95. Xu HP, Li ZY, Si J. Nanocarriers in Gene Therapy: A Review. J Biomed Nanotechnol. 2014; 10(12): 3483-3507

96. Farrar GJ, Millington-Ward S, Chadderton N, et al. Gene therapies for inherited retinal disorders. Visual Neuroscience. 2014; 31(4-5):289-307.

97. Shimamura M, Nakagami H, Taniyama Y. Gene therapy for peripheral arterial disease Exper opin biolo Thera 2014; 14(8):1175-1184.

98. Tan SJ, Kiatwuthinon P, Roh YH, et al. Engineering Nanocarriers for siRNA Delivery. Small. 2011; 7(7):841-56.

99. Mansouri S, Lavigne P, Corsi K, et al. Chitosan-DNA nanoparticles as non-viral vectors in gene therapy: strategies to improve transfection efficacy. Eur J Pharm Biopharm. 2004; 57(1):1-8.

100. Fathabadi EG, Shelling AN, Al-Kassas R. Nanocarrier systems for delivery of siRNA to ovarian cancer tissues. Expert Opin Drug Deliv. 2012; 9(7):743-54.

101. Kim JK, Choi SH, Kim CO, et al. Enhancement of polyethylene glycol (PEG)-modified cationic liposome-mediated gene deliveries: effects onserum stability and transfection efficiency. J Pharm Pharmacol. 2003; 55(4):453-60.

102. Ma K, Shen H, Shen S, et al. Development of a successive targeting liposome with multi-ligand for efficient targeting gene delivery. J Gene Med. 2011; 13(5):290-301.

103. Ryuke Y, Mizuno M, Natsume A, et al.Growth inhibition of subcutaneous mouse melanoma and induction of natural killer cells by liposome-mediatedinterferon-beta gene therapy. Melanoma Res. 2003; 13(4):349-56.

104. Stopeck AT, Jones A, Hersh EM, et al. Phase II study of direct intralesional gene transfer of allovectin-7, an HLA-B7/beta2-microglobulin DNA-liposomecomplex, in patients with metastatic melanoma. Clin Cancer Res. 2001; 7(8):2285-91.

105. Mockey M, Bourseau E, Chandrashekhar V, et al. mRNA-based cancer vaccine: prevention of B16 melanoma progression and metastasis by systemic injection of MART1 mRNA histidylated lipopolyplexes. Cancer Gene Ther. 2007; 14(9):802-14.

106. Fujimura T, Nakagawa S, Ohtani T, et al. Inhibitory effect of the polyinosinic-polycytidylic acid/cationic liposome on the progression of murine B16F10melanoma. Eur J Immunol. 2006; 36(12):3371-80.

107. Okumura K, Nakase M, Inui M, et al. Bax mRNA therapy using cationic liposomes for human malignant melanoma. J Gene Med. 2008; 10(8):910-7.

108. Noble GT, Stefanick JF, Ashley JD, et al. Ligand targeted liposome design: challenges and fundamental considerations. Trends Biotechnol. 2014; 32(1):32-45.

109. Evans MS, Madhunapantula SV, Robertson GP, Drabick JJ. Current and future trials of targeted therapies in cutaneous melanoma. Adv Exp Med Biol. 2013; 779:223-55.

110. Del Vecchio S, Reynolds JC, Carrasquillo JA, et al. Local distribution and concentration of intravenously injected 131I-9.2.27 monoclonal antibody in human malignant melanoma. Cancer Res. 1989; 49(10):2783-9.

111. Shiku H, Takahashi T, Oettgen HF. Cell surface antigens of human malignant melanoma. II. Serological typing with immune adherence assays and definition of two new surface antigens. J Exp Med. 1976; 144(4):873-81.

112. Pastorino F, Brignole C, Marimpietri D, et al. Targeted liposomal c-myc antisense oligodeoxynucleotides induce apoptosis and inhibit tumor growth and metastases in human melanoma models. Clin Cancer Res. 2003; 9(12):4595-605.

113. Besić E. Physical mechanisms and methods employed in drug delivery to tumors. Acta Pharm. 2007; 57(3):249-68.

114. Campana LG, Testori A, Mozzillo N, Rossi CR. Treatment of metastatic melanoma with electrochemotherapy. J Surg Oncol. 2014; 109(4):301-7.

115. Sounni NE, Noel A. Targeting the tumor microenvironment for cancer therapy. Clin Chem. 2013; 59(1):85-93.

116. Kontopodis E, Kentepozidis N, Christophyllakis C, et al. Docetaxel, gemcitabine and bevacizumab as salvage chemotherapy for HER-2-negative metastatic breast cancer. Cancer Chemother Pharmacol. 2014 Nov 15.

117. Qin M, Lee YE, Ray A, Kopelman R. Overcoming cancer multidrug resistance by codelivery of doxorubicin and verapamil with hydrogelnanoparticles. Macromol Biosci. 2014; 14 (8):1106-15.

118. Kolishetti N, Dhar S, Valencia PM, et al. Engineering of self-assembled nanoparticle platform for precisely controlled combination drug therapy. Proc Natl Acad Sci U S A. 2010; 107(42):17939-44.

119. Kretzer IF, Maria DA, Maranhão RC. Drug targeting in combined cancer chemotherapy: tumor growth inhibition in mice by association of paclitaxel and etoposide with a cholesterol-rich nanoemulsion. Cell Oncol (Dordr). 2012; 35(6):451-60.

120. Mitrus I, Sochanik A, Cichoń T, Szala S. Combination of combretastatin A4 phosphate and doxorubicin-containing liposomes affects growth of B16-F10 tumors. Acta Biochim Pol. 2009; 56(1):161-5.

121. Shiraga E, Barichello JM, Ishida T, Kiwada H. A metronomic schedule of cyclophosphamide combined with PEGylated liposomal doxorubicin has a highly antitumor effect in an experimental pulmonary metastatic mouse model. Int J Pharm. 2008; 353(1-2):65-73.

122. Liu Y, Fang J, Kim YJ, et al. Codelivery of doxorubicin and paclitaxel by cross-linked multilamellar liposome enables synergistic antitumor activity. Mol Pharm. 2014; 11(5):1651-61.

123. Hu CM, Zhang L. Nanoparticle-based combination therapy toward overcoming drug resistance in cancer. Biochem Pharmacol. 2012; 83(8):1104-11.

124. Pritchard JR, Bruno PM, Gilbert LA, et al. Defining principles of combination drug mechanisms of action. Proc Natl Acad Sci U S A. 2013; 110(2):E170-9.

125. Cao L, Zeng Q, Xu C, et al. Enhanced antitumor response mediated by the codelivery of paclitaxel and adenoviral vector expressing IL-12. Mol Pharm. 2013; 10(5):1804-14.

126. Takeda S , Nakao A, Miyoshi K, Takagi H. Gene therapy for pancreatic cancer. Sem Surg Oncol. 1998; 15 (1): 57-61

127. Park SY, Lee W, Lee J, Kim IS. Combination gene therapy using multidrug resistance (MDR1) gene shRNA and herpes simplex virus-thymidinekinase. Cancer Lett. 2008; 261(2):205-14.

128. Han Y, Zhang Y, Li D, et al. Transferrin-modified nanostructured lipid carriers as multifunctional nanomedicine for codelivery of DNA anddoxorubicin. Int J Nanomedicine. 2014; 9: 4107-16.

129. Yin T, Wang P, Li J, et al. Tumor-penetrating codelivery of siRNA and paclitaxel with ultrasound-responsive nanobubbles hetero-assembled from polymeric micelles and liposomes. Biomaterials. 2014; 35(22):5932-43.

130. Balbino TA, Azzoni AR, de la Torre LG. Microfluidic devices for continuous production of pDNA/cationic liposome complexes for gene delivery and vaccine therapy. Colloids Surf B Biointerfaces. 201; 111: 203-10.

131. Shi S, Zhu X, Guo Q. Self-assembled mPEG-PCL-g-PEI micelles for simultaneous codelivery of chemotherapeutic drugs and DNA: synthesis and characterization in vitro. Int J Nanomedicine. 2012; 7: 1749-59.

132. Somani S, Blatchford DR, Millington O, et al. Transferrin-bearing polypropylenimine dendrimer for targeted gene delivery to the brain. J Control Release. 2014; 188:78-86.

133. Saha K, Kim ST, Yan B, et al. Surface functionality of nanoparticles determines cellular uptake mechanisms in mammalian cells. Small. 2013; 9(2):300-5.

134. Xiao Y, Jaskula-Sztul R, Javadi A, et al. Co-delivery of doxorubicin and siRNA using octreotide-conjugated gold nanorods for targeted neuroendocrine cancer therapy. Nanoscale. 2012; 4(22):7185-93.

135. Legha SS, Ring S, Bedikian A, et al. Treatment of metastatic melanoma with combined chemotherapy containing cisplatin, vinblastine and dacarbazine (CVD) and biotherapy using interleukin-2 and interferon-alpha. Ann Oncol. 1996; 7(8):827-35.

2. Oxidized Phospholipid based pH Sensitive Micelles for Delivery of Anthracyclines: *in vitro* Study in Resistant Leukemia Cells

2.1 Abstract

A self-assembled micelle drug delivery system constructed by an oxidized phospholipid for anthracycline anti-cancer drug delivery is presented. An oxidized phospholipid, 1-palmitoyl-2-azelaoyl-sn-glycero-3-phosphocholine (PazPC), was chosen to fabricate micellar formulation via both electrostatic and hydrophobic interaction for delivery of Doxorubicin (DOX) and Idarubicin (IDA). The formation of ion-pair complexes between PazPC and DOX was first investigated under different pH values, and then the drug-loaded PazPC micelles at 5:1 molar ratio of lipid/drug under pH 7.0 were prepared by solvent evaporation method. The empty and drug-loaded PazPC micelles exhibited a small particle size (~10 nm) and high encapsulation efficiency. In vitro stability and release profile indicated that micelles were stable at physiological conditions, but exhibited pH-sensitive behavior with accelerated release of DOX or IDA in acidic endosome environment. Finally, in vitro uptake and cytotoxicity were evaluated on leukemia P388 and its resistant subline P388/ADR. The drug-loaded PazPC micelles enhanced drug uptake and exhibited higher cytotoxicity in both leukemia cells in comparison to free drugs. In conclusion, we developed a novel pH sensitive oxidized phospholipid-based micellar formulation which could potentially be useful in delivering anthracycline anti-cancer drugs and provide a novel strategy for increasing the therapeutic index and overcoming multidrug resistance for leukemia treatment.

2.2 Introduction

Self-assembled micelles from amphiphilic molecules have attracted considerable interest and been comprehensively studied due to the unique advantage as a drug delivery system for anticancer drug (1-3). The benefits of micellar formulation include the small size ranging from tens of nanometers to hundred nanometers, core-shell structure which leads to increased solubility and metabolic stability of associated drugs, and passive or active targeting capability which enhances the specificity of drug activity (3). The core of micellar system serves as a micro-reservoir that associates drug molecules through a combination of hydrophobic, electrostatic interaction, hydrogen bonding and in some cases *via* chemical conjugate (1,3). Among the micellar drug delivery system, many amphiphilic polymers, including block copolymer, graft copolymer and linear dentritic polymer have been widely used to fabricate micelles to improve drug efficacy and therapeutic index. For instance, a poloxamer-based micellar formulation of Doxorubicin (DOX), SP1049C, was shown to be safe and effective in animal and human (4-5).

Among amphiphilic polymers, lipid derivative polymers are widely investigated in the literature so far. For instance, some phospholipid derivatives, e.g., PEG-DSPE and PEG-DOPE, have been demonstrated many advantages for delivery of hydrophobic drugs due to phospholipid itself represent a well-known class of biocompatible and non-cytotoxic amphiphilic biomolecules (6-7). Phospholipids are aliphatics comprised of a hydrophilic phosphate ester as the headgroup and two hydrophobic tails, as a result they typically form bilayer vesicles, *i.e.* liposome, not the micellar structure. However, some lipid derivatives can form micellar structure instead of vesicles when their headgroups are modified with hydrophilic polymers, e.g. PEG or PVP, etc (6). In addition, when one of two hydrophobical aliphatic chains at the glycerol backbone is oxidatively truncated (e.g. oxidized phospholipids), this class of phospholipid derivatives also

spontaneously forms micellar structure in water (8-9). Oxidized phospholipids (OxPLs) are metabolic products of phosphatidylcholine through tissue damages, oxidative stress or inflammatory stimulation. They are components on cell membrane and circulating lipid particles, constituting an important subclass of phospholipids and exhibiting unique physical and biological properties not found in their parent phospholipids. As endogenous phospholipid derivatives, they are widely characterized for their biological activities, including anti- and pro-inflammatory effects, apoptotic effects, and potent ligands for scavenger receptors (10, 11). However, to the best of our knowledge, only few papers discussed the physicochemical properties of the micellar aggregates of oxidized phospholipids *in vitro* so far (8, 12). Furthermore, no work has yet described the micellar system formed by these phospholipid derivatives to support drug delivery *in vitro* and *in vivo*.

Due to the unique features of their structure organization and biological activity, oxidized phospholipids could be used to construct drug delivery system. In this study, we examine the possible use of oxidized phospholipid-based micelles for delivery of anthracyclines. An oxidized phospholipid, 1-palmitoyl-2-azelaoyl-sn-glycero-3-phosphocholine (PazPC, Figure 2.1A), was chosen to show the proof-of-principle. PazPC is a truncated oxidized phosphotidylcholine with a 9-carbon azelaoyl chain at the sn-2 position, and a 16-carbon palmitoyl chain at the sn-1 position, produced from the oxidation of 1-palmitoyl-2-linoleoyl-sn-glycero-3-phosphocholine (PLPC) (12). It is predicted that the polar carboxyl group of the truncated sn-2 acyl chain reverses its orientation and reaches the lipid-water interface when micellar aggregates are spontaneously formed at neutral pH in aqueous water (12-13). We hypothesize that the negative charged carboxyl group of the azelaoyl chain at the sn-2 position could form ion-pair (Figure 2.1C) with primary amine of anthracyclines *i.e.* DOX and IDA

(Figure 2.1B) existing in the micellar solution. At the same time, the hydrophobic interaction between aromatic rings of the drug with the sn-1 chain of the lipid will further stabilize the micelles. Therefore, once the micelle is formed, the drugs will be effectively encapsulated in the core of the micelle (Figure 2.1D).

In the present study, the conditions of ion-pair complex formation and subsequent micelle preparation were optimized. Then characterization of OxPLs-based micellar delivery system and *in vitro* drug release studies under different pH value were performed. Finally, uptake and cytotoxicity of micellar drug formulation in sensitive and drug resistance leukemia cell lines were tested.

2.3 Materials and Methods

2.3.1 Materials

1-palmitoyl-2-azelaoyl-sn-glycero-3-phosphocholine (PazPC) was obtained from Avanti Polar Lipids (Alabaster, AL). Doxorubicin hydrochloride (DOX), Idarubicin hydrochloride (IDA), HEPES, Sephadex G75 and PBS were purchased from Sigma-Aldrich (St. Louis, MO). Fetal bovine serum, RPMI1640 medium and other reagents for cell culture were purchased from Mediatech (Manassas, VA). Murine leukemia cell lines, P388 and P388/ADR, were obtained from National Cancer Institute at Frederick (Frederick, MD).

2.3.2 Formation of PazPC/DOX Ion-Pair Complexes

DOX solution (3 mM) in 20 mM HEPES buffer at different pH (pH 4.5-9.0) was freshly prepared. PazPC films were formed in glass tubes under nitrogen and desiccated under vacuum. Predetermined volume of the DOX solutions were then added into the lipid films-containing tubes, and hydrated at 60°C for 30 min to obtain 1:1 molar ratio of PazPC/DOX. Scattering

intensities of the hydration mixtures were determined using Nicomp 380 Submicron Particle Sizer (PSS, Santa Barbara, CA). The mixtures were then centrifuged for 10 min at 10,000 rpm. The concentrations of DOX in the supernatant were measured fluorometrically at 480 nm (excitation) and 590 nm (emission). The percentage of the drug ion-paired with PazPC (mole/mole) was calculated as follows (14):

$$\%\ \text{of the drug ion\_paired with PazPC} = 100\% - (\%\text{drug in supernatant}) \quad (1)$$

In order to eliminate an influence of the solubility of DOX solubility, control experiments used DOX solutions without PazPC (pH 4.5-9.0) and the % precipitates formed were subtracted to obtain the net % of DOX ion-paired with PazPC.

2.3.3 Preparation of PazPC/DOX or IDA Micelles

100 µl PazPC (10mg/ml) in chloroform was pipetted into a glass tube, and the solvent was removed under a stream of nitrogen, and the lipid films subsequently maintained under vacuum condition for at least 2 hours. The dry lipid films were hydrated at 60°C for 30 min in 1 ml DOX or IDA (0.3 mM) in 20 mM HEPES buffer (pH 7.0) to yield 5:1 molar ratio of PazPC/drug, and the drug-containing PazPC micelle solution was further placed in a bath-type sonicator for 10 min.

2.3.4 Characterization of PazPC/DOX or IDA Micelles

2.3.4.1 Encapsulation Efficiency and Drug Loading Content

The ratios of DOX or IDA encapsulated in PazPC micelle were determined using column separation method. Sephadex G75 was employed to separate the PazPC/DOX or PazPC/IDA micelle solution. 0.5 ml micelle sample was pipetted into the column, and was eluted using 20

mM HEPES buffer (pH 7.0) as mobile phase, and then fractions were collected. The concentrations of DOX in each collection tube were measured fluorometrically at 480 nm (excitation) and 590 nm (emission) using microplate reader (Fluostar, BMG labtechnologies, Germany). Elution profiles of DOX or IDA were then plotted versus elution volumes. The first peak reflects the micellar drug, and the second peak reflects the free drug. The encapsulation efficiency (EE %) and drug loading content (DL %) of PazPC micelle were calculated as follows (15) :

$$\text{Encapsulation efficiency}\,(\%) = \frac{\text{amount of micellar drug}}{\text{total amount of drug}} \times 100\% \quad (2)$$

$$\text{Drug loading}\,(\%) = \frac{\text{amount of micellar drug}}{\text{total amount of lipid} + \text{amount of micellar drug}} \times 100\ \% \quad (3)$$

2.3.4.2 Particle Size and Zeta Potential Characterization

Particle size and zeta potential of PazPC micelles were determined based on dynamic light scattering (DLS) and Electrophoretic light scattering (ELS), respectively, using a Nicomp Model 380/ZLS particle sizer (PSS, Santa Barbara, CA).

2.3.4.3 Stability in Acidic pH, PBS and Serum

The stability of drug-loaded PazPC micelles was evaluated under different conditions. The PazPC/DOX and PazPC/IDA micelle at pH 7.0 were prepared according to the above method. In order to evaluate the micelle stability at a lower pH condition, the pH of the sample was adjusted to 6.0 using 0.6 M HCl , incubated at 37°C for 30 min, applied to Sephadex G75 column, and eluted with 20 mM HEPES buffer at pH 6.0. In order to evaluate its stability at a physiological ionic strength or in normal cell culture medium, aliquots of 25×PBS or fetal bovine

serum (FBS) were added into the micelle solution to yield a final concentration of 1×PBS or 10% serum, respectively. Two samples were incubated at 37°C for 30 min, applied to a Sephadex G75 column, and eluted with 1× PBS-containing 20 mM HEPES buffer or 10% FBS-containing 20 mM HEPES buffer, respectively. Elution profiles of DOX or IDA were plotted versus elution volumes according to the fluorescence (λex=480 and λem=590) of DOX or IDA fraction in collection tubes.

2.3.4.4 *In vitro* Release Property

DOX or IDA release from PazPC micelles was studied in different pH buffers. 1 ml of PazPC/DOX or PazPC/IDA or free drug solutions (0.3mM DOX or IDA is in each sample) was placed in dialysis membrane (MWCO 15K, Spectra/por membrane tubing, Spectrum Labs, CA) and immersed in tubes containing 40 ml of release buffers with different pH (1×PBS, pH 7.4 or pH 6.5; 0.1 M citrate buffer, pH 6.0). All tubes were incubated at 37°C under mild agitation. 0.5ml of the dialyzate sample was collected at different time intervals and the same volume of the fresh release medium was replenished immediately. The concentration of DOX or IDA in dialyzate was analyzed fluorometrically at 480 nm (excitation) and 590 nm (emission), and cumulative release profiles were then plotted verse release times.

2.3.4.5 Uptake of DOX and IDA Micelle by Leukemia Cells

The cellular uptake of PazPC micellar drug or free drug was first visualized by a fluorescent microscope (EVOS fl Microscope, AMG, USA). Briefly, P388 and P388/ADR cells were seed into 12-well plates at a cell density of 10^6cells/ml and PazPC micellar drug or free drug (DOX: 10 μM, IDA: 1 μM) was then added into 12-well plate to yield a proper drug concentration. After 2 hours incubation, the cells were fixed with fixation buffer (4%

paraformaldehyde, Biolegend) for 20 min at room temperature. Cellular uptake of micellar drug or free drug was finally visualized under the light channel of RFP.

The extent of cellular uptake of PazPC micellar drug or free drug was further quantitatively determined using flow cytometry (Accuri C6 Cytometer, Ann Arbor, MI) by measurement of the cell associated fluorescence (16-18). P388 and P388/ADR cells were seeded on 12-well plates at a cell density of 10^6cells/ml. The appropriate concentration of each formulation or free drug (DOX: 10 μM, IDA: 1 μM) was given to the cells and incubated at 37°C for different time. The fluorescence was then measured with flow cytometry by collecting 20000 events for each sample at predetermined time. Each experiment was performed in triplicate.

2.3.4.6 Cytotoxicity on Leukemia Cells

The MTT (3-[4, 5-dimethylthiazol-2-yl]-2, 5-diphenyl tetrazolium bromide) assay was utilized to assess cytotoxicity of the PazPC micelle. Cells were seeded in 96-well plates at 5,000 cells in 100μl RPMI1640 medium with 10% FBS/well. Serial dilutions of DOX or IDA formulations were added to the plate with 10% FBS at 37°C in 5% CO_2 for 48 hr. 10μl MTT stock solution (5 mg/mL in PBS; pH 7.4) was then added into the wells and the plates were incubated at 37°C for another 4 hours. Cell suspensions were spun down for 10 min at 1,000 rpm. The medium was removed and 100μl DMSO was then added to each well to solubilize the dye. The absorbance was measured using microplate reader (Fluostar, BMG labtechnologies, Germany) at 540 nm, and the concentration of drug that inhibited cell survival by 50% (IC_{50}) was determined from cell survival plots using "DoseResp" function of OriginPro 8.0.

2.3.4.7 Statistical Analysis

The data were expressed as mean ± S.D. of the mean. Statistical significance in uptake and cytotoxicity were determined using one-way ANOVA followed by a Student's *t* test for multiple comparison tests. P value of <0.05 is considered as statistically significant.

2.4 Results

In order to obtain an optimal pH for formation of ion-pair complex between oxidized phospholipid and DOX, the changes of the scattering intensity and the resultant precipitates of mixtures of PazPC and DOX (molar ratio=1:1) as a function of pH were first investigated. As shown in Figure 2.2A, the scattering intensities reached maximum at pH 7.0 and pH 7.5, and the intensity values decreased when pH was less than 7.0 or more than 7.5, as indicated by the bell-shaped curve. The similar results are shown by the experiment of centrifugation of the mixtures of PazPC and DOX. The percentage of the drug ion-paired with PazPC was greater than 60% at pH 7.0 and pH 7.5, but it dramatically decreased when pH was less than 7.0 or more than 7.5. Therefore, pH 7.0 - 7.5 is the proper pH range to form the PazPC/DOX ion-pair complexes. In order to optimize a proper ratio of lipid to drug for preparation of drug-loaded micelle with reasonable particle size and encapsulation efficiency, DOX concentration was kept constant (0.3mM) and different concentration of PazPC was used to prepare PazPC/DOX micelle. The changes of particle size, scattering intensity, encapsulation efficiency and drug loading content of PazPC/DOX micelles as a function of PazPC/DOX molar ratio is shown in Figure 2.2B and 2.2C. When the ratio of PazPC/DOX was over 2:1, the intensity of PazPC/DOX mixture dramatically decreased to around 25 KHz compared to 170 KHz (sample with 1:1 ratio) or 260 KHz (samples with 1:2 or 1:10 ratio). The particle size also showed similar changes when the ratio was over 2:1 (Figure 2.2B). This indicated that the DOX-loaded PazPC micelle was formed through ion-pair interaction between PazPC and DOX when the ratio was more than 2:1. Figure

2.2C also shows that encapsulation efficiency (%) increased and drug loading (%) decreased with increasing of the ratio, respectively. When the ratio was over 5:1, the encapsulation efficiency (%) reached above 60%, and drug loading (%) was around 10%. Figure 2.2D is the representative size distribution analysis of the PazPC/DOX micelle with the molar ratio of 5:1 by DLS. Blank PazPC micelles and PazPC/IDA micelles were demonstrated similar size distribution by DLS (data not shown). This molar ratio of 5:1 (PazPC: DOX or IDA) was then chosen in subsequent experiments.

The characterization of resultant PazPC/DOX and PazPC/IDA micelle prepared at 5:1 molar ratio of lipid/drug is summarized in Table 2.1. The particle size of blank PazPC micelle, PazPC/DOX micelle and PazPC/IDA micelle, measured by DLS method, was in the range of 8 - 10 nm. Table 2.1 also shows the PazPC/IDA micelle had comparable zeta potential and higher encapsulation efficiency (%) compared to PazPC/DOX micelle. More IDA was entrapped in the core of PazPC micelle than DOX presumably due to higher hydrophobicity of IDA, and that resulted in less carboxyl group of PazPC on the surface of the micelle and therefore, less zeta potential of PazPC/IDA micelle. This data also indicated that both electrostatic and hydrophobic interactions were involved in the driven force of micelle formation.

Next, the stability of PazPC/drug micelle was studied using G75 size exclusion chromatography. Figure 2.3 shows the stability of drug-loaded PazPC micelle under different conditions: acidic pH, neutral physiological salt concentration and 10% serum. As shown in Figure 2.3A and B, DOX or IDA was significantly dissociated from the PazPC micelle when the micelles were incubated at pH 6.0 for 30 min, resulting in the area of the first peak dramatically decreased and the second peak increased. When the micelles were incubated in 1×PBS buffer for 30 min, the second peak of PazPC/DOX and PazPC/IDA micelle increased just slightly (Figure

2.3C& D), and encapsulation efficiency of the micelle were maintained at over 60% (for DOX) or 80% (for IDA) (Table 2.2). When the micelles were incubated in 10% fetal bovine serum for 30 min, the changes of elution profiles of the micelle were similar to that in 1×PBS buffer (Figure 2.3E&F).

The pH-dependent release profiles of DOX or IDA from the drug-loaded PazPC micelles are shown in Figure 2.4. A control experiment with free DOX and IDA confirmed that the high MWCO (15K) of dialysis membrane tubing couldn't restrict diffusion of the released drugs, and they were able to reach 100% release after 3.5 hours. However, the release of DOX or IDA from the micelle at different pH couldn't reach a plateau until at least 10 hours. The total released drug from the micelle was significantly different under different pH conditions. The release rate of drug from PazPC micelle increased with decreasing of the pH of release medium. Interestingly, at any given pH, the release of IDA from the micelle displayed slightly slower rate than DOX before the plateau was reached.

The cellular uptake of DOX and IDA with micellar formulations containing different concentration of DOX and IDA was examined in sensitive p388 and resistant p388/ADR leukemia cell lines with fluorescence microscope. After period of 2 h incubation, the enhanced uptake of PazPC/DOX micelle was observed in resistant leukemia cell line p388/ADR compared to free DOX. As for PazPC/IDA micelle, the enhanced uptake was also observed in resistance leukemia cell line compared to free IDA (Figure 2.5, *A-D*). The uptake of DOX or IDA by leukemia cells was then quantitatively investigated using a flow cytometry by measurement of cell-associated fluorescence intensity (16). Figure 2.5*E*&*F* shows that the cellular uptake of DOX and IDA increased significantly in the micelle formulation compared to free drugs in p388/ADR resistant cells after a period of 2 hr incubation. Figure 2.5*G* &*H* present the 4h time

courses of DOX and IDA uptake by leukemia cells treated with DOX (10 μM) or IDA (1.0 μM) micellar formulations or with free drugs. Cellular DOX or IDA levels in both cells gradually increased with different increment rate during 4-h treatment. In the case of DOX uptake (Figure 5G), in sensitive P388 cells treated with free drug or micellar drug, there is no difference of DOX uptake, but in resistant P388/ADR cells, the treatment of micellar DOX increased DOX uptake compared to free DOX treatment ($p<0.01$) after 1h treatment. When the cells were treated with free IDA or PazPC/IDA micelle, micellar formulation induced higher IDA uptake in both sensitive and resistant cells than free IDA. However, in sensitive cells, the p values are less than 0.05 for all the time points after 2h treatment, whereas in resistant P388/ADR cells, the p values are less than 0.01 for all the time points after 0.5h treatment (Figure 5H). In order to determine whether the enhancement of cellular uptake was simply resulted from the effects of lipid, the leukemia cells were treated with blank PazPC micelle and free drug by simple mixing or sequentially. When both cell lines were first incubated with blank micelles for 2h, then washed, and treated again with free drug for another 2h, the uptake of DOX or IDA didn't increase compared to that of free drugs. Furthermore, simple mixing blank micelles with free drug together for 2h only slightly increased the drug uptake in sensitive cell lines. In summary, the micelle drug formulations induced higher cellular drug uptake than free drugs or simple mixture of drugs and empty micelles in both resistant and sensitive leukemia cells.

In vitro cytotoxicity of free DOX, IDA PazPC/DOX, PazPC/IDA micelles, and blank PazPC micelle were conducted in the sensitive P388 and resistant P388/ADR cells. The IC_{50} values are listed in Table 3, and cell viability of both leukemia cells were shown in Figure 6. PazPC/DOX micelle and PazPC/IDA micelle exhibited significantly higher cytotoxicity ($p < 0.01$) in both cells compared to free drug, respectively. In the case of resistant P388/ADR cell,

the IC_{50} values of PazPC/DOX micelle were 14-fold lower than that of free DOX, and PazPC/IDA micelle were 8-fold lower than free IDA. In contrast, the IC_{50} values showed 8-fold lower for DOX micelle and 5-fold lower for IDA micelle in the sensitive P388 cells. Therefore, the resistant P388/ADR cell is more susceptive to the PazPC micellar drugs than their sensitive counterparts. More important, the cytotoxicity of PazPC micellar drug in resistant cells was increased to the point where the sensitive cells responded to free drug (Figure 2.6), resulting in the comparable IC_{50} values of the same order of magnitude (166 nM vs 221 nM for DOX, and 45 nM vs 59 nM for IDA, Table 2.3). Table 2.3 also shows that the blank PazPC micelle had very high IC_{50} values in sensitive P388 cells (93 μM) and resistant P388/ADR cells (136 μM), and it showed no cytotoxicity on both cells with the equivalent concentration of drug-loaded PazPC micelle (Figure 2.6).

2.5 Discussion

The CMC value of PazPC was about 18.7-23.1 μM (8, 12), which is slightly higher than the established lipid micelle drug delivery system, such as DSPE-PEG2000 (CMC=11 μM) (6). Although we did not measure the CMC of drug loaded micelles, once PazPC/drug ion-pair complexes are formed, the CMC of the ion-pair complexes is predicted to decrease to the level of natural phospholipids. The previous report indicated that both hydrophobic and electrostatic interactions are involved in the interaction between DOX and PazPC. When forming the ion-pair complexes, the anionic charge of carboxylic group of azelaoyl chain at the sn-2 position of PazPC can be shielded by cationic charge of drug, and accordingly, the hydrophobic interaction between the drug and sn-1 chain will force the sn-2 short chain to turn back and parallelize with sn-1 chain. The both hydrophobic and ion-pair interactions in lipid/drug complex make the complex a structure mimic of intact phosphotidylcholine, e.g. DPPC (dipalmitoylPhsophatidyl

choline). Natural phospholipids are reported to have very low CMC values in the range of 0.01 to 10 nM. For example, the CMC of DPPC in water is 0.5 nM (19), so it has tendency to form the bilayer structure of liposomes. In Figure 2.2B, the 1:1 molar ratio of PazPC to DOX actually formed around 400 nm size particles, which is the range of size of liposome formed by nature phosphatidylcholine. In our system, however, the drug-loaded PazPC micellar system was prepared at the 5:1 molar ratio of PazPC/drug, containing excessive PazPC in comparison to the ion-pair complexes of PazPC/drug. Therefore, the resultant micellar system may be considered as mixed binary micelle system consisting of PazPC/drug ion-pair complexes and pure PazPC itself. According to the report on CMC prediction of mixed binary surfactants in aqueous solution, the CMC of mixed binary surfactant can be calculated as follow equation (20):

$$\frac{1}{CMC_{mix}} = \frac{\alpha}{\mathrm{CMC_A}} + \frac{1-\alpha}{\mathrm{CMC_B}} \qquad (4)$$

Where CMC_{mix}, CMC_A and CMC_B represent the CMC of the mixed surfactants, pure surfactant A, and pure surfactant B, respectively. α is the mole fraction of surfactant A in a binary system. In our study, the EE% of DOX is around 62%, representing α is around 0.124 at 5:1 molar ratio of PazPC/drug. Due to similarity of the structure between ion-pair complexes and DPPC, the CMC_A, CMC of ion-pair complexes is considered as the same as that of DPPC, 0.5 nM. The CMC_B, CMC of PazPC is around 20 µM. Therefore, the CMC of the DOX-loaded PazPC micellar system prepared in this study is roughly around 4.0 nM based on this equation.

In order to maintain its stability, the ion-pair complexes must be effectively formed between PazPC and drug. If destroying the conditions of formation of the complexes, the micelle cannot be stable and drug will be dissociated from the micelle. This is confirmed by the stability data at pH 6.0, from which only about 5% (DOX) and 14% (IDA) drug associated in the micelle

were observed compared to 62% (DOX) and 87% (IDA) at pH 7.0. pH-sensitive drug release from the nanoparticle system is believed to be advantageous for tumor targeting and endolysosomal compartments escaping due to a lower pH in the interstitial space of solid tumors and intracellular lysosome and endosomes compartments (1,21) . Due to higher hydrophobicity of IDA, the IDA-loaded PazPC micelles have higher EE%, resulting in greater number of IDA molecules entrapped into the core of the micelle and lower CMC of the binary system. As a result, IDA-loaded PazPC micelle remains relatively high stability against dilution.

Our data indicates that when the cells were pretreated with PazPC first, and then treated with free drug, drug uptake didn't increase. Furthermore, no or only slightly enhancement of cellular uptake was achieved by simply mixing the drugs and PazPC in the medium for treatment of cells. Probably, the lower enhancement of uptake induced by the simple mixture of drug and PazPC is resulted from the spontaneous formation of ion-pair complexes and micelles between PazPC and drug in cell culture medium due to its neutral pH (pH 7.0 - 7.5). This phenomenon of lower enhancement induced by mixture of drug and PazPC was further confirmed by the MTT assay on P388 and P388/ADR cells. The IC_{50} of simple mixture of free drug and PazPC on both resistant P388/ADR and sensitive P388 cells is the same order of magnitude of that of free DOX or IDA, respectively. These observations suggest that in order to achieve enhanced DOX or IDA uptake the drugs must be entrapped inside of the PazPC micelles to be recognized and up-taken by target cells. It is reported that some oxidized phospholipids, such as PazPC, account for almost two-third of oxidized phospholipid in oxidized LDL (OxLDL) (22) , and some receptors, such as scavenger receptor, toll-like receptor, expressed on macrophages were reported to recognize free OxPLs present in OxLDL and mediates the uptake of OxLDL (10,11) . Considering that murine leukemia P388 is a neoplastic cell of macrophage lineage (23, 24), it is

highly possible that the PazPC-based micellar system may exert its advantage on drug uptake and cytotoxicity on these cell lines through scavenger receptor. Interestingly, the micelle/drug formulation did not enhance the uptake of drugs in normal bone marrow cells, suggesting specificity of this system for leukemia treatment. Recent report also demonstrated negatively charged liposome mediated selective accumulation of cytotoxic agents within leukemic cells residing in the bone marrow through scavenger receptor (25). Importantly, increased expression of scavenger receptors have been reported in tumor cells of leukemia patients (26-28) and in leukemia cells (29).

Furthermore, the resistant P388/ADR cell shows more susceptive to drug-loaded PazPC micelle than sensitive P388 cell with regard to both uptake and cytotoxicity. These differences between P388 and P388/ADR are probably due to different pattern of uptake, intracellular retention and distribution, as well as subsequently biological effects among free drug, PazPC micelle, and the ion-pair complexes of PazPC and drug. So far, it is not clear how the PazPC and its micelle enter the P388 and p388/ADR leukemia to induce enhanced uptake and cytotoxicity. However, it should be mentioned that oxidized phospholipids are a type of endogenous substances, exhibiting a variety of biological activities (11). It was reported that PazPC, can associate with mitochondria, resulting in cytochrome *c* and apoptosis-inducing factor escaped from mitochondria to the cytoplasm and nucleus, respectively (22, 30). Mitochondria damage can not only initiate apoptosis cascade, but depress the production of ATP. The former effect can probably kill the tumor cell synergistically with anti-tumor drug, and the latter can subsequently affect the function of ATP-dependent MDR-related protein, such as PgP, resulting in increasing intracellular drug. It was also reported that some OxPLs, e.g. OxPAPC, can increase intracellular levels of reactive oxygen species (ROS) (11), and cancer cells would be more vulnerable to

further oxidative stress induced by exogenous ROS-generating agents (31). The increased ROS level in P388 and P388/ADR cells by PazPC was observed in our lab (data not shown). Probably, this increased ROS induced by PazPc in leukemia could be another mechanism to kill cancer cell synergistically with the drug. The specific mechanisms that induces enhanced uptake and cytotoxicity of DOX and IDA by PazPC micellar system in leukemia P388 and P388/ADR is under investigation in our lab.

2.6 Conclusion

In conclusion, we designed and developed a novel micellar formulation, constructed by a single oxidized phospholipid PazPC for delivery of anthracycline anticancer drugs, DOX and IDA. The ion-pair complexes between PazPC and DOX were effectively formed and subsequently the drug-loaded PazPC micelles were prepared at 5:1 molar ratio of lipid to drug and with high encapsulation efficiency (62% for DOX, 87% for IDA) and small particle size (7-8 nm), as well as good stability at physiological condition. Meanwhile, the drug-loaded PazPC micelles were sensitive to the pH change with accelerated release of DOX or IDA in acidic environment. Importantly, they significantly enhanced drug uptake and exhibited higher cytotoxicity effect on both sensitive and resistant leukemia cells in comparison to free drugs. Therefore, oxidized phospholipid-based micelle system could be a promising carrier that may improve the therapeutic outcomes of leukemia.

2.7 Acknowledgements

This study was supported by the Department of Drug Discovery and Development, Harrison School of Pharmacy, Auburn University.

2.8 References

1. Kim JO, Kabanov AV, Bronich TK. Polymer micelles with cross-linked polyanion core for delivery of a cationic drug doxorubicin. Journal of Controlled Release 2009**;** 138:197-204.
2. Liu JY, Pang Y, Huang W, Zhu XY, Zhou YF, Yan DY. Self-Assembly of phospholipid-analogous hyperbranched polymers nanomicelles for drug delivery. Biomaterials 2010**;** 31:1334-41.
3. Tyrrell ZL, Shen YQ, Radosz M. Fabrication of micellar nanoparticles for drug delivery through the self-assembly of block copolymers. Prog Polym Sci 2010**;** 35:1128-43.
4. Alakhov V, Klinski E, Li SM, Pietrzynski G, Venne A, Batrakova E, et al. Block copolymer-based formulation of doxorubicin. From cell screen to clinical trials. Colloid Surface B 1999**;** 16:113-34.
5. Danson S, Ferry D, Alakhov V, Margison J, Kerr D, Jowle D, et al. Phase I dose escalation and pharmacokinetic study of pluronic polymer-bound doxorubicin (SP 1049C) in patients with advanced cancer. Brit J Cancer 2004**;** 90:2085-91.
6. Lukyanov AN, Torchilin VP. Micelles from lipid derivatives of water-soluble polymers as delivery systems for poorly soluble drugs. Adv Drug Deliver Rev 2004**;** 56:1273-89.
7. Koo OM, Rubinstein I, Onyuksel H. Camptothecin in sterically stabilized phospholipid micelles: a novel nanomedicine. Nanomedicine 2005**;** 1:77-84.
8. Mattila JP, Sabatini K, Kinnunen PKJ. Oxidized phospholipids as potential novel drug targets. Biophysical Journal 2007**;** 93:3105-12.

9. Vitiello G, Ciccarelli D, Ortona O, D'Errico G. Microstructural characterization of lysophosphatidylcholine micellar aggregates: The structural basis for their use as biomembrane mimics. Journal of Colloid and Interface Science 2009**;** 336:827-33.

10. Fruhwirth GO, Loidl A, Hermetter A. Oxidized phospholipids: from molecular properties to disease. Biochim Biophys Acta 2007**;** 1772:718-36.

11. Bochkov VN, Oskolkova OV, Birukov KG, Levonen AL, Binder CJ, Stockl J. Generation and biological activities of oxidized phospholipids. Antioxid Redox Signal 2010**;** 12:1009-59.

12. Pande AH, Kar S, Tripathy RK. Oxidatively modified fatty acyl chain determines physicochemical properties of aggregates of oxidized phospholipids. Biochim Biophys Acta 2010**;** 1798:442-52.

13. Khandelia H, Mouritsen OG. Lipid Gymnastics: Evidence of Complete Acyl Chain Reversal in Oxidized Phospholipids from Molecular Simulations. Biophysical Journal 2009**;** 96:2734-43.

14. Ma P, Dong X, Swadley CL, Gupte A, Leggas M, Ledebur HC, et al. Development of idarubicin and doxorubicin solid lipid nanoparticles to overcome Pgp-mediated multiple drug resistance in leukemia. J Biomed Nanotechnol 2009**;** 5:151-61.

15. Wang YZ, Yu L, Han LM, Sha XY, Fang XL. Difunctional Pluronic copolymer micelles for paclitaxel delivery: Synergistic effect of folate-mediated targeting and Pluronic-mediated overcoming multidrug resistance in tumor cell lines. Int J Pharmaceut 2007**;** 337:63-73.

16. Chen YC, Bathula SR, Li J, Huang L. Multifunctional Nanoparticles Delivering Small Interfering RNA and Doxorubicin Overcome Drug Resistance in Cancer. Journal of Biological Chemistry 2010**;** 285:22639-50.

17. Szaraz I, Forsling W. PVP and azelaic acid adsorption on gamma-alumina studied by FT-IR spectroscopy. Vib Spectrosc 2002**;** 29:15-20.

18. Tian Y, Bromberg L, Lin SN, Alan Hatton T, Tam KC. Complexation and release of doxorubicin from its complexes with pluronic P85-b-poly(acrylic acid) block copolymers. Journal of Controlled Release 2007**;** 121:137-45.

19. Tieleman DP, Marrink SJ. Lipids out of equilibrium: Energetics of desorption and pore mediated flip-flop. Journal of the American Chemical Society 2006**;** 128:12462-7.

20. Cheng JS, Chen YP. Correlation of the critical micelle concentration for aqueous solutions of nonionic surfactants. Fluid Phase Equilibr 2005**;** 232:37-43.

21. Gao WW, Chan JM, Farokhzad OC. pH-Responsive Nanoparticles for Drug Delivery. Molecular Pharmaceutics 2010**;** 7:1913-20.

22. Chen R, Yang L, McIntyre TM. Cytotoxic phospholipid oxidation products. Cell death from mitochondrial damage and the intrinsic caspase cascade. J Biol Chem 2007**;** 282:24842-50.

23. Bauer SR, Holmes KL, Morse HC, Potter M. Clonal Relationship of the Lymphoblastic Cell-Line P388 to the Macrophage Cell-Line P388d1 as Evidence by Immunoglobulin Gene Rearrangements and Expression of Cell-Surface Antigens. Journal of Immunology 1986**;** 136:4695-9.

24. Lechleitner M, Auer B, Zilian U, Hoppichler F, Schirmer M, Foger B, et al. The Immunosuppressive Substance 2-Chloro-2-Deoxyadenosine Modulates Lipoprotein Metabolism in a Murine Macrophage Cell-Line (P388 Cells). Lipids 1994**;** 29:627-33.

25. Lim WS, Tardi PG, Dos Santos N, Xie XW, Fan MN, Liboiron BD, et al. Leukemia-selective uptake and cytotoxicity of CPX-351, a synergistic fixed-ratio cytarabine:daunorubicin formulation, in bone marrow xenografts. Leukemia Res 2010**;** 34:1214-23.

26. Belov L, de la Vega O, dos Remedios CG, Mulligan SP, Christopherson RI. Immunophenotyping of leukemias using a cluster of differentiation antibody microarray. Cancer Research 2001**;** 61:4483-9.

27. Xu Y, McKenna RW, Wilson KS, Karandikar NJ, Schultz RA, Kroft SH. Immunophenotypic identification of acute myeloid leukemia with monocytic differentiation. Leukemia 2006**;** 20:1321-4.

28. Banker DE, Mayer SJ, Li HY, Willman CL, Appelbaum FR, Zager RA. Cholesterol synthesis and import contribute to protective cholesterol increments in acute myeloid leukemia cells. Blood 2004**;** 104:1816-24.

29. Scherf U, Ross DT, Waltham M, Smith LH, Lee JK, Tanabe L, et al. A gene expression database for the molecular pharmacology of cancer. Nat Genet 2000**;** 24:236-44.

30. Chen R, Feldstein AE, McIntyre TM. Suppression of mitochondrial function by oxidatively truncated phospholipids is reversible, aided by bid, and suppressed by Bcl-XL. J Biol Chem 2009**;** 284:26297-308.

31. Trachootham D, Alexandre J, Huang P. Targeting cancer cells by ROS-mediated mechanisms: a radical therapeutic approach? Nat Rev Drug Discov 2009**;** 8:579-91.

Table 2.1 Characterization of PazPC/DOX micelle and PazPc/IDA micelle

(PazPc/drug=5:1, molar ratio)

	Particle Size (nm)	**Zeta Potential (mV)**	**Encapsulation Efficiency (%)**	**Drug Loading (%)**
Blank PazPC micelle	7.7 ± 0.9	-39.2 ± 5.3	-	-
PazPC/DOX mcielle	8.5 ± 1.0	-27.8 ± 2.5	62.5	10.4
PazPC/IDA micelle	8.9 ± 0.9	-24.3 ± 3.7	87.1	14.8

Table 2.2 Encapsulation efficiency (EE %) of PazPC/DOX and PazPC/IDA micelle under different conditions

	pH=7.0			pH=6.0
	**	1×PBS	10% serum	
PazPC/DOX micelle*	61.87	60.96	58.24	4.83
PazPC/IDA micelle*	86.63	84.65	81.89	14.39

Note: * PazPC/drug=5:1, molar ratio, and [drug] = 0.3mM;
** Normal drug-loaded PazPC micelle, without 1×PBS or 10% serum.

Table 2.3 IC_{50} values (nM) of free DOX, IDA and their PazPC micelles (PazPC/drug=5:1, molar ratio) on leukemia cells (48 hours)

	P388	**P388/ADR**
Free DOX	221 ± 63	2,425 ± 290
PazPC/DOX	26.3 ± 3.0*	166 ± 49.8*
Free IDA	59.9 ± 15.6	361 ± 5.1
PazPC/IDA	10.9 ± 2.8*	45.1 ± 10.0*
Blank PazPC (μM**)	93.3 ± 2.55	137 ± 1.29

Note: *P < 0.01, as compared with free drug

**the unit of IC_{50} value for the Blank PazPC micelle is μM

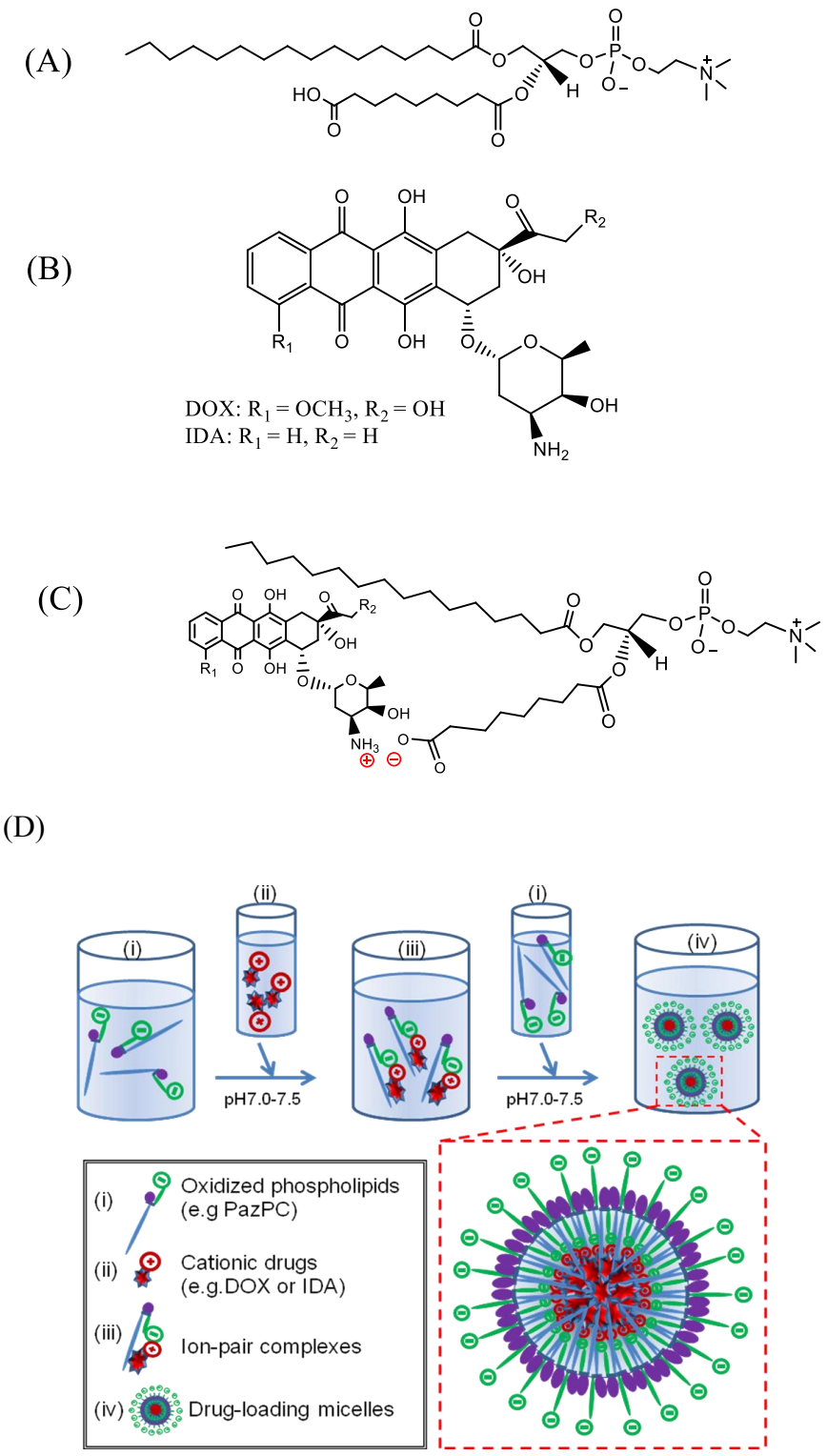

Figure 2.1 The structure of oxidized lipid, PazPC (A) and cationic drugs, doxorubicin (DOX) and idarubicin (IDA) (B), ion-pair complexes between PazPC and DOX or IDA (C) and self-assembly of drug loaded micelle (D).

(A)

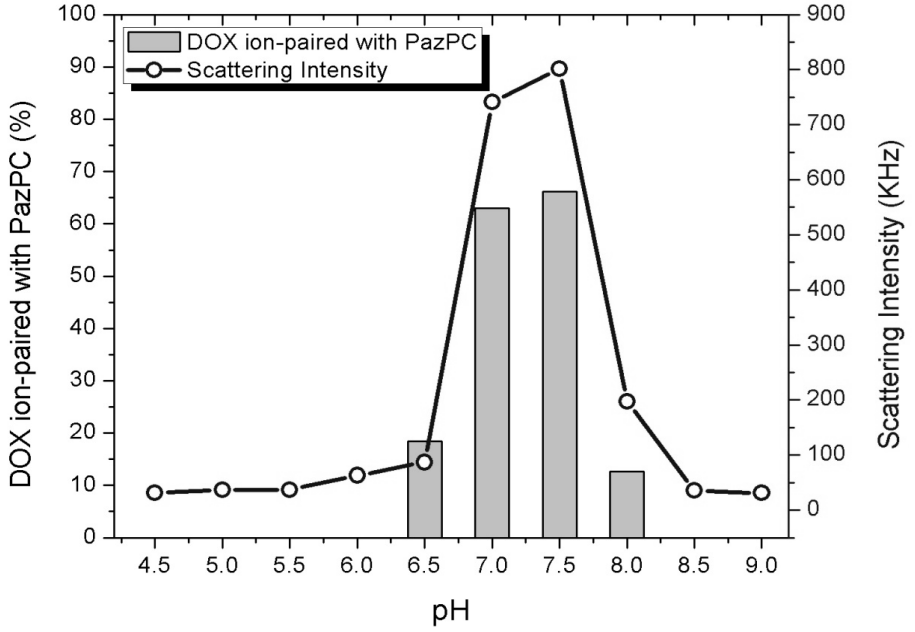
DOX ion-paired with PazPC
Scattering Intensity
DOX ion-paired with PazPC (%)
Scattering Intensity (KHz)
pH

(B)

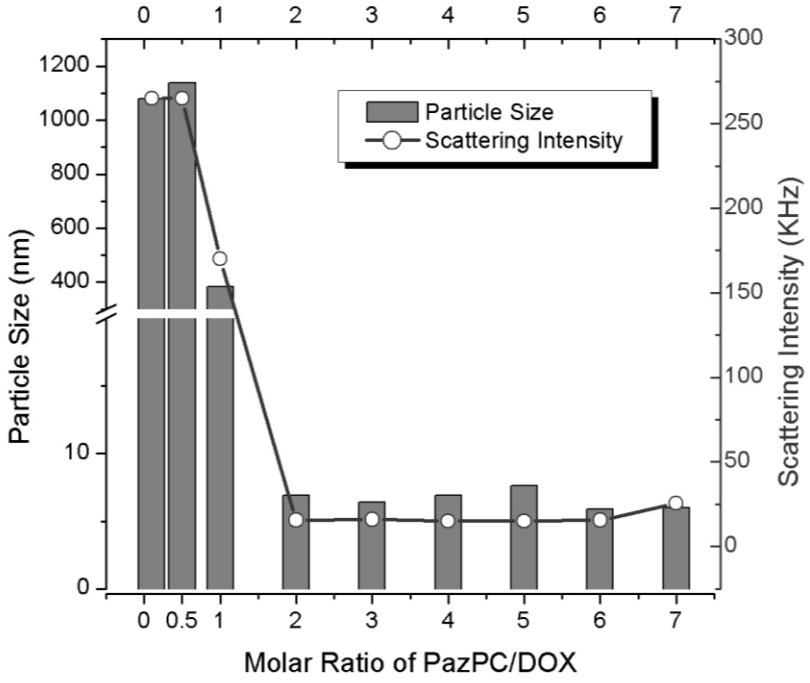
Particle Size
Scattering Intensity
Particle Size (nm)
Scattering Intensity (KHz)
Molar Ratio of PazPC/DOX

(C)

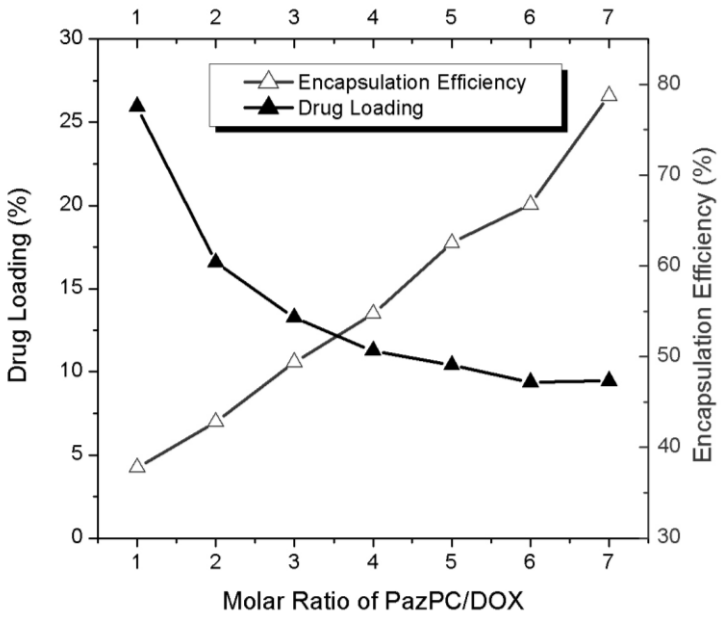

(D)

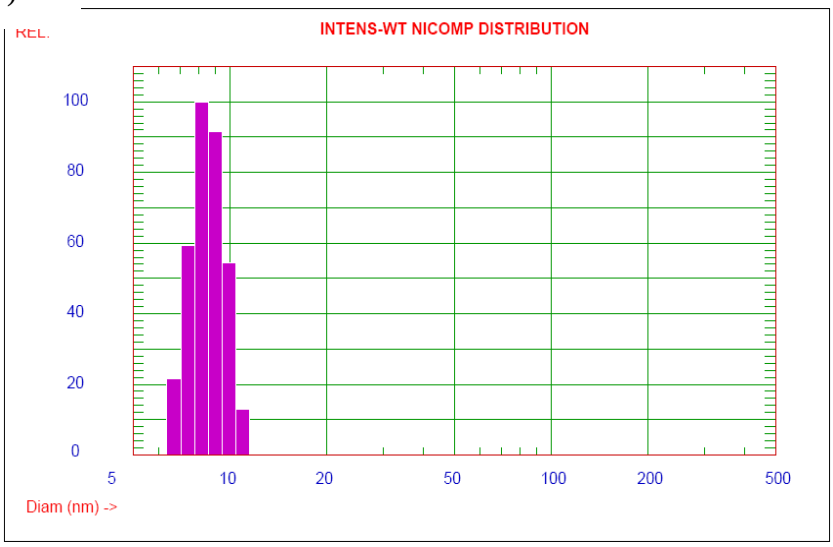

Figure 2.2 Formation and characterization of PazPC/DOX ion-pair complex and micelles. (A) The effect of pH on the formation of PazPC/DOX ion-pair complexes. The molar ratios were 1:1. (B) The effect of PazPC/DOX molar ratio on particle size of DOX-loaded PazPC micelle. (C) The effect of PazPC/DOX molar ratio on encapsulation efficiency and drug loading content of DOX-loaded PazPC micelle. (D) Representative Nicomp distribution analysis (intensity-weighted) of the PazPC/DOX micelle (8.5±1.0 nm) by DSL. All measurements were done in triplicate.

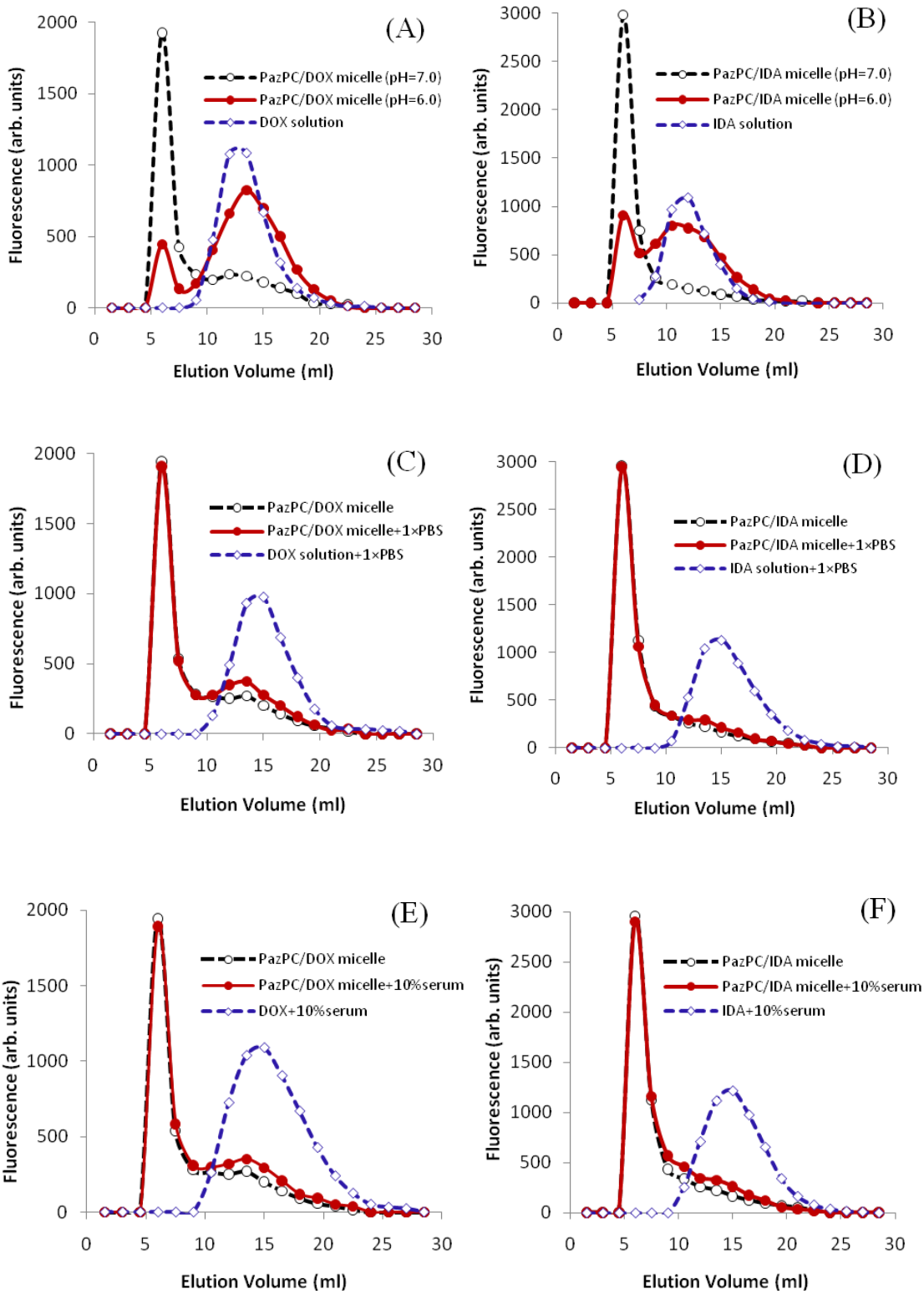

Figure 2.3 *In vitro* stability of PazPC/DOX and PazPC/IDA micelle (PazPC/drug=5:1, molar ratio) under different conditions: acidic pH (A-B), 1×PBS (C-D) and 10% serum (E-F).

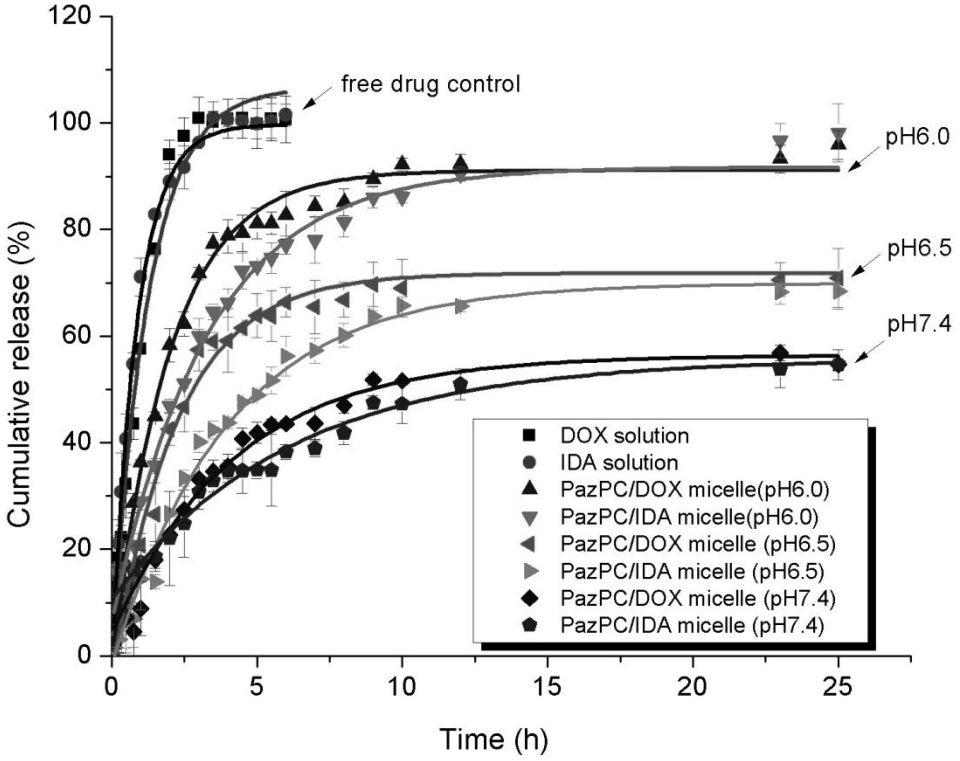

Figure 2.4 *In vitro* release profiles of DOX and IDA from drug-loaded PazPC micelles (PazPC/drug=5:1, molar ratio) at different pH.

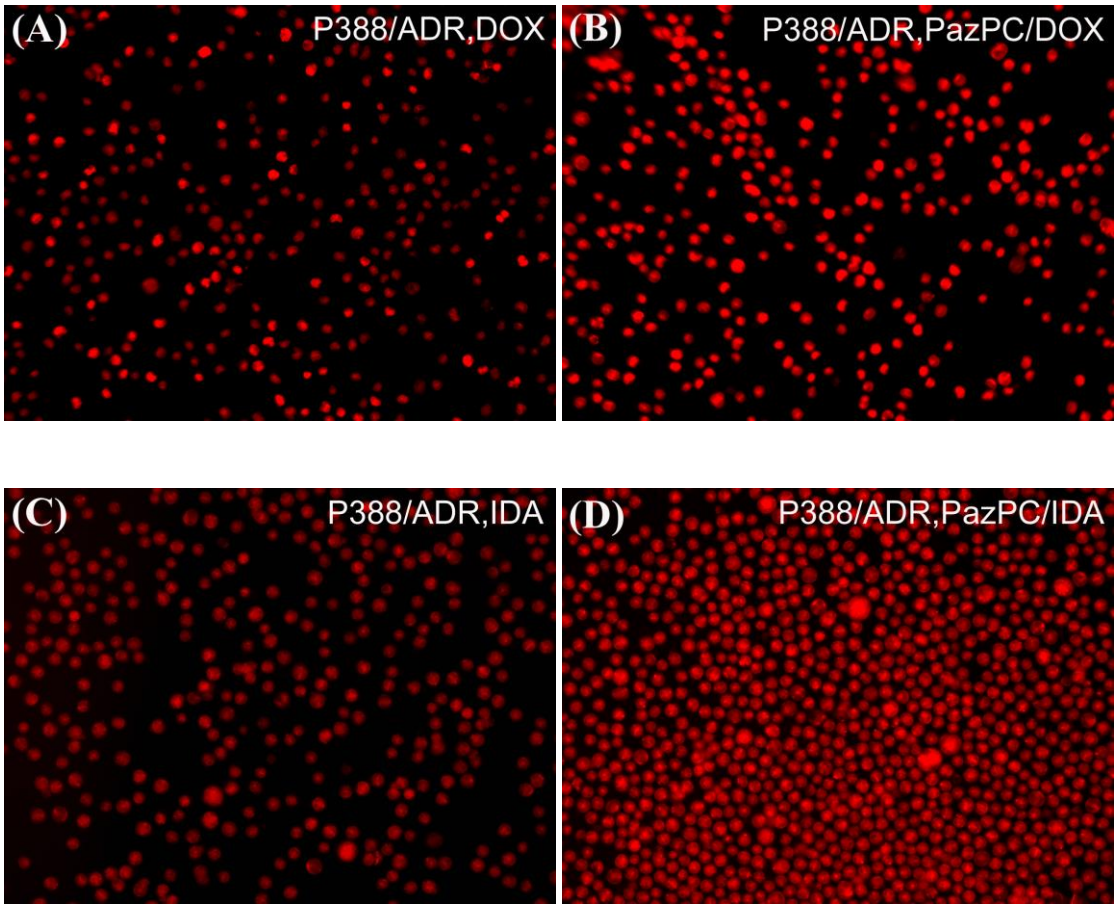
(A)
P388/ADR,DOX
(B)
P388/ADR,PazPC/DOX
(C)
P388/ADR,IDA
(D)
P388/ADR,PazPC/IDA

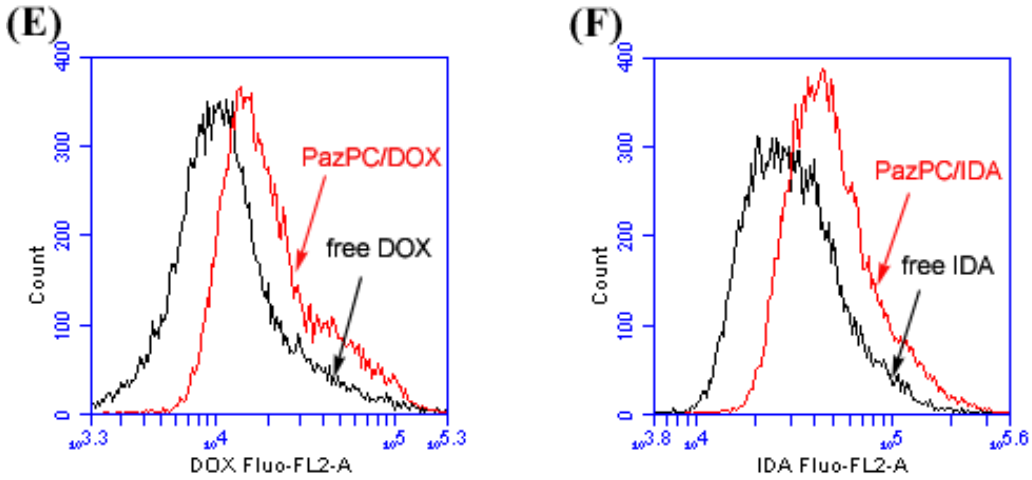
(E)
PazPC/DOX
free DOX
Count
DOX Fluo-FL2-A
(F)
PazPC/IDA
free IDA
Count
IDA Fluo-FL2-A

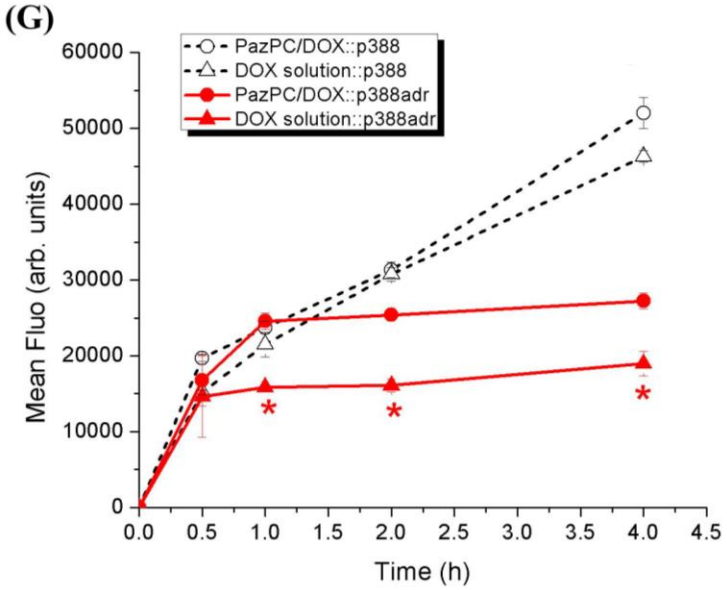
(G)
PazPC/DOX::p388
DOX solution::p388
PazPC/DOX::p388adr
DOX solution::p388adr
Mean Fluo (arb. units)
Time (h)

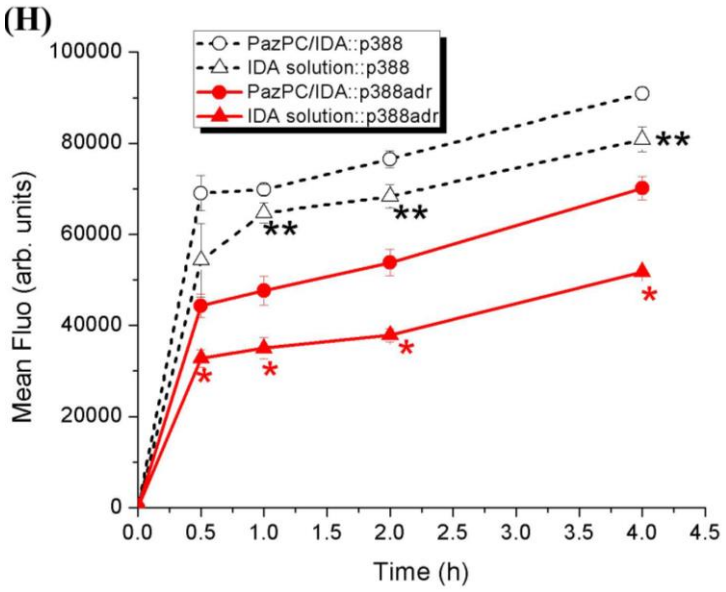

Figure 2.5 Cellular uptake of drug-loaded PazPC micelle. A-D: Cellular uptake visualized by fluorescence microscope (20 X) through treating cells for 2 hours in leukemia resistant cell line p388/ADR, (A) free DOX, (B) PazPC DOX micelle, (C) Free IDA, (D) PazPC IDA micelle; E-F: Cellular uptake analysis by flow cytometry through treating cells for 2 hours, (E) Free DOX and PazPC DOX micelle, (F) Free IDA and PazPC IDA micelle. G-H: The time courses of PazPC micellar DOX or IDA uptake by flow cytometric analysis in leukemia cells treated with drug-loaded PazPC micelles (PazPC/drug=5:1, molar ratio): (G) DOX for 0-4 hours, (H) IDA for 0-4 hours. *$p<0.01$, and **$p<0.05$, as compared with free drugs.

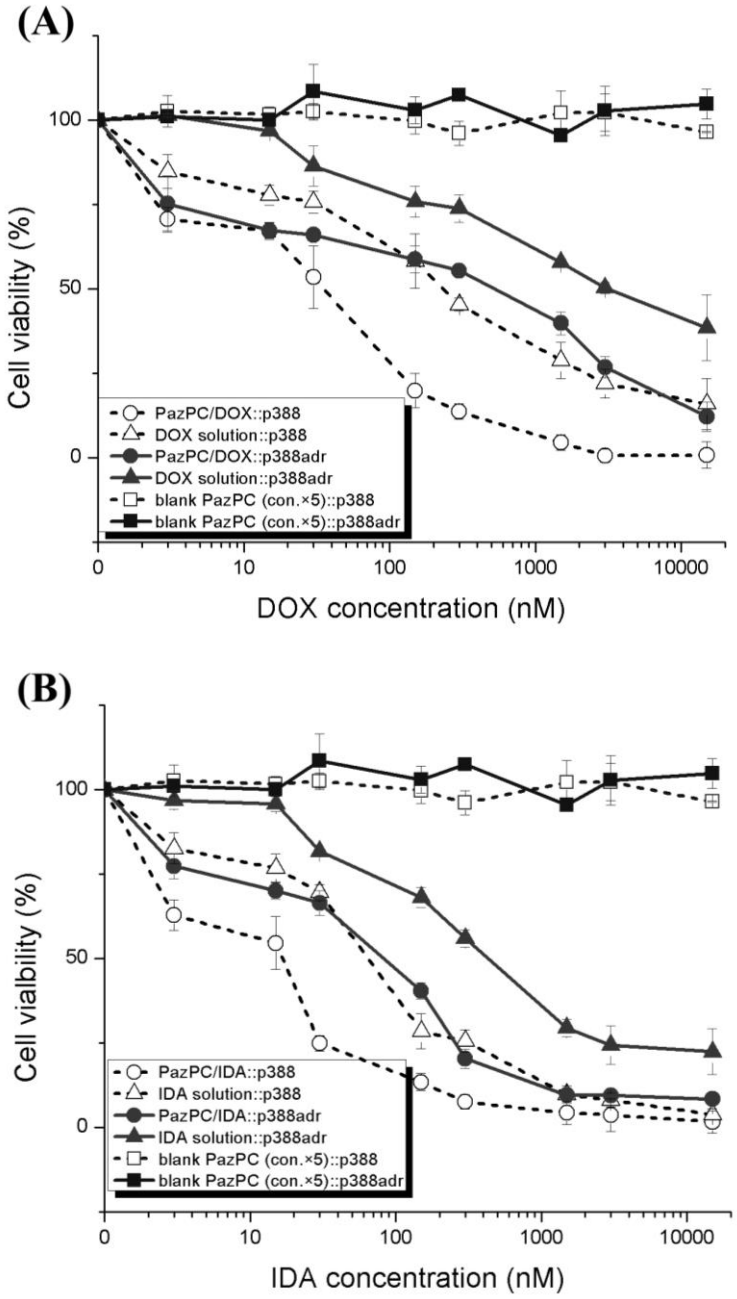

Figure 2.6 Cell viability of leukemia treated with PazPC/DOX micelle (A) or PazPC/IDA micelle (B) (PazPC/drug=5:1, molar ratio) for 48 hours.

3. Co-delivery of Zoledronic Acid and Double-strand RNA from Core-shell Nanoparticles

3.1 Abstract

Zoledronic acid, an inhibitor of osteoclast-mediated bone resorption, has been shown to have both direct and indirect antitumor activity. However, its use in extraskeletal malignancy is limited due to rapid uptake and accumulation within bone. Polyinosinic acid-polycytidylic acid [poly (I:C)] is a synthetic double-stranded RNA with direct antitumor cytotoxicity if it can be delivered to tumor cells intracellularly. Cationic lipid-coated calcium phosphate nanoparticles (LCP) were developed to enable intracellular codelivery of zoledronic acid and poly (I:C). LCP codelivering zoledronic acid and poly (I:C) were prepared using an ethanol injection method. Briefly, the ethanol solution of lipids was rapidly injected into newly formed calcium phosphate crystals containing poly (I:C) and zoledronic acid, and the mixture was then sonicated briefly to form LCP. The LCP were characterized for mean diameter size and zeta potential, efficiency in loading zoledronic acid, cytotoxic effect in a B16BL6 melanoma cell line in vitro, and antitumor effect in B16BL6 melanoma-bearing mice. LCP with a mean diameter around 200 nm and a narrow size distribution (polydispersity index 0.17) and high zoledronic acid encapsulation efficiency (94%) were achieved. LCP loaded with zoledronic acid and poly (I:C) had significantly greater antitumor activity than the free drugs in the B16BL6 melanoma cell line ($P < 0.05$). Furthermore, codelivery of zoledronic acid and poly (I:C) by LCP had higher cytotoxicity than delivering poly (I:C) alone by LCP ($P < 0.05$), indicating a synergism between zoledronic acid and poly (I:C). Finally, the antitumor study in melanoma-bearing mice also

demonstrated synergism between zoledronic acid and poly (I:C) codelivered by LCP. Cationic lipid-coated calcium phosphate nanoparticles constructed for codelivery of zoledronic acid and double-stranded RNA poly (I:C) had better antitumor activity both in vitro and in vivo. Future preclinical development of LCP encapsulating zoledronic acid and poly (I:C) for the treatment of human cancer is under way.

3.2 Introduction

Zoledronic acid (ZOL) and other nitrogen-containing bisphosphonates are potent inhibitors of osteoclast proliferation, and are used to treat osteoporosis and cancer-related bone metastasis (1). Moreover, preclinical studies have demonstrated the anti-tumor effects of zoledronic acid in various nonskeletal tumor models, including breast cancer, myeloma and others, suggesting that zoledronic acid has direct tumor inhibitory activity (2). Zoledronic acid can directly induce apoptosis in tumor cells and inhibit tumor cell growth and angiogenesis (3-6). For example, zoledronic acid directly suppresses cell proliferation and induces apoptosis in highly tumorigenic prostate and breast cancers (7). The anticancer activity of zoledronic acid has also been seen in the induction of γδ T-cell activation needed to initiate both the innate and the adaptive immune responses (8, 9).

However, zoledronic acid is rapidly eliminated after intravenous injection due to preferential uptake and accumulation within bone, which results in ineffective concentration of zoledronic acid in non-skeletal cancer tissues (10). In addition, accumulation of ZOL in bone would pose a serious health risk (11). These problems could be solved by a nanoparticle drug delivery system shielding the zoledronic acid from directly binding to bone while in the circulation (12-16). The enhanced permeation and retention effect of the nanoparticle drug delivery system can also improve accumulation of zoledronic acid in solid tumors (17, 18).

Synthetic double-stranded RNA polyinosinic–polycytidylic acid [poly (I:C)], a ligand for endosomal receptor TLR3 (19), can induce expression of inflammatory cytokines and type I interferon via the NF-κB, mitogen-activated protein kinase, and interferon regulatory factor 3 pathways, so enhancing the antitumor immune responses (11,20,21). Furthermore, poly (I:C) can be a ligand for cytoplasmic melanoma differentiation–associated gene 5 (22). In human melanoma, transfection of poly (I:C) into the cytoplasm can induce autophagy-mediated apoptosis via the melanoma differentiation-associated gene 5- mediated signaling pathway (21,23,24). Thus, delivering poly (I:C) to solid tumor can induce tumor apoptosis directly if delivery to cytoplasm can be achieved.

Complexes containing nucleic acid and calcium phosphate precipitation have been used in gene transfection studies for many years (25) .They can be easily taken up by cells through endocytosis and subsequently dissolved in endosomes (26). Also, calcium phosphate has low toxicity and good biocompatibility because it is the inorganic component of hard biological hard tissues, *i.e.*, bones and teeth (27). Therefore, it has the potential to be a good carrier system for drug delivery, especially for nucleic acid-based therapeutics. However, large aggregates are easily formed as a result of rapid crystal growth, so use of these complexes is limited to *in vitro* gene transfection (28). The key issue when fabricating calcium phosphate nanoparticles is to halt continuous growth of crystals. Synthesis of calcium phosphate nanoparticles can be done by various methods ,including wet precipitation (29), solid state reaction (30), flame spray pyrolysis (31), and hydrothermal (32), spray-drying (33), micelle-mediated (34), reverse micelle-mediated (35, 36) and double emulsion-mediated synthesis (37). These calcium phosphate nanoparticle fabrication methods usually involve multiple steps, which are not easily scaled up in pharmaceutical manufacturing process.

In this study, we devised a simple method of wet precipitation combined with cationic lipid surface coating for fabrication of calcium phosphate nanoparticles and co-delivery of zoledronic acid and poly (I:C). Being a polyanion, poly (I:C) is not only a therapeutic agent, but has a unique role in the process of fabricating calcium phosphate nanoparticles. In this study, binding poly (I:C) prevented continuous growth of calcium phosphate crystals and imparted a negative charge to the surface of calcium phosphate crystals for subsequent cationic lipid coating. We also tested whether codelivery of zoledronic acid and poly (I:C) has a synergistic inhibitory effect on growth of the mouse melanoma both *in vitro* and *in vivo*.

3.3 Materials and Methods

3.3.1 Materials

DOTAP (1, 2-dioleoyl-3-trimethylammonium-propane) was purchased from Avanti Polar Lipids Inc. (Alabaster, AL). Poly I:C was sourced from EMD Chemicals (San Diego, CA). Zoledronic acid was obtained from Alexis Corporation (San Diego, CA). Cholesterol and tetrabutylammonium hydrogen sulfate were purchased from JT Baker (Phillipsburg, NJ). Calcium nitrate, phosphate salt and all other reagents were purchased from VWR International (West Chester, PA). Fetal bovine serum, Dulbecco's Modified Eagle's Medium, and other reagents needed for cell culture were purchased from Mediatech (Manassas, VA). The mouse melanoma cell line (B16BL6) was obtained from National Cancer Institute at Frederick (Frederick, MD).

3.3.2 Preparation of Lipid-coated Calcium Phosphate Nanoparticles

Calcium phosphate nanoparticles were prepared by a wet precipitation method (28, 38) (Figure 3.1). Briefly 500 µl of aqueous solution of calcium (6.25 mM) was mixed with 500 µl of

aqueous solution of diammonium hydrogen phosphate (3.74 mM). The pH of both solutions was preadjusted to 9.0 with 0.1M NaOH (39). Mixing was accomplished by rapidly injecting both solutions using an 1 ml insulin syringe into a 1.5 ml tube into which 15 µl of poly (I:C) aqueous solution (5 µg/µl or higher concentrations in some experiments) was added before injection. The suspension was then mixed well by vortex for 10 s. Finally 7.5 µL of 10 mg/ml zoledronic acid was added to the calcium-poly (I:C) complex to form a calcium phosphate -poly (I:C)-zoledronic acid core.

The lipids mixture, composed of DOTAP-cholesterol (1:1 mol/mol), was dissolved in absolute ethanol and coated onto the surface of calcium phosphate-poly (I:C)-zoledronic acid complex. Briefly, 80 µL of the lipid mixture in 25 mg/ml ethanol solution was rapidly injected into the calcium phosphate-poly (I:C)-zoledronic acid core, and the mixture was then sonicated for 2 minutes in a bath sonicator to form lipid-coated nanoparticles consisting of a lipid shell and calcium phosphate-poly (I:C)-zoledronic acid core. The nanoparticles formed were extensively dialyzed against pH 8.0 Tris-HCl buffer to remove residue ethanol.

3.3.3 Preparation of Cationic Liposomes

DOTAP cationic liposomes were prepared using the ethanol injection method (40). Briefly, 80 µL of lipid ethanol solution (DOTAP to cholesterol, 1:1,25mg/ml) was injected rapidly into a 1.5 ml tube containing 1.0 ml of filtered sterilized water, and the suspension was then sonicated in a bath sonicatior for 2 min to form liposomes. The cationic liposomes formed were extensively dialyzed against water to remove the residue ethanol.

3.3.4 Preparation of Nanoparticles

Because poly (I:C) has a unique role in stabilizing LCP, the LCP containing various amounts of poly (I:C) (25, 75, 150, 300 µg/ml, respectively) was prepared to investigate the effect of amount of poly(I:C) on nanoparticles size. The mean diameters of the calcium phosphate nanoparticles, cationic liposomes, and LCP were compared between these three formulations. LCP containing various amounts of zoledronic acid (25, 50 and 75µg/ml) and a fixed amount of poly (I:C) (75µg/ml) were prepared using the method described above and evaluated for particle size and cytotoxicity in a B16BL6 melanoma cell line.

3.3.5 Particle Size and Zeta Potential of Calcium Phosphate Nanoparticles, Cationic Liposomes, and LCP

Mean diameter and Polydispersity index were used to characterize the size distribution of nanoparticles. The particle size and zeta potential of the different formulations were determined at room temperature using a particle sizer (Nicomp Model 380/ZLS, Particle Sizing System, Santa Barbara, CA). Each sample was diluted 20-fold with 0.22um filtered water before the measurement. All these values were calculated as the mean of the three separate batches.

3.3.6 Quantitative Analysis and Calculation of Zoledronic Acid Encapsulation Efficiency in LCP

Quantitative analysis of zoledronic acid was performed by reverse-phase high-performance liquid chromatography on a Luna C18 (2) column (3 µm, 150*4.6 mm) using a mobile phase composed of 5:95 methanol to phosphate buffer (8 mM, pH 7.4), 3 mM Tetrabutylammonium hydrogen sulfate and 2.3 µg/ml ethylenediamine tetra-acetic acid at a flow rate of 0.6 ml per minute at room temperature, with ultraviolet detection at 215 nm (41). Briefly, 1ml of liposomes or nanoparticles was centrifuged through a centrifugal device with a molecule

cut-off of 100,000 (Nanosep, Pall Life Sciences, Menlo Park, CA) at 12000 rpm for 20 minutes. The supernatants containing free zoledronic acid were then carefully collected, and the zoledronic acid concentration was determined by high performance liquid chromatography (42). The zolic acid encapsulation efficiency was calculated by the following equation:

Encapsulation efficiency (%) = (Total amount of zoledronic acid in formulation – Free zoledronic acid) / Total amount of zoledronic acid*100%

3.3.7 Stability Study

To determine the stability of LCP under storage conditions, LCP was freshly prepared and then stored at 4^{o}C in 10 mM pH 8.0 Tris-HCl buffer, and then the particle size and zoledronic acid encapsulation efficiency were then monitored during 30 days of storage.

3.3.8 Cell Viability Assay

In vitro cytotoxicity was determined by MTT assay, as described previously (43). The B16BL6 cells were grown in Dullbecco's Modified Eagle's medium supplemented with 10% fetal bovine serum (FBS), 100 U/ml penicillin, and 100 µg/ml streptomycin at 37^{o}C in a humidified atmosphere containing 5%$CO_{2.}$ The B16BL6 cells were seeded in 96-well plates at 8 X 10^{3} cells/well in 100 µl medium. After 16 hours, the cells were treated with the different formulations diluted in Dullbecco's Modified Eagle's medium to provide the same mass concentration (µg/mL) of poly (I:C) , zoledronic acid, or their combination, and incubated for 48 hours prior to MTT assay. Briefly, MTT reagent was added to the culture medium at a final concentration of 0.5 mg/ml and the cells were incubated at 37^{o}C for an additional 4 hours. Finally, the medium was removed, the cells with dye compounds were dissolved in dimethylsulfoxide, and absorption was measured at 544 nm using a microplate reader (Fluostar,

BMG LabTech GmbH, Ortenbery, Germany). Viability was expressed as a percentage of the untreated control cells (100% viability).

3.3.9 Animal Study

Female 8-week-old Charles River C57BL/6 mice were used to evaluate the in vivo efficacy of the different formulations. The animal experiments complied with the rules set down in the National Institutes of Health Guide for the Care and Use of Laboratory Animals and the Institutional Animal Care and Use Committee. B16BL6 mouse melanoma cells were used as the tumor development model. B16BL6 cells (5×10^5) were inoculated subcutaneously into the mice to induce tumor formation and growth. After 5 days, when the tumor volume had reached approximately 50 mm^3, mice were divided randomly into four groups (n=6) to receive phosphate-buffered solution (control), free zoledronic acid, LCP-poly (I:C), or LCP-poly (I:C)-zoledronic acid, and received four peritumoral injections on days 0, 2, 4 and 6 after tumor formation at a dose of 4.5 μg per mouse. The doses of 4.5 μg per mouse were calculated as free zoledronic acid or poly (I:C) or their 1:1 combination in the three treatment groups mentioned above. Following treatment, the animals were monitored regularly for body weight, tumor growth, and survival. Tumor volumes were assessed by measuring two perpendicular diameters with digital calipers and using the formula $(L*W^2)/2$, where L is the longest diameter and W is perpendicular to L (43). Results are expressed as the mean tumor volume ± standard deviation for six mice.

3.3.10 Statistical Analysis

The student's t-test was used to identify differences between groups. $P < 0.05$ was considered to be statistically significant.

3. 4 Results and Discussion

3.4.1 Nanoparticle Preparation and Characterization

As shown in Figure 3.2A, the diameter of LCP without poly (I:C) prepared by the newly formed calcium phosphate crystals and DOTAP was about 8.3 μm, suggesting no affinity between calcium phosphate crystals and DOTAP. Therefore, the surface of the calcium phosphate crystal needed to be functionalized by negative charges for further coating with cationic liposomes. Poly (I:C), a negatively charged synthetic nucleic acid, was chosen to functionalize the surface of calcium phosphate because of its high affinity for calcium phosphate and therapeutic effects. We then investigated the effect of poly (I:C) on the particle size of LCP. The particle size was still large with the addition of poly (I:C) 25 μg/ml (Figure 3.2A). However, the diameter of LCP was dramatically decreased to the size range of nanoparticles (around 200 nm) by addition of poly (I:C) 75 μg/ml to the preparation. There was no significant difference in particle size between the three poly (I:C) concentrations used (75, 150, 300 μg/ml), indicating that 75 μg/ml of poly (I:C) was enough to prevent continuous growth of calcium phosphate crystals. Meanwhile, under such conditions, the charge (+/−) to N/P ratio (for DOTAP and poly (I:C), respectively), was 4:1, and this ratio was appropriate for DOTAP coating to achieve colloidal stability of LCP. It was confirmed that all the poly (I:C) was associated with LCP, with an N/P ratio of 4:1 by agarose gel retardation assay (data not shown). The agarose gel retardation assay also indicated that increasing poly (I:C) to >150 μg/ml in the preparation resulted in gradual accumulation of free poly (I:C) in the formulation (data not shown), so an N/P ratio of 4:1 was used for subsequent experiments.

In order to codeliver poly (I:C) and zoledronic acid, different weight ratios of poly (I:C) to zoledronic acid with a fixed 75 μg/ml amount of poly (I:C) were used in the fabrication of

LCP, and their sizes were compared (Figure 3.2B). There were no obvious increases in LCP particle size when the weight ratios were varied from 3:1 to 3:3 [poly (I:C) to zoledronic acid], but the size increased to around 300 nm at a ratio of 3:6. Because zoledronic acid has high affinity for calcium phosphate (12), it will compete with poly (I:C) binding to calcium phosphate, leading to compromise of the stabilization effects of poly (I:C).

Four different delivery systems were prepared and characterized, and the results were summarized in Table 1, which shows that LCP is capable of delivery of poly (I:C) alone. The size of LCP-poly (I:C) is around 180 nm. The lipoplex formed by mixing of cationic liposomes, poly (I:C), and zoledronic acid, had the smallest particle size of 138 nm but the broadest size distribution (polydispersity index 0.33) of all the formulations tested. It appeared that only 42% of the total amount of zoledronic acid was associated with the lipoplex. This is probably due to the rapid diffusion of zoledronic acid from the lipoplex because the molecular weight of zoledronic acid is less than 300 Da. The LCP-poly (I:C)- zoledronic acid, formed by a calcium phosphate core and DOTAP coating, had higher zoledronic acid encapsulation efficiency (94%) and a relatively small size (205 nm). Being one of the bisphosphonates, zoledronic acid anions are suitable for coordinating calcium cations in the calcium phosphate phase through bidentate chelation (44). The high affinity between calcium phosphate and zoledronic acid decreased the diffusion of zoledronic acid from LCP. The lipid coating added another diffusion barrier to zoledronic acid, leading to overall high encapsulation efficiency. Interestingly, without a lipid coating, the freshly prepared intermediate core formed by calcium phosphate, poly (I:C), and zoledronic acid had a negative charge (-10 mV) and a high loading efficiency for zoledronic acid (90%), suggesting that the major contribution to the high encapsulation efficiency of zoledronic

acid in LCP was the high affinity between zoledronic acid and calcium phosphate. The size distribution of LCP-poly (I:C)-zoledronic acid is shown in Figure 3.3.

We then studied the stability of LCP in pH 8.0 Tris- HCl buffer protected form light and stored at 4°C for 30 days. Although the calcium phosphate-poly (I:C)-zoledronic acid complex had a relatively small size of 360 nm when freshly prepared, its size gradually increased to more than 1 μm after 24 hours (Figure 3.4). However, LCP-poly (I:C)-zoledronic acid demonstrated good colloidal stability. Figure 3.4 shows that the particle size of LCP-poly (I:C)-zoledronic acid remained unchanged over 30 days. Therefore, the cationic DOTAP coating on the LCP nanoparticle contributed to its good colloidal stability. The cationic liposome drug delivery system has been widely studied for gene transfection, vaccine delivery, and antitumor targeting. LCP may have some characteristics similar to those of a cationic liposome, such as good colloidal stability. However, more experiments are required for a better understanding of the difference between these two drug delivery systems.

3.4.2 Co-delivery of Poly (I: C) and Zoledronic Acid had Superior Cytotoxicity in Melanoma Cells

It has been reported that poly (I:C) induces direct apoptotic cytotoxicity in cancer cells, including melanoma (45), lung cancer (46) and breast cancer (45, 47), if poly (I:C) can be delivered into the cytoplasm (48). Therefore, we formulated poly (I:C) using calcium phosphate nanoparticles, a DOTAP lipoplex, and LCP, and compared their cytotoxicity in B16BL6 mouse melanoma cells. As shown in Figure 3.5, at the same poly (I:C) concentration of 0.5 μg/ml, LCP-poly (I:C) showed the highest cytotoxicity to B16BL6 cells, followed by the poly (I:C)-lipoplex, and finally poly (I:C)-calcium phosphate nanoparticles. Cell viability was 47.1%, 61.2%, and 86.3%, respectively. Blank calcium phosphate nanoparticles, DOTAP liposomes, or their

combination had no cytotoxic effect on B16BL6 cells (data not shown). The enhanced cytotoxic effect of LCP could be explained by delivery of more poly (I:C) into the cytoplasm by LCP. It has been reported that the calcium phosphate core in LCP is unstable in an acidic endosomal environment, so its decomposition to free calcium and phosphate ions in the endosome will increase osmotic pressure and cause swelling and rupture of the endosomes, and release of their contents into the cytosol (26, 49, 50). However, without DOTAP, the negatively charged calcium phosphate-poly (I:C) nanoparticles are not easily taken up by melanoma cells, leading to a compromised cytotoxic effect (48).

Next, the cytotoxicity of LCP codelivering poly (I:C) and zoledronic acid was tested in B16BL6 cells. Like free poly (I:C), free zoledronic acid at a concentration of 0.5 μg/ml had no cytotoxic effect in B16BL6 cells. We then prepared LCP codelivering poly (I:C) and zoledronic acid in different ratios, but the combined concentration of both drugs (poly (I:C) + zoledronic acid) in LCP was kept constant (0.5 μg/ml) in the subsequent MTT assay. The results demonstrated that the drug combination was more potent in its ability to generate cytotoxicity in melanoma cells than were the individual drugs used alone (Figure 3.6). As shown in Figure 3.6, the cell viabilities after treatment with free zoledronic acid and LCP-poly (I:C) were 91.8% and 49.0%, respectively. Codelivery of poly (I:C) and zoledronic acid (1:1) by LCP showed enhanced cell cytotoxicity, with a cell cytotoxicity of 14.4%. Interestingly, the greater the amount of zoledronic acid in the LCP-poly (I:C)-zoledronic acid complex, the greater the potency of the cytotoxicity to B16BL6 cells, although the combined concentration of the two drugs was the same. However, from previous formulation studies, zoledronic acid could not be increased to more than 50%, because more zoledronic acid led to instability of LCP during the fabrication process.

3.4.3 Tumor Inhibition by Co-delivering Poly (I:C) and Zoledronic Acid in Melanoma-bearing mice

Based on the superior cytotoxicity of LCP co-delivering poly (I:C) and zoledronic acid in the B16BL6 melanoma cell line, we investigated its antitumor activity in B16BL6 tumor-bearing mice. The tumors were allowed to grow subcutaneously for 5 days, and the tumor-bearing mice were then treated with phosphate-buffered solution (control), free zoledronic acid, LCP-poly (I:C), or LCP-poly (I:C)-zoledronic acid by peritumoral injection on days 0, 2, 4, and 6. As shown in Figure 3.7, the control mice had the largest tumors at day 11. Mice treated with LCP-poly (I:C)-zoledronic acid showed significant tumor growth inhibition compared with the other groups ($P < 0.05$). Mice treated with LCP-poly (I:C) also showed slight tumor growth inhibition.

Poly (I:C) has multiple actions in the inhibition of tumor growth, including direct apoptosis effects on tumor cells and modulation of the immune system (51-55). One of the side effects of poly (I:C) is induction of toxic cytokines, so its use in cancer is limited (56-58). In our study, by encapsulating zoledronic acid and poly (I:C) in LCP, the effective doses of both poly (I:C) and zoledronic acid could be decreased, so this formulation may have less toxic effects. The current peritumoral injection of LCP-poly (I:C)-zoledronic acid in melanoma-bearing mice confirmed the in vivo efficacy of codelivery of poly (I:C) and zoledronic acid by LCP. However, further development of LCP by surface PEGylation and targeting ligands is required for intravenous injection, and is suitable for treatment of other type of tumors.

3.5 Conclusion

LCP were developed for simultaneous delivery of zoledronic acid and poly (I:C). Lipid-coated nanoparticles including a calcium phosphate core and lipid shell had a narrow particle

size distribution and high loading efficiency for poly (I:C) and zoledronic acid, with good stability. In addition, codelivery of zoledronic acid and poly (I:C) offered superior antitumor activity in both *in vitro* and *in vivo* studies. These results suggest a potential for future preclinical development of zoledronic acid and poly (I:C)-encapsulating LCP for the treatment of human cancer.

3.6 References

1. M.S. Aapro, R.E. Coleman, Bone health management in patients with breast cancer: current standards and emerging strategies, Breast, 21 (2012) 8-19.
2. I. Benzaid, H. Monkkonen, V. Stresing, E. Bonnelye, J. Green, J. Monkkonen, J.L. Touraine, P. Clezardin. High phosphoantigen levels in bisphosphonate-treated human breast tumors promote Vgamma9Vdelta2 T-cell chemotaxis and cytotoxicity in vivo, Cancer research, 71 (2011) 4562-4572.
3. M.V. Lee, E.M. Fong, F.R. Singer, R.S. Guenette, Bisphosphonate treatment inhibits the growth of prostate cancer cells, Cancer research, 61 (2001) 2602-2608.
4. S.G. Senaratne, G. Pirianov, J.L. Mansi, T.R. Arnett, K.W. Colston, Bisphosphonates induce apoptosis in human breast cancer cell lines, British journal of cancer, 82 (2000) 1459-1468.
5. P. Clezardin, Bisphosphonates' antitumor activity: an unravelled side of a multifaceted drug class, Bone, 48 (2011) 71-79.
6. E. Giraduo, D. Hanahan, Zoledronic acid inhibits angiogenesis and impairs tumorigenesis in a mouse model of cervical carcinogenesis,, Haematological reports (2006) 39-41.

7. H. Almubarak, A. Jones, R. Chaisuparat, M. Zhang, T.F. Meiller, M.A. Scheper, Zoledronic acid directly suppresses cell proliferation and induces apoptosis in highly tumorigenic prostate and breast cancers, Journal of carcinogenesis, 10 (2011) 2.

8. V. Kunzmann, M. Wilhelm, Adjuvant zoledronic acid for breast cancer: mechanism of action?, The lancet oncology, 12 (2011) 991-992.

9. E. Cimini, P. Piacentini, A. Sacchi, C. Gioia, S. Leone, G.M. Lauro, F. Martini, C. Agrati, Zoledronic acid enhances Vdelta2 T-lymphocyte antitumor response to human glioma cell lines, International journal of immunopathology and pharmacology, 24 (2011) 139-148.

10. M. Caraglia, M. Marra, S. Naviglio, G. Botti, R. Addeo, A. Abbruzzese, Zoledronic acid: an unending tale for an antiresorptive agent, Expert opinion on pharmacotherapy, 11 (2010) 141-154.

11. G. Salzano, M. Marra, M. Porru, S. Zappavigna, A. Abbruzzese, M.I. La Rotonda, C. Leonetti, M. Caraglia, G. De Rosa, Self-assembly nanoparticles for the delivery of bisphosphonates into tumors, International journal of pharmaceutics, 403 (2011) 292-297.

12. M. Scheper, R. Chaisuparat, K. Cullen, T. Meiller, A novel soft-tissue in vitro model for bisphosphonate-associated osteonecrosis, Fibrogenesis & tissue repair, 3 (2010) 6.

13. O.C. Farokhzad, R. Langer, Impact of nanotechnology on drug delivery, ACS nano, 3 (2009) 16-20.

14. C. Agrati, C. Marianecci, S. Sennato, e. al., Multicompartment vectors as novel drug delivery systems: selective activation of Tγδ lymphocytes after zoledronic acid delivery., Nanomedicine, 7 (2011) 153-161.

15. Rooijen V, K.-H.E. V, Clodronate liposomes: perspectives in research and therapeutics, J Liposome Res, 12 (2002) 81-94.

16. H.D. Danenberg, G. Golomb, A. Groothuis, J. Gao, H. Epstein, R.V. Swaminathan, P. Seifert, E.R. Edelman, Liposomal alendronate inhibits systemic innate immunity and reduces in-stent neointimal hyperplasia in rabbits, Circulation, 108 (2003) 2798-2804.

17. M. Marra, G. Salzano, C.L. Leonetti, Carlo)3., Nanotechnologies to use bisphosphonates as potent anticancer agents: the effects of zoledronic acid encapsulated into liposomes, Nanomedicine : nanotechnology, biology, and medicine, 7 (2011) 955-964.

18. S. Guo, L. Huang, Nanoparticles Escaping RES and Endosome: Challenges for siRNA Delivery for Cancer Therapy, Journal of nanomaterials 2011 (2011).

19. A. Hafner, B. Corthesy, M. Textor, H. Merkle, Tuning the immune response of dendritic cells to surface-assembled poly(I:C) on microspheres through synergistic interactions between phagocytic and TLR3 signaling, Biomaterials, 32 (2011) 2651-2661.

20. Y. Zheng, H. An, M. Yao, J. Hou, Y. Yu, G. Feng, X. Cao, Scaffolding adaptor protein Gab1 is required for TLR3/4- and RIG-I-mediated production of proinflammatory cytokines and type I IFN in macrophages, J Immunol, 184 (2010) 6447-6456.

21. R. Besch, H. Poeck, T. Hohenauer, D. Senft, G. Hacker, C. Berking, V. Hornung, S. Endres, T. Ruzicka, S. Rothenfusser, G. Hartmann, Proapoptotic signaling induced by RIG-I and MDA-5 results in type I interferon-independent apoptosis in human melanoma cells, The Journal of clinical investigation, 119 (2009) 2399-2411.

22. D. Alonso-Curbelo, M.S. Soengas, Self-killing of melanoma cells by cytosolic delivery of dsRNA: wiring innate immunity for a coordinated mobilization of endosomes,

autophagosomes and the apoptotic machinery in tumor cells, Autophagy, 6 (2010) 148-150.

23. Y.S. Cheng, F. Xu, Anticancer function of polyinosinic-polycytidylic acid, Cancer biology & therapy, 10 (2011) 1219-1223.

24. D. Tormo, A. Checinska, D. Alonso-Curbelo, E. Perez-Guijarro, E. Canon, E. Riveiro-Falkenbach, T.G. Calvo, L. Larribere, D. Megias, F. Mulero, M.A. Piris, R. Dash, P.M. Barral, J.L. Rodriguez-Peralto, P. Ortiz-Romero, T. Tuting, P.B. Fisher, M.S. Soengas, Targeted activation of innate immunity for therapeutic induction of autophagy and apoptosis in melanoma cells, Cancer cell, 16 (2009) 103-114.

25. M. Jordan, A. Schallhorn, F.M. Wurm, Transfecting mammalian cells: optimization of critical parameters affecting calcium-phosphate precipitate formation, Nucleic acids research, 24 (1996) 596-601.

26. J. Li, Y.C. Chen, Y.C. Tseng, S. Mozumdar, L. Huang, Biodegradable calcium phosphate nanoparticle with lipid coating for systemic siRNA delivery, Journal of controlled release : official journal of the Controlled Release Society, 142 (2010) 416-421.

27. M. Zhang, K. Kataoka, Nano-structured composites based on calcium phosphate for cellular delivery of therapeutic and diagnostic agents, Nanotoday 4(2009) 508-517.

28. S. Bisht, G. Bhakta, S. Mitra, A. Maitra, pDNA loaded calcium phosphate nanoparticles: highly efficient non-viral vector for gene delivery, International journal of pharmaceutics, 288 (2005) 157-168.

29. V.V. Sokolova, I. Radtke, R. Heumann, M. Epple, Effective transfection of cells with multi-shell calcium phosphate-DNA nanoparticles, Biomaterials, 27 (2006) 3147-3153.

30. C. Silva, M. Graca, A. Sombra, M. Valente, Structural and electrical study of calcium phosphate obtained by a microwave radiation assisted procedure., Physica b-condensed matter, 404 (2009) 1503-1508.

31. J.S. Cho, Y.N. Ko, H.Y. Koo, Y.C. Kang, Synthesis of nano-sized biphasic calcium phosphate ceramics with spherical shape by flame spray pyrolysis, Journal of materials science. Materials in medicine, 21 (2010) 1143-1149.

32. K. Li, S.C. Tjong, Hydrothermal synthesis and biocompatibility of hydroxyapatite nanorods, Journal of nanoscience and nanotechnology, 11 (2011) 10444-10448.

33. H.H. Xu, J.L. Moreau, L. Sun, L.C. Chow, Nanocomposite containing amorphous calcium phosphate nanoparticles for caries inhibition, Dental materials : official publication of the Academy of Dental Materials, 27 (2011) 762-769.

34. S. Thachepan, M. Li, S. Mann, Mesoscale crystallization of calcium phosphate nanostructures in protein (casein) micelles, Nanoscale, 2 (2010) 2400-2405.

35. S. Dasgupta, S. Bose, Reverse Micelle-Mediated Synthesis and Characterization of Tricalcium Phosphate Nanopowder for Bone Graft Applications, Journal of the american ceramic society, 92 (2009) 2528-2536.

36. J. Han, T. Tan, J. Loo, Utilizing inverse micelles to synthesize calcium phosphate nanoparticles as nano-carriers, J nanopart Res, 13 (2011) 3441-3454.

37. H. Shum, A. Bandyopadhyay, S. Bose, D. Weitz, Double Emulsion Droplets as Microreactors for Synthesis of Mesoporous Hydroxyapatite, Chemistry of materials 21 (2009) 5548-5555.

38. C. Ergun, Z. Evis, T. Webster, F.C. Sahin, Synthesis and microstructural characterization of nano-size calcium phosphates with different stoichiometry, Ceramics International 37 (2011) 971-977.

39. V. Sokolova, T. Knuschke, A. Kovtun, J. Buer, M. Epple, A. Westendorf, The use of calcium phosphate nanoparticles encapsulating Toll-like receptor ligands and the antigen hemagglutinin to induce dendritic cell maturation and T cell activation., Biomaterials, 31 (2010) 5627-5633.

40. C. Zhou, B. Yu, X. Yang, T. Huo, L.J. Lee, R.F. Barth, R.J. Lee, Lipid-coated nano-calcium-phosphate (LNCP) for gene delivery, International journal of pharmaceutics, 392 (2010) 201-208.

41. H. Shmeeda, Y. Amitay, J. Gorin, D. Tzemach, Delivery of zoledronic acid encapsulated in folate-targeted liposome results in potent in vitro cytotoxic activity on tumor cells., Journal of controlled release, 146 (2010) 76-83.

42. M. Marra, G. Salzano, C. Leonetti, M. Porru, R. Franco, S. Zappavigna, G. Liguori, G. Botti, P. Chieffi, M. Lamberti, G. Vitale, A. Abbruzzese, M.I. La Rotonda, G. De Rosa, M. Caraglia, New self-assembly nanoparticles and stealth liposomes for the delivery of zoledronic acid: a comparative study, Biotechnology advances, 30 (2012) 302-309.

43. J.J. Sudimack, W. Guo, W. Tjarks, R.J. Lee, A novel pH-sensitive liposome formulation containing oleyl alcohol, Biochimica et biophysica acta, 1564 (2002) 31-37.

44. C.W. Kim, Y.P. Yun, H.J. Lee, Y.S. Hwang, I.K. Kwon, S.C. Lee, In situ fabrication of alendronate-loaded calcium phosphate microspheres: controlled release for inhibition of osteoclastogenesis, Journal of controlled release : official journal of the Controlled Release Society, 147 (2010) 45-53.

45. C. Y, X. F., Anticancer function of polyinosinic-polycytidylic acid, Cancer Biology & Therapy 10 (2010) 1219-1223.

46. G. Forte, A. Rega, S. Morello, A. Luciano, C. Arra, A. Pinto, R. Sorrentino, Polyinosinic-polycytidylic acid limits tumor outgrowth in a mouse model of metastatic lung cancer, J Immunol, 188 (2012) 5357-5364.

47. S. B, C. I, R. MC, L. SJ, R. T., TLR3 can directly trigger apoptosis in human cancer cells., J Immunol, 176 (2006) 4894-4901.

48. K. Hirabayashi, J. Yano, T. Inoue, T. Yamaguchi, K. Tanigawara, G.E. Smyth, K. Ishiyama, T. Ohgi, K. Kimura, T. Irimura, Inhibition of cancer cell growth by polyinosinic-polycytidylic acid/cationic liposome complex: a new biological activity, Cancer research, 59 (1999) 4325-4333.

49. Sokolova V, E. M., Inorganic nanoparticles as carriers of nucleic acids into cells., Angew Chem Int Ed Engl., 47 (2008) 1382-1395.

50. F.L. Graham, A.J. van der Eb, A new technique for the assay of infectivity of human adenovirus 5 DNA, Virology, 52 (1973) 456-467.

51. A. Shir, M. Ogris, W. Roedl, E. Wagner, A. Levitzki, EGFR-homing dsRNA activates cancer-targeted immune response and eliminates disseminated EGFR-overexpressing tumors in mice, Clinical cancer research : an official journal of the American Association for Cancer Research, 17 (2011) 1033-1043.

52. K. Kubler, C. tho Pesch, N. Gehrke, S. Riemann, J. Dassler, C. Coch, J. Landsberg, V. Wimmenauer, M. Polcher, C. Rudlowski, T. Tuting, W. Kuhn, G. Hartmann, W. Barchet, Immunogenic cell death of human ovarian cancer cells induced by cytosolic poly(I:C)

leads to myeloid cell maturation and activates NK cells, European journal of immunology, 41 (2011) 3028-3039.

53. C.Y. Wu, H.Y. Yang, A. Monie, B. Ma, H.H. Tsai, T.C. Wu, C.F. Hung, Intraperitoneal administration of poly(I:C) with polyethylenimine leads to significant antitumor immunity against murine ovarian tumors, Cancer immunology, immunotherapy : CII, 60 (2011) 1085-1096.

54. T. Inao, N. Harashima, H. Monma, S. Okano, M. Itakura, T. Tanaka, Y. Tajima, M. Harada, Antitumor effects of cytoplasmic delivery of an innate adjuvant receptor ligand, poly(I:C), on human breast cancer, Breast cancer research and treatment, 134 (2012) 89-100.

55. N. Harashima, T. Inao, R. Imamura, S. Okano, T. Suda, M. Harada, Roles of the PI3K/Akt pathway and autophagy in TLR3 signaling-induced apoptosis and growth arrest of human prostate cancer cells, Cancer immunology, immunotherapy : CII, 61 (2012) 667-676.

56. A.J. Steelman, J. Li, Poly(I:C) promotes TNFalpha/TNFR1-dependent oligodendrocyte death in mixed glial cultures, Journal of neuroinflammation, 8 (2011) 89.

57. S.M. Ngoi, M.C. St Rose, A.M. Menoret, D.E. Smith, M.G. Tovey, A.J. Adler, A.T. Vella, Presensitizing with a Toll-like receptor 3 ligand impairs CD8 T-cell effector differentiation and IL-33 responsiveness, Proceedings of the National Academy of Sciences of the United States of America, 109 (2012) 10486-10491.

58. P.S. Morahan, A.E. Munson, W. Regelson, S.L. Commerford, L.D. Hamilton, Antiviral activity and side effects of polyriboinosinic-cytidylic acid complexes as affected by

molecular size, Proceedings of the National Academy of Sciences of the United States of America, 69 (1972) 842-846.

Table 3.1 Diameter, PI, Zeta Potential and Encapsulation Efficiency of Different Nanoparticles.

Formulation	Diameter (nm)	PI	Zeta Potential (mv)	Encapsulation Efficiency (% zol)
LCP-poly（I:C）	184 ± 25	0.22 ± 0.02	43.2 ± 5.3	N/A
Lipoplex-poly (I:C)-zoledronic acid[2]	138 ± 40	0.33 ± 0.30	44.2 ± 6.3	42 ± 5.7
CaP-poly (I:C)-zoledronic acid[2]	359 ± 15	0.12 ± 0.10	-10.1 ± 2.5	90 ± 2.4
LCP-poly (I:C)-zoledronic aicd [2]	205 ± 20	0.17 ± 0.04	21.7 ± 4.2	94 ± 1.3

Notes: Data are presented as the Mean ± standard deviation; poly (I:C)-zoledronic acid =1:1 (w/w)

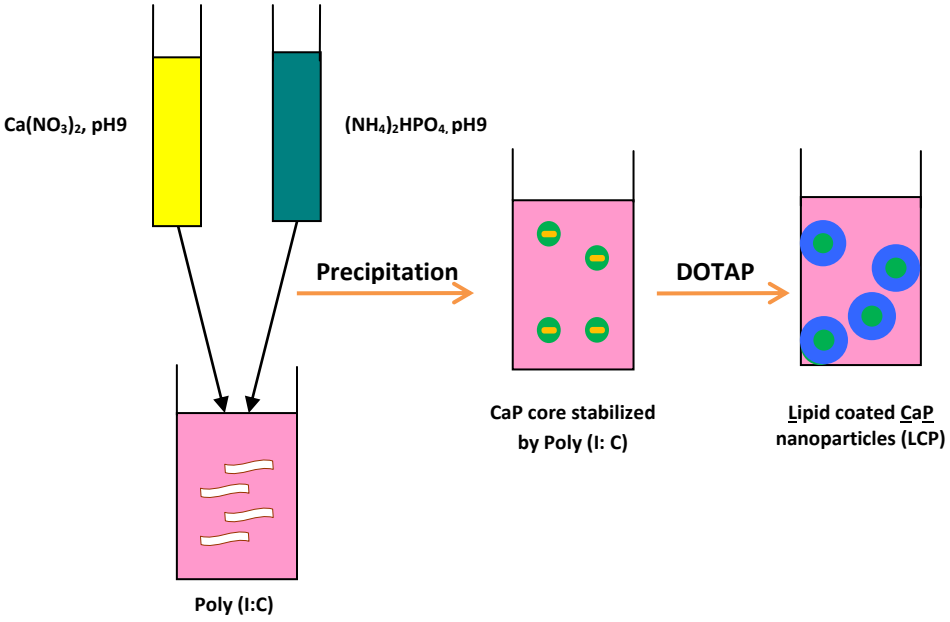

Figure 3.1 Fabrication of lipid-coated calcium phosphate nanoparticles.

A

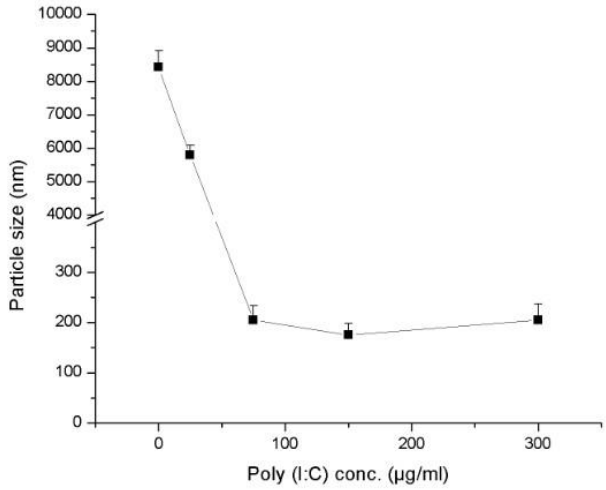

B

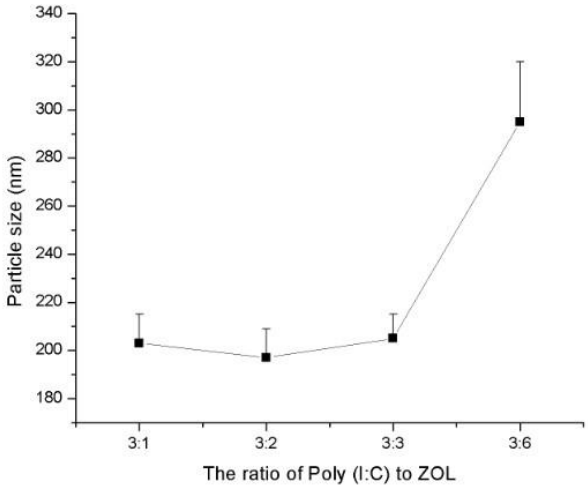

Figure 3.2 (A) Effect of Poly (I:C) on particle size of LCP without zoledronic acid. (B) Effect of ratio of Poly (I:C) to zoledronic acid on particle size of LCP.

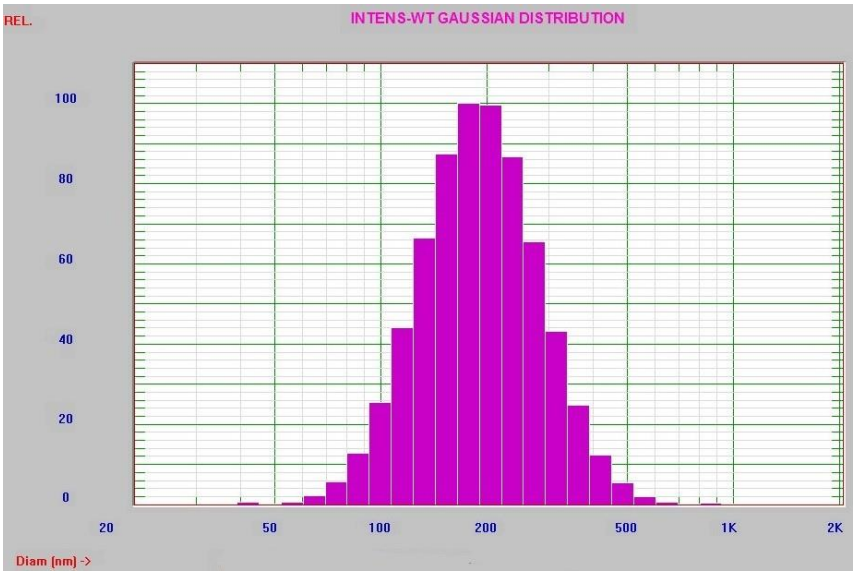

Figure 3.3 Size distribution of LCP-poly (I:C)-zoledronic acid.

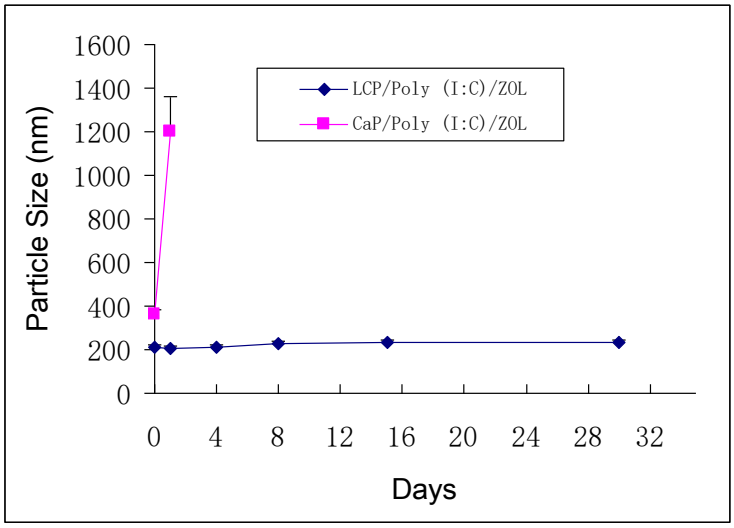

Figure 3.4 Change of particle size of LCP-poly(I:C)-zoledronic acid and CaP-poly (I:C)-zoledronic acid at 4^{o}C within 30 days.

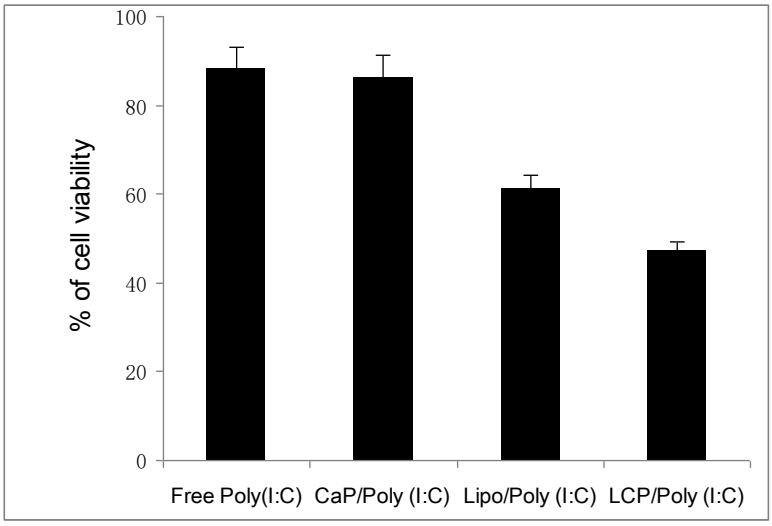

Figure 3.5 *In vitro* cytotoxicity of free poly (I:C), CaP-poly (I:C), Lipoplex-poly (I:C) and LCP poly (I:C) in B16BL6 cell line, with a poly (I:C) concentration of 0.5 μg/ml.

Notes: *$p<0.05$, compared to free poly (I:C), **$p<0.05$, compared to Lipoplex-poly (I:C).

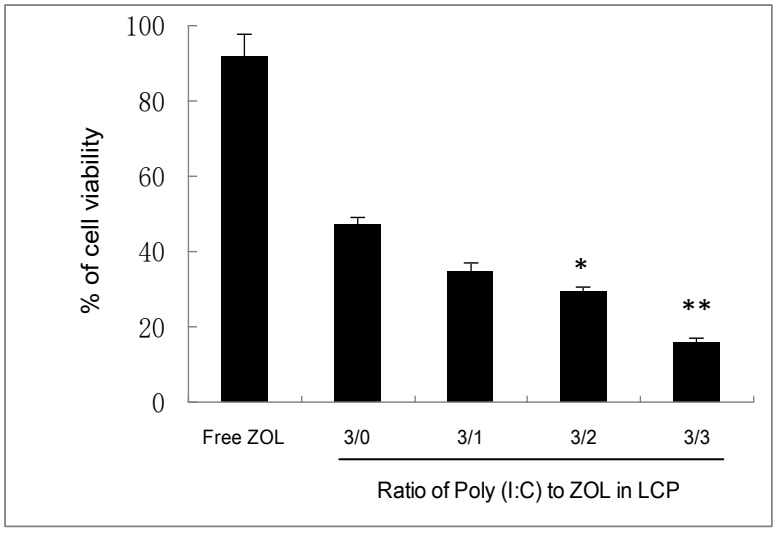

Figure 3.6 In vitro cytotoxicity of LCP-poly (I:C)-zoledronic acid in B16BL6 cell line with different weight ratios of poly (I:C) to zoledronic acid.

Notes: The concentration of total drugs (poly (I: C) & zoledronic acid) was 0.5 μg/ml. *$p < 0.05$, compared with the ratio of 3:0; **$p<0.01$, compared with the ratio of 3:0.

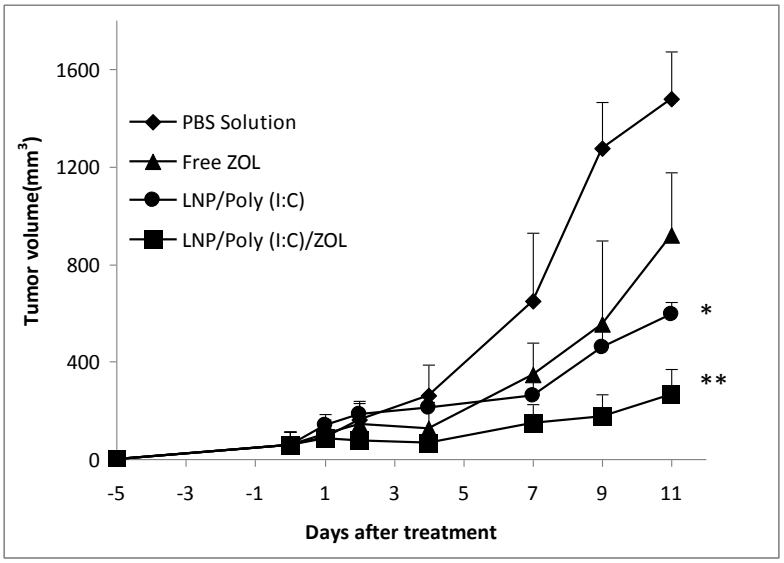

Figure 3.7 Tumor growth inhibition by poly (I:C) and zoledronic acid co-delivered by LCP in melanoma-bearing mice.

Notes: *$p < 0.05$ compared with PBS; **$p < 0.01$ compared with PBS.

4. Formulation of Genistein Microemulsion for Enhanced Transdermal Delivery

4.1 Abstract

Genistein, a soy isoflavone, is a well-known anti-oxidant effective in preventing UV induced skin damage. This study reports the formulation of microemulsions for enhanced transdermal delivery of genistein, *in vitro*. A stability indicating HPLC method for genistein was established for quantification of genistein in the microemulsions. The formulations were optimized for the stable microemulsions region in the pseudo-ternary phase diagrams and maximizing the transdermal flux of genistein. The ternary phase diagrams were constructed with different oil phases (oleic acid, medium chain triglyceride), surfactants (cremophor EL, cremophor RH 40 and polysorbate 80), co-surfactants (ethanol and transcutol P) and the ratio of surfactant to co-surfactant (5:11, 1:1 and 11:5). The formulation was optimized further by using various water contents (0%, 10%, 20%, 30% and 40%). The influence of formulation factors and stratum corneum on permeation through dermatomed human skin was determined using Franz Diffusion Cells. The ternary phase diagrams revealed that the oleic acid microemulsion had a much higher area under the curve (AUC) compared to labrafac WL1349 (38% versus 14%), due to better compatibility of oleic acid with other components in the microemulsion. All three surfactants produced similar AUC values (~36%), but the combination of Cremophor EL/ethanol (5:11) provided the maximum AUC at 38.06%. The water content in the formulation played an important role in the microemulsion stability, droplet size and transdermal flux. The oleic acid based microemulsions with 20% water exhibited a 40 fold higher fluxes than the control

(genistein aqueous suspension). The optimized formulation consisted of 2% genistein, 18% oleic acid, 60% Cremophor EL/ethanol (5:11) and 20% water. It exhibited small particle size and the highest skin permeation rate. A microemulsion system for enhanced transdermal delivery of genistein using oleic acid, cremophor EL and transcutol P was developed. Various formulation factors were evaluated to identify an optimum formulation with a high skin permeation rate for genistein.

4.2 Introduction

Non-melanoma skin cancer is the most common human malignancy. It is estimated that over 1.3 million such cancers are diagnosed each year in the USA alone (1). Moreover, malignant melanoma has exhibited the most rapid increase in incidence compared to any other type of cancer (2). Chronic exposure to solar UV radiation, in particular its UVB component, is the primary cause for the vast majority of cutaneous malignancies (3-5). The development of preventive and therapeutic agents against photo carcinogenesis has become an important subject in dermatological research (6). Genistein, a soy isoflavone, is a well-known anti-oxidant effective in preventing UV induced skin damage and melanoma (7). Genistein can alleviate hormone-dependent physiological symptoms (8), prevent skin aging and inhibit UVB-induced skin carcinogenesis and photo-damage in animals (6, 9, 10). The possible mechanisms of the anti-carcinogenic action include scavenging of reactive oxygen species (11, 12), blocking of oxidative and photodynamic damage to DNA (13), inhibition of tyrosine protein kinase (14), down-regulation of Mitogen-Activated Protein Kinases (MAPK) activation and suppression of oncoprotein expression in UVB-irradiated cells (15). Topical administration is a viable route for delivering genistein as a protective agent against photo-induced skin damage. Topical delivery may also be a suitable route for genistein to attain systemic bioavailability (16).

However, intradermal delivery of genistein is inefficient due to its low permeability as well as low solubility in both aqueous and organic media (17). Many delivery systems, such as gels (18), emulsions (19) and liposomes (20), have been developed to enhance the skin permeation of genistein. Microemulsions (ME) provide another means for dermal and transdermal delivery of drugs. Microemulsions are commonly known as oil-in-water or water-in-oil emulsions producing a transparent product having a droplet size from 10 to 100 nm that does not have the tendency to coalesce (21). It is a spontaneously formed, single-phase colloidal dispersion of either oil-in-water or water-in-oil, stabilized by an interfacial film of surfactants and co-surfactants. Also, it is a transparent, optically isotropic, thermodynamically stable system (22). They have been studied as transdermal drug delivery systems because of their capacity to increase the solubility of poorly water-soluble drugs, as well as their ability to improve topical and systemic drug availability (23-25). Several mechanisms have been proposed to explain the advantages of microemulsions for the topical and dermal delivery of drugs: the high drug loading capacity of microemulsions and their in situ super-saturation could provide a higher concentration gradient that increases the driving force across the skin; the penetration enhancing effect of the microemulsion components; direct transfer of drug from the microemulsion droplet to the stratum corneum; and the very low interfacial tension that causes excellent spreading and contact between the microemulsion and skin surface (26-30).

In this study, we validated a high performance liquid chromatography (HPLC) method for analyzing genistein in microemulsions and skin permeation studies. Pseudo-ternary phase diagrams were then used for the selection of concentration ranges of different components (oil, surfactant and co-surfactant). Finally, the formulations were further optimized based on in vitro skin permeation and skin retention studies.

4.3 Materials and Methods

4.3.1 Reagents and Chemicals

Genistein was obtained from LC laboratories (Woburn, MA). Oleic acid was purchased from Spectrum Chemical Corporation (Gardena, CA). Cremophor-EL and Cremophor-RH40 were purchased from BASF (Ludwigshafen, Germany). Ethanol and polysorbate 80 were purchased from Letco Medical (Decatur, AL). Labrafac WL1349 and Transcutol P were samples donated by Gaffeose (Cedex, France). Trifluoroacetic acid and acetonitrile were purchased from EMD Chemical Inc. (Gibbstown, NJ). All other reagents were purchased from VWR International (West Chester, PA).

4.3.2 Methods

4.3.2.1 HPLC Method Validation

A Waters high performance liquid chromatography (HPLC) system equipped with PDA-UV detector (Alliance 2695 Separation module and 996 PDA detector) (Waters Corporation, Milford, MA) was used in this study. The system was interfaced with Empower 2 software. The chromatographic separation was carried out on a reversed phase Phenomenex, Luna® C18 Column (5 µm, 250 × 4.6 mm). Standards were prepared by accurately weighing and transfering about 25 mg of genistein into a clean, dry 25 mL volumetric flask. About 15 mL of ethanol was added followed by sonication to dissolve and the volume was made up to 25 mL with ethanol and mixed thoroughly. This provided 1 mg/ml of genistein standard solution. The diluent solutions was prepared by mixing 100 and 900 ml each of water and ethanol, respectively, and filtering through a 0.45 µm nylon filter. The final concentration of genistein of approximately 60 µg/ml was achieved by diluting the standard solution with diluent. The sample

preparation followed the same procedure as the standard preparation except for replacing genistein with genistein loaded formulation.

A full validation of the method was performed according to the current FDA Guidelines. It was validated for system suitability, linearity, accuracy and recovery, precision, intermediate precision, solution stability, limit of detection (LOD), limit of quantitation (LOQ) and forced degradation (stress).

4.3.2.1.1 System Suitability: system suitability was tested by injecting the working standard preparation (60 µg/ml standard genistein solution, 25 µl) six times at the beginning of the run. Injecting the working standard preparation once after every six sample preparation injections (60 µg/mL solution of genistein formulation, 25 µl), and at the end of the run is required. Three parameters: resolution factors, tailing factor and column efficiency (number of theoretical plates) were calculated using the Enpower2 software provided by Waters Corporation (Milford, MA).

4.3.2.1.2 Linearity: standard solutions of the analyte were prepared at eight different linearity levels ranging from 10% to 200% of the theoretical sample concentration (60 µg/ml). For each run, the sample was analyzed with three independent injections. The calibration curve equations and the corresponding correlation coefficients (R^2) were calculated.

4.3.2.1.3 Accuracy: accuracy was determined by analyzing three known concentrations of samples of genistein emulsion formulation in triplicate, corresponding to approximately 80%, 100% and 120% of the analyte concentrations at the theoretical assay levels.

4.3.2.1.4 Precision: Method Precision/Repeatability was determined by analyzing six test preparations of genistein emulsion formulation. Intermediate precision of the assay method was determined by evaluating two independent sets of assay sample preparations. The first set was taken from the precision samples. The second was taken from six assay sample preparations prepared by a second analyst on a different day. Precision was assessed by calculating the mean and the coefficient of variation (RSD %) of these values.

4.3.2.1.5 Solution Stability: the stability of sample and standard solutions from method precision experiments was determined when these solutions were stored under laboratory conditions for at least 48 h. At 72 h intervals the responses of the aged solutions against freshly prepared standards were measured and any changes between the chromatographic profile of aged and fresh solutions were compared.

4.3.2.1.6 Limit of Detection (LOD) and Limit of Quantitation (LOQ): the Limit of Detection and Quantitation (LOD and LOQ) were determined according to signal to noise ratio (s/n) of diluted standard solution. The diluted standard solutions were prepared by serial dilutions of the working standard with signal-to-noise ratio around 2-3 for LOD and 6-15 for LOQ， then the diluted standards solutions were injected three times for LOD and six times for LOQ.

4.3.2.1.7 Stress Study: genistein microemusion was subjected to forced degradation under acid, alkaline, light and oxidative (hydrogen peroxide) conditions in the solution state. 1.5 g of genistein microemulsion or placebo microemulsion was placed in 25 ml volumetric flasks and exposed to various stress conditions. In order to achieve approximately 30% genistein degradation, various stress conditions were adjusted as follows: 1) Acid: 1 ml, 1N HCl, 60^{o}C, 4

h; 2) Base: 1 ml, 0.1N NaOH, 60^{o}C, 1 h; 3) Oxidation: 1 ml,1% H_2O_2, Ambient, 8 h; 4) UV light: ambient, 24h; 5) Control: Untreated sample, Ambient, 1 h. After exposures, the samples were quenched (if necessary), brought to room temperature and the volume was made to 25 mL with diluent as stated in the above HPLC method. Samples were periodically analyzed by HPLC to determine the extent of degradation under different stress conditions.

4.3.2.2 Formulation Optimization

Initially, the solubility of genistein in various solvents was determined to select appropriate oils (oleic Acid and labrafac WL1349), surfactants (polysorbate 80, cremophor-EL and cremophor-RH40) and co-surfactants (ethanol and transcutol P). An excess of genistein was added to 5 ml of oil or surfactant or co-surfactant and the resulting mixture was shaken reciprocally at 37 ^{o}C for 72 h followed by centrifugation for 10 min at 15,000 g (31). The supernatant was filtered through a nylon membrane filter (0.45 µm) and the filtrate was analyzed by HPLC. The oil, surfactant and co-surfactant that showed the highest solubility of genistein were chosen for future formulations for human skin permeation studies.

The microemulsion was evaluated by a pseudo-ternary phase diagram indicating the phase behavior and miscibility of various microemulsion components. For each phase diagram, a specific surfactant to co-surfactant weight ratio (S/CoS), oily mixture, surfactant and co-surfactant were prepared with a weight ratio of oil to the mixture of surfactant and co-surfactant at 0.5:9.5, 1:9, 1.5:8.5, 2:8, 2.5:7.5, 3:7, 4:6, 5:5, 6:4,7:3, 7.5:2.5, 8:2, 8.5:1.5, 9:1 and 9.5:0.5, respectively (32). Water was added drop wise to each oily mixture with continuous stirring at 37^{o}C until the mixture became clear. The formulations were optimized by determining the existence area of microemulsions in the phase diagram with the following factors: types of oil phase, surfactant, co-surfactant and different ratios of surfactant to co-surfactant. The S/CoS

value was 5:11, 1:1 and 11:5. Finally, different water contents (w/w, at 10%, 20%, 30% and 40%) were utilized and particle size was determined by a Nicomp 380 ZLS Particle Size Analyzer. Genistein loaded microemulsions were prepared by dissolving the appropriate amount of genistein in the mixture of oil, surfactant and co-surfactant, then water was added precisely drop by drop into the oily phases with magnetic stirring at 37^{o}C. The systems were equilibrated with gentle magnetic stirring for another 30 min. The final concentration of genestein in microemulsions was 2 % (w/w).

4.3.2.3 Transdermal Delivery of Genestein by Microemulsions

4.3.2.3.1 Skin Permeation: dermatomed human skin (thickness: 0.35 mm) was obtained from Allosource (Cincinnati, Ohio). It was collected from a single donor within 8 h of death and frozen at -80 ºC until use. The frozen skin was placed at room temperature for about 30 minutes prior to skin permeation experiments. The Franz diffusion cell instrument (PermeGear, Bethlehem, PA) holding 6 diffusion cells in series was used in this study. The skin was mounted horizontally between the donor and receptor parts of the diffusion cell. The surface area of the skin exposed to the tested formulation was 0.64 cm^2. Receptor medium applied in the study was 5 mL of 0.01 M phosphate buffered saline pH 7.4 (PBS) and ethanol with a volume ratio of 4 to 1. A water circulation jacket (37ºC) system was used to maintain the temperature of skin mounted above receptor cells at a physiologic level with 600 rpm stirring rate in the receptor cells. The skin was mounted on the cells approximately 30 minutes before application of the formulations. Each formulation (0.5 ml) was applied over the surface of the skin. The donor chamber was covered with Parafilm to prevent evaporation of water from the formulations (33). Samples (1 mL) were taken from the receptor cells to measure the amount of drug transported across the skin at 0, 1, 2, 4, 6, 8, 12 and 24 h. The samples were replaced by fresh receptor

medium and accumulative amount of drugs permeated were calculated account for drug removed during sampling. Skin microporation was induced by solid metallic microneedle arrays of a Dermaroller™ (Dermaoller Deutschland, Wolfenbuttel, Germany), which wereapplied on the surface of skin 20 times to create micro-channels. This corresponds to the number of times required to produce detectable holes without damaging the microneedles and skin (34). Finally, to determine whether the stratum corneum (SC) is the major barrier for skin permeation of genistein, the permeation of various formulations were studied through stripped skin. The stripped skin samples were obtained by removing the SC with Scotch® book tape Number 845. The tape stripping numbers varied from 10 to 30 to get as much SC removal as possible from the different skin samples. SC removal was confirmed by visualization of a shiny surface (35).

4.3.2.3.2 Skin Retention: at the end of the experiment (24 h), the residual drug formulation on the surface of the skin was removed using cotton swabs by swabbing the surface with 200 µl of mixture of ethanol and water (1:1) for six times. The active diffusion area of the skin was then collected using a biopsy punch to determine the drug retention in the skin. The skin was weighed, cut into small pieces, placed in centrifugation tubes and 1 mL of a solution of ethanol and water (1:1) was added and refrigerated overnight. The samples were then warmed to room temperature, sonicated for 15 minutes and the supernatant was filtered using 0.22 µm syringe filters into HPLC vials for the assay (33).

4.4 Results and Discussion

4.4.1 HPLC Method Validation

A stability indicating HPLC method for genistein was established by optimizing isocratic flow parameters of the mobile phase. The HPLC method used a C18 column (5 µm

silica particles, 150 X 4.6 mm), mobile phase : 35% (v/v) of 0.1% trifluoroacetic acid in acetonitrile and 65% (v/v) of 0.1% trifluoroacetic acid in water at 1.5 ml/min and a PDA-UV detector set at 262 nm. The total run time was 10 minutes and the injection volume was 25 µl. All chromatographic procedures were performed at room temperature. Strong solvents such as acetonitrile or ethanol induced peak fronting or tailing issues whereas ethanol-water (v/v 9:1) used as the diluent gave better peak shape, resolution and a stable baseline. Optimum peak shape was achieved at 0.1% (v/v) trifluoroacetic acid as an ion-pairing agent (Figure 4.1). The resolution factor was 2.77, so there is no interference from other peaks and the system has good specificity for genistein. The different valuation parameters were listed in Table 4.1. This method provided an USP tailing factor of 0.98; Plate count of 5000. The parameters show that the chromatographic system is very efficient. The method was linear between 6 and 120 µg/ml for genistein, corresponding to the tested concentrations with a correlation coefficients (R^2) always greater than 0.99. As shown in Table 4.1, the accuracy, precision and intermediate precision of the assay at different genistein concentrations as represented by the coefficient of variation of the peak areas, which was always less than 1.0%, indicated that the method is precise and accurate. LOD and LOQ were 1.6 µg/ml and 6.4 µg/ml, respectively. The standard preparation is stable in solution at room temperature for 3 days and the recovery was 95.0-105.0% of the initial results. As shown in Figure 4.2, genistein is well resolved from forced degradation products under all stress conditions. The purity angle is less than the purity threshold for all stress conditions indicating that genistein peaks are pure and without interference. Under all stress conditions of the placebo emulsion formulation, all excipients and degradation products are well resolved from the expected retention times of genistein peak. Genistein was highly stable under acidic conditions, but degraded to all non-polar products under alkaline conditions, whereas the

oxidative condition produced relatively polar degradation products compared to the parent compound.

The analytical method was proven to be specific, linear, precise, rugged, accurate, and stability indicating. Therefore, the analytical method was validated and suitable for its intended use.

4.4.2 Formulation Optimization through Solubility and Pseudo-ternary Phase Diagrams

The solubility of genistein in various media was analyzed to screen components for microemulsion preparation. Table 4.2 presents the genistein solubility in different solvents. Among the three surfactants, the solubility of gensitein was highest in cremophor EL (37.11 mg/g), followed by Tween 80 (5.34 mg/g), and cremophor RH40 (5.24 mg/g). In oil, genistein had a significantly higher solubility in labrafac WL1349 (0.40 mg/g) than oleic acid (0.02 mg/g). Oleic acid is a powerful permeation enhancer for dermal delivery through increased fluidity of the lipid portion of the stratum corneum (36). Thus, oleic acid was chosen as the oil for the microemulsions containing genistein. Genistein has good solubility in both co-surfactants with the value higher in transcutol P (93.21 mg/g) than in ethanol (20.29 mg/g).

The construction of pseudo-ternary phase diagrams with the water titration method makes it easy to identify the concentration range of components for the microemulsion formation. The pseudo-ternary phase diagrams with various oil phases, surfactants, co-surfactants, and S/CoS values are presented in Figure 4.3 & 4.4. The translucent microemulsion region is presented in the phase diagrams as ME. The region labeled EM represents the turbid and conventional emulsions based on visual observation. Figure 4.3 showed that formulation with oleic acid has a 2.5 fold higher microemulsion area as compared to the one with labrafac WL 1349 (38.06% and 14.37%, respectively). The main factor determining the microemulsion

zone is the physicochemical properties of components in the formulation. The penetration and association of oil molecules with the interfacial surfactant film is essential for providing a very low surface tension (37). The oleic acid has better miscibility with other components of the microemulsion, encouraging the formation of an O/W microemulsion. Surfactant plays an important role in decreasing surface tension between oil and water, leading to the formation of microemulsion (38). There is no significant difference in microemulsion formation region using the three different surfactants. The ME areas were 36.73%, 36.59% and 35.36% for the microemulsions prepared with polysorbate 80, cremophor RH40, and cremophor EL separately (Figure 4.4 (a) (b) (c)). This may be due to the similar HLB (Hydrophilic-Lipophilic Balance) values for all three surfactants.

However, since surfactants are unable to lower the interfacial tension between the oil and water to ultra-low values, co-surfactant is frequently necessary in a microemulsion system. Incorporation of co-surfactant can further reduce the interfacial tension between the oil and water, adjust the flexibility of the interfacial membrane, and reduce the amount of surfactant needed (39). A similar result was obtained from transcutol P-based and ethanol-based microemulsion system (Figure 4.4 (c) (d)). The area of microemulsion isotropic region changed slightly in size with increased S/CoS value (Km). In the system using oleic acid, cremophor EL as surfactant, ethanol as co-surfactant, the area of microemulsion was largest when Km was 5 to 11, followed by 1 to 1 and 11 to 5. This indicated that increasing the amount of ethanol facilitated the formation of microemulsion. Ethanol has good miscibility with surfactant and oil (40). As water plays an important role in both microemulsion formulation and skin permeation (41), the formulations were prepared with different amounts of water and the particle size changed significantly (Figure 4.5). The particle size remained below 200 nm when the water

content was below 20%. However, the particle size increased dramatically to approximately 4000 nm with 30% water and to 7000 nm with 40% water. This suggested the absence of microemulsion in formulations with 30% and 40% water. The increased water content led to a decreased percentage of other components in the formulation, especially the surfactant and co-surfactant, which increased surface tension, which inhibited the formation of microemulsion.

4.4.3 Human Skin permeation and Retention of Genestein

Skin permeation studies were conducted to obtain an optimum formulation with enhanced skin permeation. Figure 4.6 shows that the oleic acid based formulation increased skin permeation and deposition 3-fold as compared to the microemulsion made with Labrafac WL 1349 ($P<0.001$). OA-induced skin penetration enhancement was due to a mechanism involving both SC lipid fluidization and phase separation; with the latter is probably predominating (42). Unsaturated hydrocarbons in OA could induce lipid disordering in the superficial layers of the SC, whereas labrafac WL1349 has no influence on this process. Unsaturated fatty acids (like oleic acid) form a separate fluid domain when introduced into a solid, saturated lipid mixture (like SC lipids). OA-induced transdermal penetration enhancement occurs as a result of increased permeability at the interface between solid and fluid lipid domains formed by the incorporation of OA into the membrane. The formation of such pools provides permeability defects within the bilayer lipids, thus facilitating permeation of drugs through the membrane (36, 43). The effects of three different nonionic surfactants on skin permeation and retention were also investigated (Figure 4.7). Formulations with Cremophor EL and Cremophor RH40 have similar skin permeation rate, while the one with polysorbate 80 has slightly lower skin permeation. Generally, nonionic surfactants have low toxicity (44, 45). This group of surfactants has an enhancement effect in human skin permeation which could be attributed to disruption of

lipid bilayers in SC. The system with ethanol as a co-surfactant demonstrated 7 and 2.5 fold higher skin permeation and retention, respectively, as compared to the one with Transcutol P ($P<0.001$) (Figure 4.8).

Ethanol is well-known compound commonly used in transdermal formulations. It has a superior ability to facilitate skin permeation of drugs and excellent miscibility with other components of microemulsions. It is capable of extracting lipids from SC to improve drug permeation. Additionally, permeation of ethanol into the SC can alter the solubility properties of the tissue with a consequent improvement of drug partitioning into the membrane (46). Additionally, it is feasible that the rapid permeation of ethanol or evaporative loss of this volatile solvent from the donor phase modifies the thermodynamic activity of the drug within the formulation (47). The value of S/CoS in ME affected the skin permeation rate of genistein significantly (Figure 4.9). As the value decreased from 11 to 5, the skin permeation rate of genistein increased 3-fold. This confirms that ethanol contributed to improved permeation of genistein across intact skin.

Water is a critical factor that affects the transdermal delivery of drugs (41). The genistein permeation across both intact human skin (Figure 4.10) and microneedle treated skin (Figure 4.11) for different water contents and two controls: aqueous base and emulsion base. The genistien permeation with changed water content exhibited a parabolic profile in both intact skin and microneedle treated skin. Increasing the content of water led to improved skin permeation and retention of genistein. The formulation with 20% water demonstrated 3.5 fold higher skin permeation as compared to 10% water ($P<0.001$) (Figure 4.10). Permeation reached a maximum at 30% water. This is because drug has to be dissolved in the aqueous phase to diffuse into the skin lipid bilayer. However, the genistein permeation decreased dramatically with 40% water

compared with 30% water in the formulation. The genistein retention on both intact skin and microneedle treated skin (Figure 4.12) demonstrated a similar trend as in the permeation studies. These results can be explained by two possible mechanisms: the decreased soluble fraction drug in the formulation as the percentage of water increased. The thermodynamic activity decreased with increased water content which impaired skin penetration.

The outermost layer of skin, the stratum corneum (SC), presents a significant barrier to the transdermal delivery of drugs (48, 49). Microneedles have been used to overcome the stratum corneum barrier. Microneedles are minimally invasive devices that can deliver drug into or through the skin barrier. Surprisingly, Figure 4.12 & 13 showed that microneedle treated skin did not significantly increase the permeation and retention of genistein from any of the formulations ($P>0.05$). This suggests that the SC barrier was overcome by the permeation enhancement of the microemulsion formulations. This is due to both formulation components and the combination of these components in the nanoparticle based delivery system. To further confirm this phenomenon, the SC was removed through tape-stripping. The tape stripped skin showed no significant increase in genistein permeation compared to intact skin.

4. 5 Conclusion

A stability indicating HPLC method was developed for genistein for use in studying the stability and degradation profiles of genistein in topical based formulations. Various factors affecting the microemulsion formulation, and skin permeation and deposition of genistein were studied. The optimum microemulsion formulation for stability and skin permeation is composed of oleic acid (18%), cremophor EL-ethanol (1:2.2) (60%) and water (20%), and genistein (2%). This formulation had significantly increased skin permeation and deposition compared with microemulsions made with other components and both aqueous base and emulsion base controls.

4.6 References

1. Nevillek JA, Welch E, Leffell DJ. Management of nonmelanoma skin cancer in 2007. Nat Clin Pract.2007; 4: 462-469.
2. Moore JO, Wang Y, Stebbins WG, et al. Photoprotective effect of isoflavone genistein on ultraviolet B-induced pyrimidine dimer formation and PCNA expression in human reconstituted skin and its implications in dermatology and prevention of cutaneous carcinogenesis. Carcinogenesis.2006; 27: 1627–1635.
3. Afaq F, Syed DN, Malik A, et al. Delphinidin, an anthocyanidin in pigmented fruits and vegetables, protects human HaCaT keratinocytes and mouse skin against UVB-mediated oxidative stress and apoptosis. J Invest Dermatol. 2007; 127: 222–232.
4. Kelfkens G, Cruijl FR, van der Leun JC. Tumorigenesis by short-wave ultraviolet A: papillomas versus squamous cell carcinomas. Carcninogenesis. 1991; 12: 1377–1382.
5. Cruijl FR, Sterenborg HJCM, Cole C, et al. Wavelength dependence of skin cancer induction by ultraviolet irradiation of albino hairless. Cancer Res.1993; 53: 53-60.
6. Wei H, Zhang X, Wang Y, Lebwohl M.Inhibition of ultraviolet light-induced oxidative events in the skin and internal organs of hairless mice by isoflavone genistein. Cancer Lett. 2002; 185(1):21-9.
7. Brand RM, Jendrzejewski JL. Topical treatment with (-)-epigallocatechin-3-gallate and genistein after a single UV exposure can reduce skin damage. J Dermatol Sci.2008; 50: 69–72.
8. Daniel S, Esther B, Sandra Meister. Use of soy isoflavones for stimulation of skin collagen systhesis. Mibelle Biochemistry, Switzerland. 2008.

9. Widyarini S, Husband AJ, Reeve VE. Protective effect of the isoflavonoid equol against hairless mouse skin carcinogenesis induced by UV radiation alone or with a chemical cocarcinogen. Photochem Photobiol. 2005; 81: 32–37.

10. Shyong EQ, Lu Y, Lazinsky A, et al. Effects of the isoflavone 4,5,7-trihydroxyisoflavone (genistein) on psorelen plus ultra-violet A radiation (PUVA)-induced photodamage. Carcinogenesis. 2002; 23: 317–321.

11. Peak MJ, Peak JG. Solar-ultraviolet-induced damage to DNA. Photodermatology.1982; 6: 1–15.

12. Beehler BC, Przybyszewski J, Box HB, Kulesz-Martin MF. Formation of 8-hydroxydeoxyguanosine within DNA of mouse keratinocytes exposed in culture to UVB and H_2O_2. Carcinogenesis, 1992; 13: 2003–2007.

13. Kim SY, Na YJ, Kim D, et al. Development of estimation methods of skin oxidation and evaluation of anti-oxidative effects of genistein in topical formulations. Korean J Physiol Pharmacol. 2012; 16(3):205-9.

14. Foti P, Erba D, Riso P, et al. Comparsion between daidzein and genistein antioxidant activity in primary and cancer lymphocytes. Arch Biochem Biophys. 2005; 433(2):421-7.

15. Pavese JM, Farmer RL, Bergan RC. Inhibition of cancer cell invasion and metastasis by genistein. Cancer Metastasis Rev. 2010; 29(3):465-82.

16. Busby MG, Jeffcoat AR, Bloedon LT, et al. Clinical characteristics and pharmacokinetics of purified soy isoflavones: single-dose administration to healthy men. Am J Clin Nutr. 2002, 75: 126–136.

17. Kitagawa S, Inoue K, Teraoka R, Morita SY. Enhanced skin delivery of genistein and other two isoflavones by microemulsion and prevention against UV irradiation-induced erythema formation. Chem Pharm Bull. 2010; 58(3):398-401.

18. Chadha G, Sathigari S, Parsons DL, Jayachandra Babu R. In vitro percutaneous absorption of genistein from topical gels through human skin.Drug Dev Ind Pharm. 2011; 37(5):498-505.

19. Silva AP, Nunes BR, Oliveira MC, et al. Development of topical nanoemulsions containing the isoflavone genistein. Pharmazie. 2009; 64(1):32-5.20.

20. Kang KH, Kang MJ, Lee J, Choi YW. Influence of Liposome Type and Skin Model on Skin Permeation and Accumulation Properties of Genistein. J Dispers Sci Technol, 2010, 31:1061–1066.

21. Rhee YS, Choi JG, Park ES, Chi SC. Transdermal delivery of ketoprofen using microemulsions. Int J Pharm. 2001; 228(1-2):161-70.

22. Wu H, Ramachandran C, Weiner ND, Roessler BJ. Topical transport of hydrophilic compounds using water-in-oil nanoemulsions. Int J Pharm. 2001; 220(1-2):63-75.

23. Ngawhirunpat T, Worachun N, Opanasopit P, et al. Cremophor RH40-PEG400 microemulsions as transdermal drug delivery carrier forketoprofen. Pharm Dev Technol. 2013; 18(4):798-803.

24. Lee J , Lee Y, Kim J, et al.Formulation of microemulsion systems for transdermal of aceclofenac. Arch Pharm Res. 2005; 28(9):1097-102.

25. Lee PJ, Langer R, Shastri VP. Novel microemulsion enhancer formulation for simultaneous transdermal delivery of hydrophilic and hydrophobic drugs. Pharm Res. 2003; 20(2):264-9.

26. Kweon JH, Chi SC, Park ES. Transdermal delivery of diclofenac using microemulsions. Arch Pharm Res. 2004; 27(3):351-6.

27. Peltola S, Saarinen-Savolainen P, Kiesvaara J, et al. Microemulsions for topical delivery of estradiol. Int J Pharm. 2003; 254(2):99-107.

28. EI Maghraby GM. Microemulsions as Transdermal Drug Delivery Systems. Current Nanoscience, 2012, 8:504-511.

29. Kreilgaard M. Influence of microemulsions on cutaneous drug delivery. Adv Drug Deliv Rev. 2002; 54:77-98.

30. Dreher F, Walde R, Walther R, Wehrli E. Interaction of a lecithin microemulsion gel with human stratum corneum and its effect on transdermal transport. J Control Release.1997; 45: 131-140.

31. Qi X, Qin J, Ma N, Chou X, Wu Z. Solid self-microemulsifying dispersible tablets of celastrol: formulation development, charaterization andbioavailability evaluation. Int J Pharm. 2014; 472(1-2):40-7.

32. Patel MR, Patel RB, Parikh JR, et al. Effect of formulation components on the in vitro permeation of microemulsion drug delivery system of fluconazole. AAPS PharmSciTech. 2009; 10(3):917-23.

33. Chadha G, Sathigari S, Parsons DL, Jayachandra Babu R. In vitro percutaneous absorption of genistein from topical gels through human skin. Drug Dev Ind Pharm. 2011; 37(5):498-505.

34. Nayak A, Das DB, Vladisavljevic GT. Microneedle assisted permeation of lidocaine carboxymethylcellulose with gelatine co-polymer hydrogel. Pharm Res. 2014; 31(5):1170-84.

35. Challapalli PV, Stinchcomb AL. In vitro experiment optimization for measuring tetrahydrocannabinol skin permeation. Int J Pharm. 2002; 241(2):329-39.

36. Francoeur ML, Golden GM, Potts RO, Oleic acid: its effects on stratum corneum in relation to transdermal drug delivery. Pharm Res.1990, 7: 621-627.

37. Malcolmson C, Satra C, Kantaria S, et al. Effect of oil on the level of solubilization of testosterone propionate into nonionic oil-in-water microemulsions. J Pharm Sci. 1998; 87(1):109-16.

38. Moghadam SH, Saliaj E, Wettig SD, et al. Effect of chemical permeation enhancers on stratum corneum barrier lipid organizational structure and interferon alpha permeability. Mol Pharm. 2013; 10(6):2248-60.

39. Chen L, Tan F, Wang J, Liu F. Microemulsion: a novel transdermal delivery system to facilitate skin penetration of indomethacin. Pharmazie. 2012; 67(4):319-23.

40. Berner B, Mazzenga GC, Otte JH, et al. Ethanol: water mutually enhanced transdermal therapeutic system: II. Skin permeation of ethanol and nitroglycerin. J Pharm Sci. 1989, 78: 402–407.

41. Adrian CW, Brian WB. Penetration enhancers. Adv Drug Deliv Rev. 2012, 64:128–13.

42. EI Maghraby GM. Transdermal delivery of hydrocortisone from eucalyptus oil microemulsion: effects of cosurfactants. Int J Pharm. 2008; 355(1-2):285-92.

43. Naik A, Pechtold LARM, Potts RO, Guy RH. Mechanism of oleic acid-induced skin penetration enhancement in vivo in humans. J Control Release.1995, 37: 299–306.

44. Sarpotdar PP, Zatz JL. Percutaneous absorption enhancement by non-ionic surfactants. Drug Dev Ind Pharm, 1986; 12:1625-1647.

45. Sarpotdar PP, Zatz JL. Evaluation of penetration enhancement of lidocaine by non-ionic surfactants through hairless mouse skin in vitro. J Pharm Sci, 1986; 75:176.

46. Pershing LK, Lambert LD, Knutson K. Mechanism of ethanol-enhanced estradiol permeation across human skin in vivo. Pharm Res, 1990, 7: 170–175.

47. Megrab NA, Williams AC, Barry BW. Estradiol permeation across human skin, silastic and snake skin membranes: the effects of ethanol/water co-solvent systems. Int J Pharm, 1995, 116:101–112.

48. Notman R, Anwar J. Breaching the skin barrier--insights from molecular simulation of model membranes. Adv Drug Deliv Rev. 2013; 65(2):237-50.

49. Lane ME. Skin penetration enhancers. Int J Pharm. 2013 Apr 15; 447(1-2):12-21.

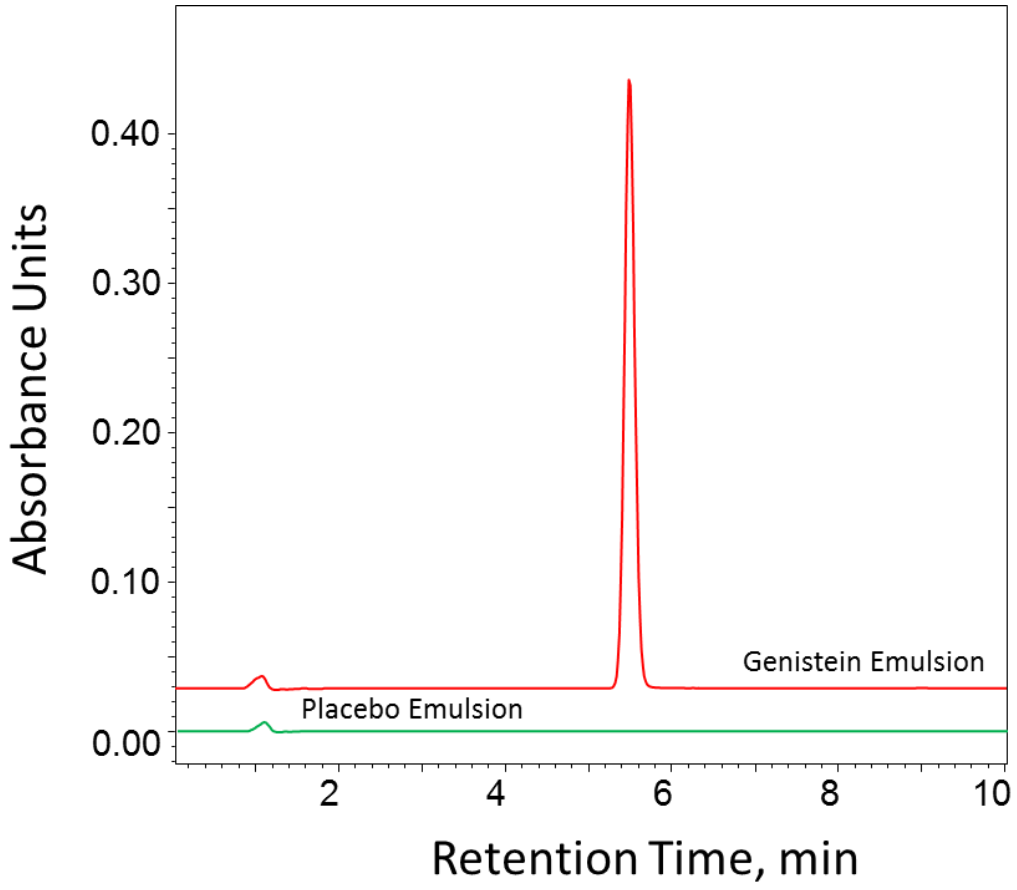

Figure 4.1 HPCL of placebo emulsion and genistein loaded microemulsions.

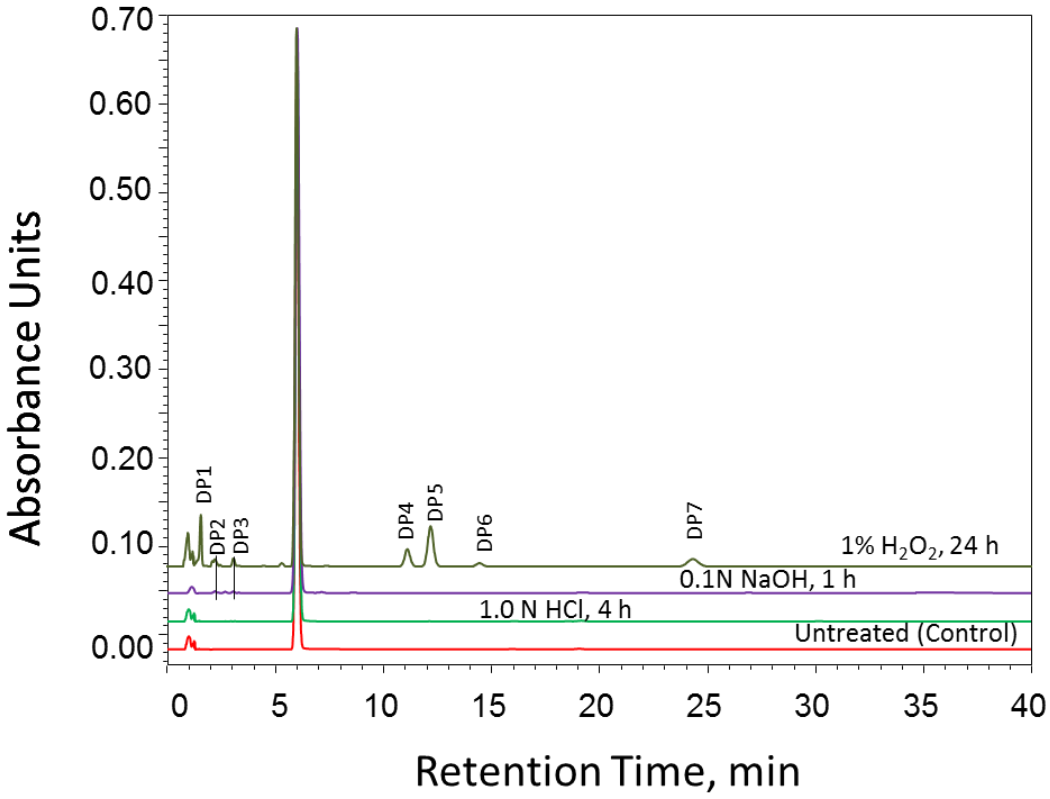

Figure 4.2 HPCL of forced degradation products of genistein microemulsions under different stress conditions.

Table 4.1 HPLC method validation parameters for genistein in a microemulsion system

System Suitability

	Tailing factor (T)	Resolution (Rs)	Theoretical plate number (N)
Specifications	≤ 2	> 2	> 2000
Experimental Results	0.98	2.77	5000

Accuracy

Conc. spiked (mg/g)	Theoretical concentration (%)	Experimental concentration (mg/g) ± SD*, n=3	% Recovery	% RSD
2.0	80	1.94 ± 0.039	97.09	0.39
2.5	100	2.46 ± 0.021	98.55	0.21
3.0	120	2.93 ± 0.041	97.57	0.41

Precision

HPLC System/ analyst	Theoretical concentration (mg/g)	Experimental concentration (μg/mL) ± SD*, n=6	% Recovery	% RSD
1	2.5	2.49 ± 0.012	99.70	0.465
2	2.5	2.44 ± 0.013	97.64	0.539

Stress study

Condition	Purity Angle	Purity Threshold	% Label Claim	% Recovery	% Degradation
Control (Untreated)	0.029	0.257	97.12	---	---
1N HCl, 70^{o}C, 4h	0.117	0.249	95.80	98.64	1.36
0.1N NaOH, 70^{o}C, 1 h	0.065	0.313	90.97	88.39	11.61
UV Light, Ambient, 24h	0.491	1.077	79.79	96.13	3.87
1% H_2O_2, 70^{o}C, 8 h	0.241	0.248	93.37	82.15	17.85

Table 4.2 The solubility of genistein in different solvents

Solvent	Solubility (mg/g)
Oleic Acid	0.02 ± 0.01
Labrafac WL139	0.40 ± 0.07
Cremophor EL	37.1 ± 2.1
Cremophor RH40	5.24 ± 0.43
Polysorbate 80	5.34 ± 0.17
Transcutol P	93.2 ± 3.0
Ethanol	20.3 ± 1.4

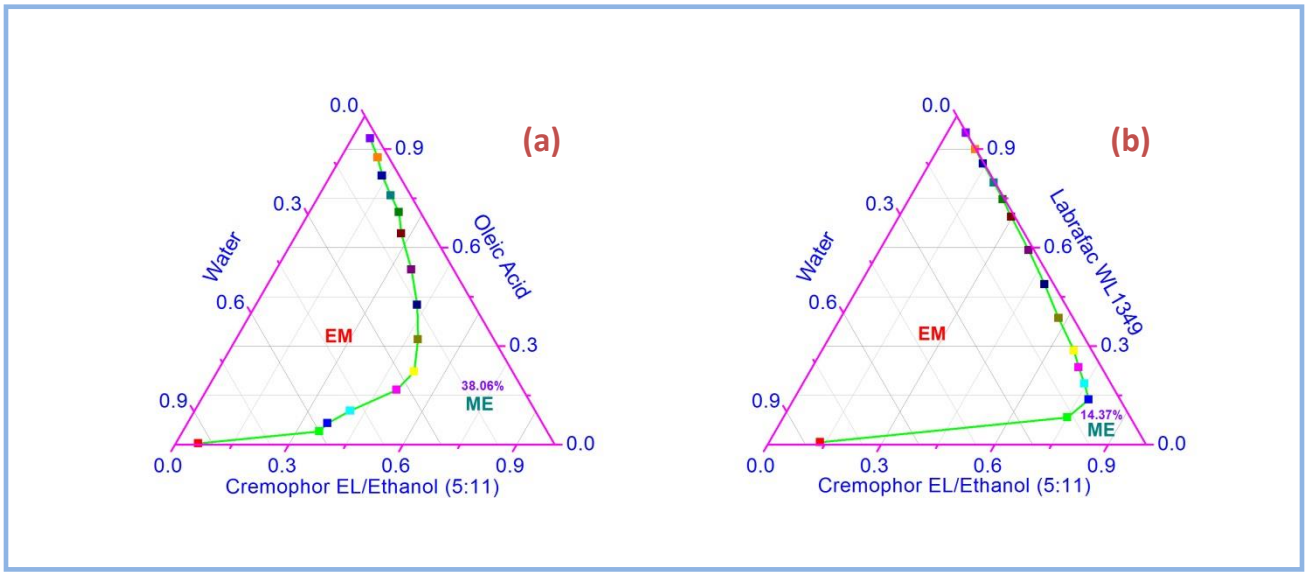

Figure 4.3 The pseudo-ternary phase diagram of cremophor EL, ethanol, water system with two different oils: (a) oleic acid and (b) labrafac WL1349.

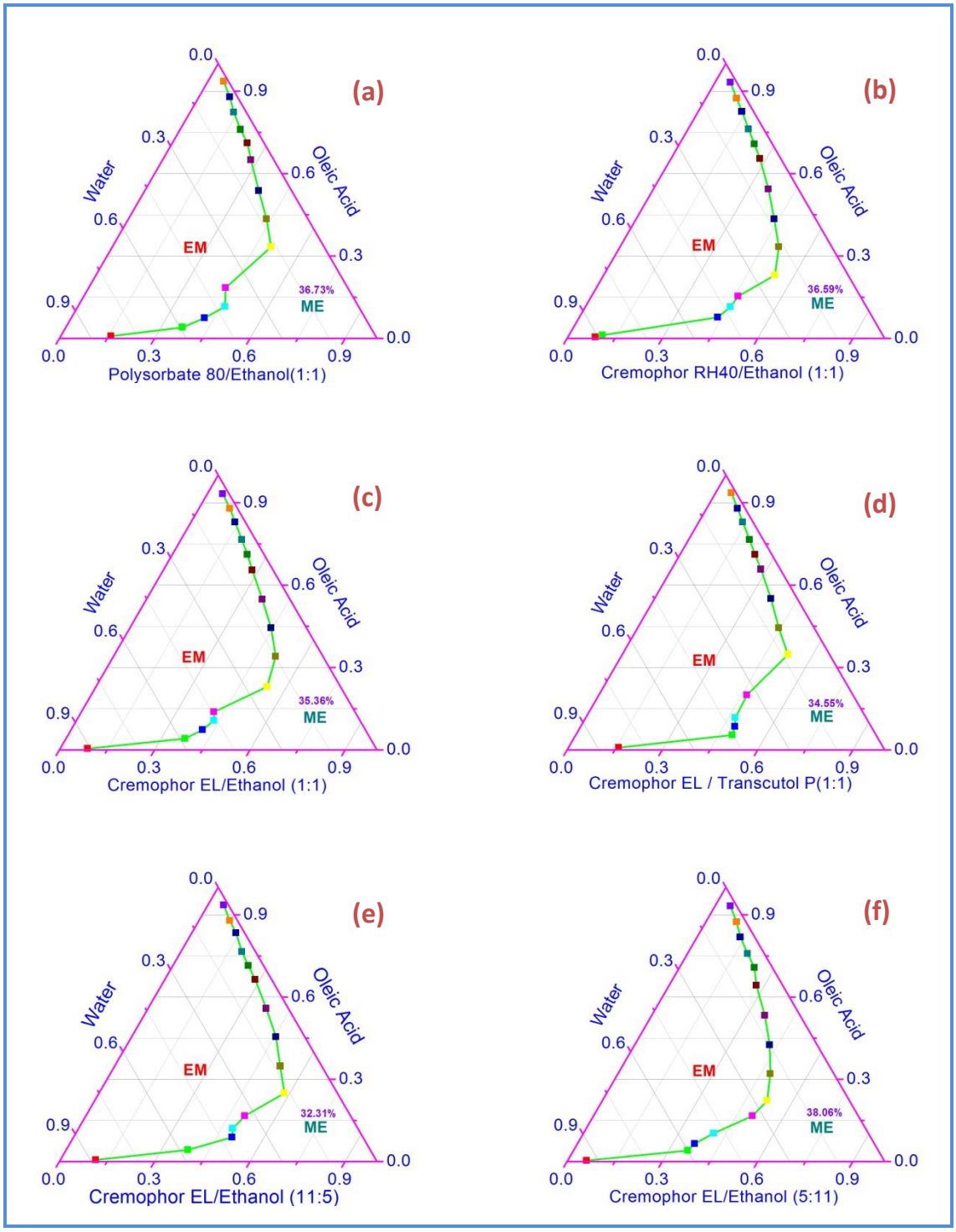

Figure 4.4 The pseudo-ternary phase diagram of oleic acid , ethanol, water system with three different surfactants: (a) polysorbate 80 (b) cremopor RH40 (c) cremophor EL with two different co-surfactants: (c) ethanol (d) transcutol P and with different Km values : (c) 1:1 and (e) 11:5 (f) 5:11.

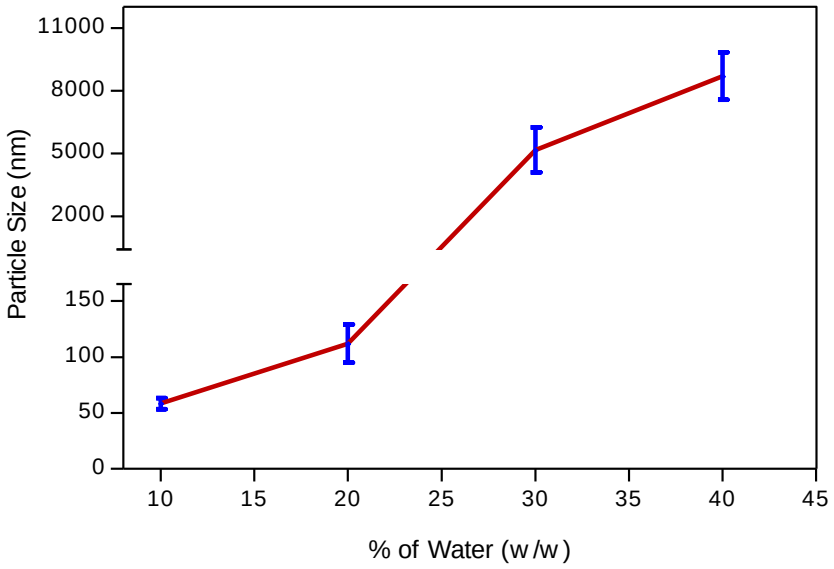

Figure 4.5 Effect of water content on the particle size of the microemulsion

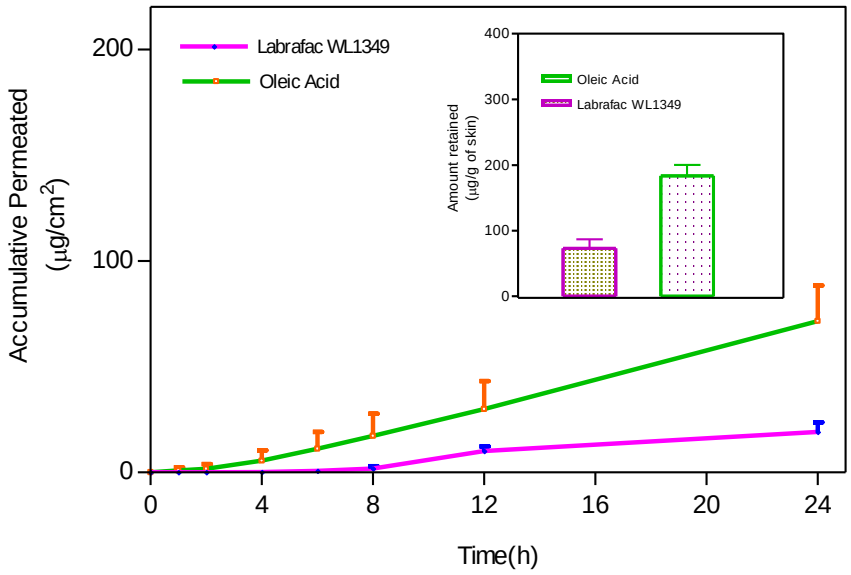

Figure 4.6 Effect of two different oils on the permeation of genistein (20mg/ml, 0.5ml) across dermatomed human skin and amount retained in the skin at 37^{o}C.

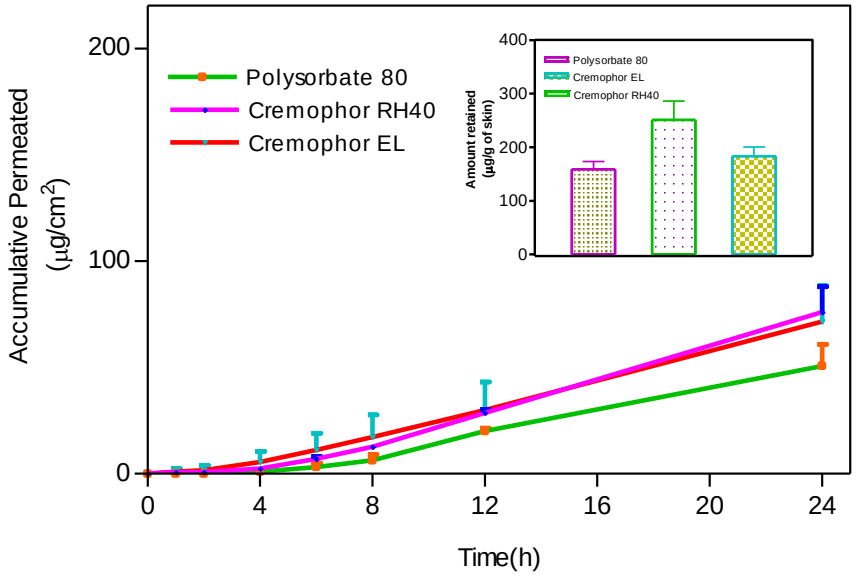

Figure 4.7 Effect of surfactants on the permeation of genistein (20mg/ml, 0.5ml) across dermatomed human skin and amount retained in the skin at 37^{o}C.

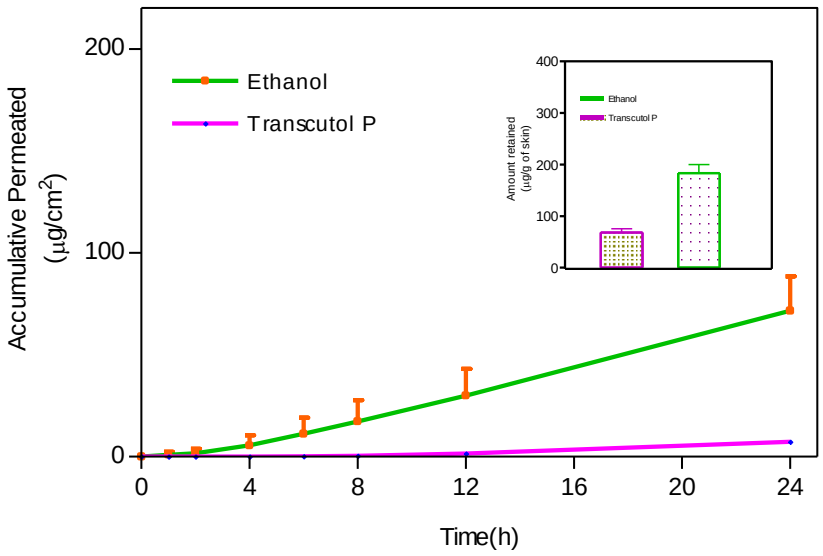

Figure 4.8 Effect of co-surfactants on the permeation of genistein (20mg/ml, 0.5ml) across dermatomed human skin and amount retained in the skin at 37^{o}C.

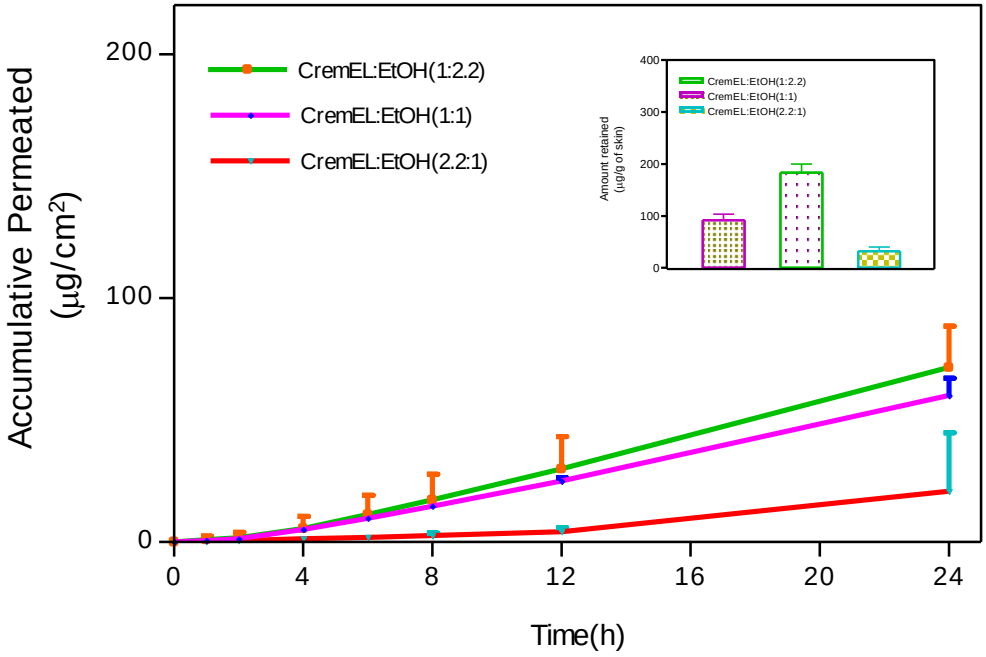

Figure 4.9 Effect of ratio of surfactant to co-surfactant (Km) on the permeation of genistein (20mg/ml, 0.5ml) across dermatomed human skin and amount retained in the skin at 37^{o}C.

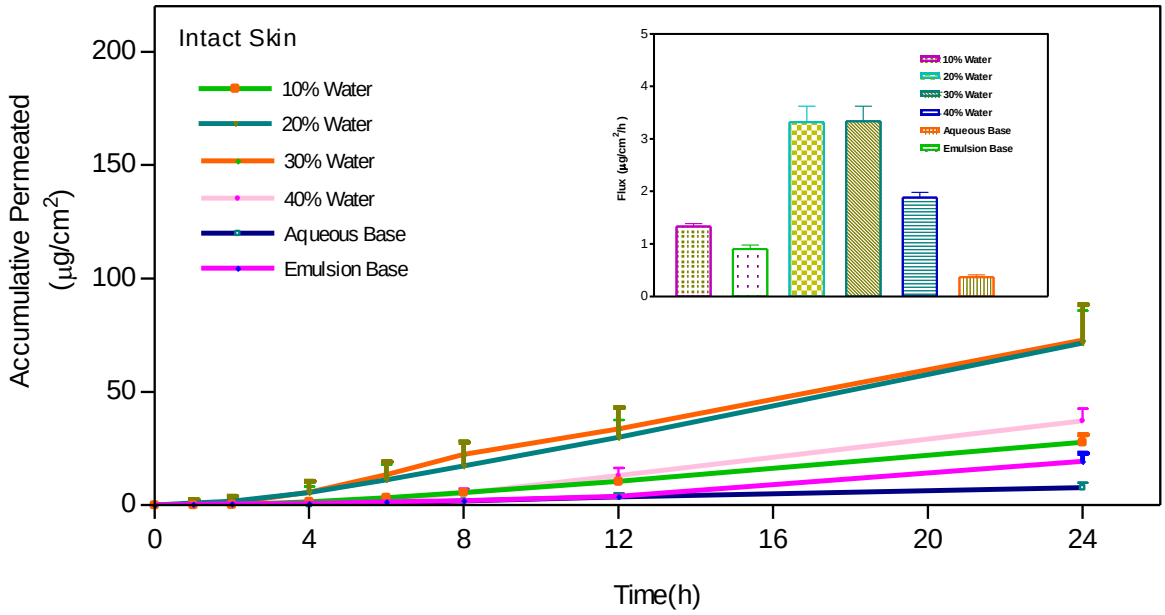

Figure 4.10 Effect of water content on the permeation of genistein (20mg/ml, 0.5ml) across intact dermatomed human skin at 37^{o}C.

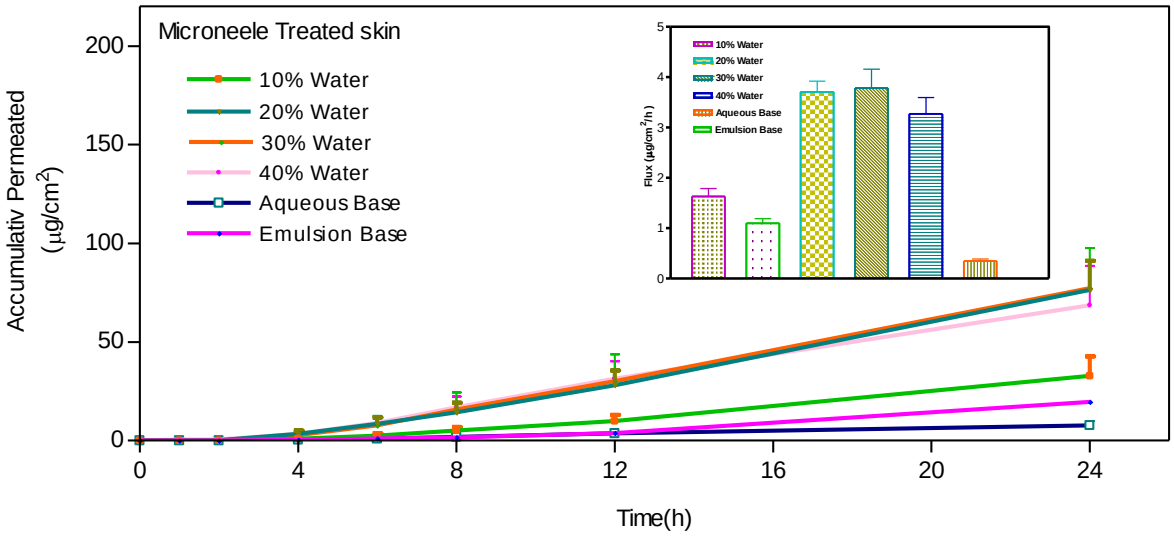

Figure 4.11 Effect of water content on the permeation of genistein (20mg/ml, 0.5ml) across microneedle treated dermatomed human skin at 37^{o}C.

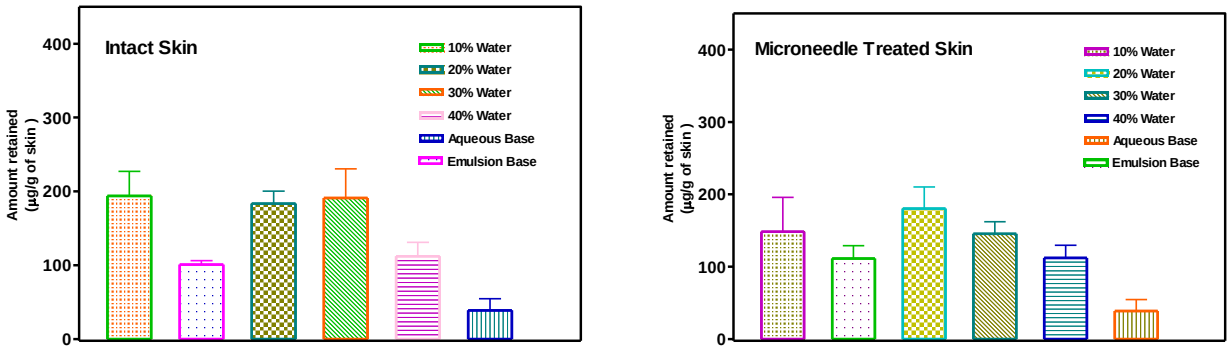

Figure 4.12 Effect of water content on genistein (20mg/ml, 0.5ml) retained in both intact skin and microneedle treated skin at 37^{o}C.

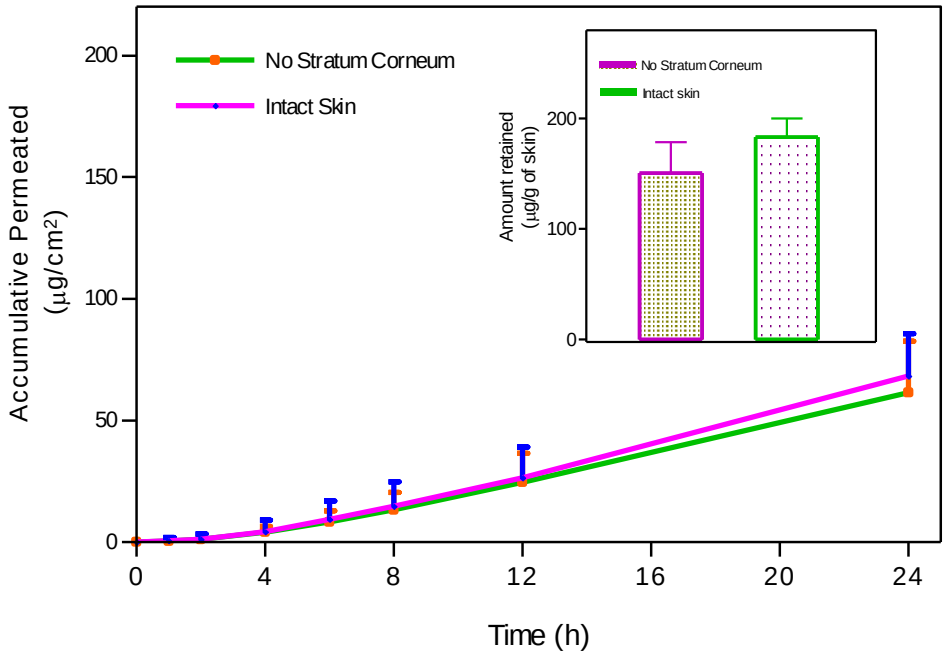

Figure 4.13 Effect of stratum corneum on the permeation of genistein (20mg/ml, 0.5ml) across dermatomed human skin and amount retained in the skin at 37^{o}C.

5. Codelivery of Doxorubicin and Ceramide as a Nanoparticle Based System for Melanoma Treatment

5.1 Abstract

Co-delivery of Doxorubicin (DOX) and ceramide using a liposomal system in B16BL6 melanoma cell lines for synergistic cytotoxic effects was investigated. Different ceramides (C_6-ceramide, C_8-ceramide and C_8-glucosylceramide) and lipids (DOTAP, DPPC, DSPE and DSPC) were utilized in the preparation of liposomes. DOX was encapsulated within liposome and ceramide acted as the component of the lipid bilayer. Liposomes were prepared by film formation and extrusion with subsequent loading of DOX. A solution of a cationic lipid, cholesterol, and ceramide, was evaporated under nitrogen to form a dry lipid film. The film was hydrated in ammonium sulfate solution to form a coarse liposome. The hydrated lipid solution was extruded 10 times through a 100 nm polycarbonate filter and then the liposomes were eluted with 100 mM citric buffer to remove extra ammonium sulfate. Finally, the liposomes were incubated with DOX solution for encapsulation process. The formulations were optimized for liposome size and size distribution, zeta potential and DOX recovery.

Cytotoxic effect on B16BL6 melanoma cell lines was measured by MTT assay. Various formulation factors influenced particle size, surface charge, and drug loading efficiency of liposomes. The optimized liposome formulation provided a mean diameter of 150 nm, a narrow size distribution (poly-dispersity index of 0.09), positive zeta potential (+34 mv), and 92% DOX encapsulation efficiency. The final optimized liposome has a 10:10:1:2:2 molar ratio of lipid/ cholesterol/PEG2000-DSPE/Ceramide/DOX. DOX and C8-Ceramide loaded DOTAP liposomes

exhibited a significantly higher anti-tumor activity in melanoma cell line B16BL6 compared with liposomes made with other lipids such as DSPC, and a combination of DSPC and DSPE) ($P < 0.05$). Co-delivery of DOX and C_8-ceramide with DOTAP lipids based liposome demonstrated a 9 fold higher cytotoxicity compared to DOX alone. Cationic liposomes were constructed for simultaneous delivery of DOX and C8-ceramide with excellent encapsulation efficiency. Co-delivery of DOX and C8-ceramide offered increased anti-proliferative effects in B16BL6 melanoma cell line than DOX alone. This study provides a basis for developing a co-delivery system of DOX and ceramide encapsulating liposomes for melanoma treatment.

5.2 Introduction

Metastatic malignant melanoma is by far one of the most common and aggressive types of cancer, with approximately 76,000 new cases diagnosed and over 9,000 estimated deaths in 2013 in the United States alone (1,2). An early-stage melanoma that has not spread or metastasized to other organs can be removed by surgery with high survival rates. However, metastatic melanoma is largely refractory to existing therapies and has a very poor prognosis, with a median survival of 6 months and a 5-year survival of less than 5% (3). Metastasized irremovable melanoma needs to be treated by other standard therapies such as chemotherapy (4, 5), radiotherapy (6), immunotherapy (7), targeted therapy and various combinations of these (8-10). Major advancements in the treatment of metastatic melanoma have recently been achieved with the approval of the Cytotoxic T-Lymphocyte Antigen 4 (CTLA-4) blocking monoclonal antibody ipilimumab and the $BRAF^{V600E}$ kinase inhibitor vemurafenib by the United States Food and Drug Administration (US FDA). Even in the era of CTLA-4 blockade and targeted therapies, chemotherapy remains an essential treatment option for metastatic disease. Many patients are ineligible for treatment with ipilimumab or do not harbor a $BRAF^{V600E}$ mutation. Additionally,

even if eligible for treatment, many patients treated with ipilimumab obtain no benefit and all patients treated with small molecule kinase inhibitors eventually relapse from therapy (11).

Doxorubicin has become one of the most often used drugs for the treatment of a wide range of cancers, such as blood cancers, like leukemia and lymphoma (12) , many types of solid tumors (breast and ovarian cancer) (13,14) and soft tissue sarcomas (15) . Nevertheless, the clinical use of this broad spectrum drug is also limited because of its poor stability and serious non-specific toxicity to normal tissues, which induces severe side effects such as acute dose limiting bone marrow toxicity and chronic cumulative cardiac toxicity (16-18). Also, most of these anthracycline drugs (e.g. doxorubicin) have slow diffusion through the plasma membrane which limits sufficient uptake within the tumor cells (19). Nanotechnology provides one approach to encapsulate therapeutic agents leading to improvements in circulation time, enhancement of tumor uptake, avoidance of reticulo-endothelial system and minimization of toxicity (20-21). Liposomes are generally considered nontoxic, biodegradable, and non-immunogenic. They have been used as drug carriers to improve harmacokinetics, resulting in reduced toxicities and enhanced therapeutic efficacies of drugs (23, 24). Recently liposomal products entrapping anthracyclines (Doxil®, Daunoxome®, Myocet®) were approved for the treatment of several types of cancers (25-27).

Ceramides, a class of sphingolipid metabolites, are known to have biological activity, serving as a lipid-derived second messenger that modulates the induction of cell differentiation, cell cycle arrest, and/or apoptosis (28-30). Ceramide has been identified as a putative therapeutic agent in cancer due to potent regulation of cell growth, differentiation, and death (31, 32). Ceramide targets the PI3K/Akt pathway through dephosphorylation of Akt, leading to increased cytotoxicity and cell apoptosis. When used in combination with other chemotherapeutics it can

enhance cell death (33). These lipids serve both a structural role in membranes and an intracellular signaling role within a cell. An obstacle that has limited clinical use of ceramide is its hydrophobicity, which can be overcome by packaging it into a nano-liposomal formulation for systemic delivery (34-36). Fortunately, nano-liposomal short-chain sphingolipid, such as C_6-Ceramide and C_8-Ceramide, and anticancer drugs (sorafenib, doxorubicin) synergistically inhibits tumor growth such as melanoma and breast cancer (37, 38). Doxorubicin can be entrapped in the aqueous compartment of liposome, while the lipid bilayer can be utilized to incorporate ceramides.

In this study, liposome formulations co-delivering doxorubicin and ceramide were optimized. Characterization of this delivery system and in vitro release profiles under certain pH values were studied. Finally, cytotoxicity of formulations was conducted in melanoma cell line B16BL6. Co-delivery of doxorubicin and ceramide has been found to facilitate the trans-membrane diffusion of doxorubicin, leading to increased cytotoxicity of melanoma cells.

5.3 Materials and methods

5.3.1 Materials

1,2-dioleoyl-3-trimethylammonium-propane (DOTAP), 1,2-dipalmitoyl-sn-glycero-3-phosphocholine (DPPC), 1,2-distearoyl-sn-glycero-3-phosphocholine (DSPC), 1,2-distearoyl-sn-glycero-3-phosphoethanolamine (DSPE), 1,2-distearoyl-sn-glycero-3-phosphoethanolamine-N-[methoxy(polyethylene glycol)-2000] (ammonium salt) (DSPE-mPEG (2000)), C6-Ceramide (C6-Cer), C8-Ceramide (C6-Cer) and C8-Glucosylceramide (C8-GlcCer) were purchased from Avanti Polar Lipids Inc (Alabaster, AL). Cholesterol was purchased from JT Baker (Phillipsburg, NJ) and other reagents were purchased from VWR International (West Chester, PA). Fetal bovine serum, Dulbecco's Modified Eagle's Medium, and other reagents for cell culture were

purchased from Mediatech (Manassa, VA). Doxorubicin hydrochloride (DOX) was purchased from AvaChem Scientific (San Antonio, TX) , HEPES Buffer and Citric Acid buffer were purchased from Amresco LLC (Solon, OH), Sephadex G75 and PBS were purchased from Sigma-Aldrich (St. Louis, MO). A mouse melanoma cell line (B16BL6) was obtained from the National Cancer Institute (Frederick, MD).

5.3.2 Methods

5.3.2.1 Formulation of DOX and ceramide encapsulated liposomes

Liposomes were prepared by lipid film hydration and extrusion and subsequent remote loading using ammonium sulfate according to Gilad and coworkers (38, 39). A schematic of preparation of empty liposomes is shown in Figure 5.1. Briefly, one of the lipids, DOTAP, DPPC, DSPC or DSPE, was dissolved at 10 mg/ml in chloroform. Similarly, 10 mg/ml solution of cholesterol; 10 mg/ml solution of one of the ceramides (C_6-ceramide, C_8-ceramide and C_8-glucosylceramide), 10 mg/ml solution of DSPE-mPEG (2000) were prepared in chloroform. These solutions were mixed well at a certain molar ratio in a test tube. This solution was then evaporated in the same test tube under a stream of nitrogen so that a thin film of the lipid contents was deposited on the walls of the test tube. The lipid film was further dried under a stream of nitrogen for 1h, followed by vacuum desiccation for 2 h. The dry lipid film was then hydrated in 250 mM ammonium sulfate solution by sonication for 10 min. This mixture was then placed in a water-bath incubator (65^{o}C) for 1 h to form coarse liposomes. The liposome mixture was then extruded through 100 nm (10 passes) polycarbonate filter using Avanti Mini Extruder (Avanti Polar Lipids, Alabaster AL). The free ammonium sulfate outside the liposomes was removed by gel permeation chromatography (GPC) using a G75 Sephadex column, eluted with 100 mM citrate buffer (pH 5.7).

5.3.2.2 Drug loading Efficiency and formulation Optimization

Liposomes with varying lipids such as DOTAP, DPPC, DSPC, and DSPE at a certain fixed concentration were prepared by varying cholesterol concentration (20 or 40 mol %) and DSPE-mPEG (2000) concentration (2, 4 or 10 mol %). Doxorubicin solution (0.3 or 0.6 mg/ml, 8 or 16% molar concentration) in 20 mM HEPES buffer, pH 7.0 was added to liposomes and incubated for 1h at 65^{o}C (40). Based on initial results of drug loading efficiency, DOX at 8% molar ratio was optimum and this concentration was used for all formulations. The effect of pH gradient (citrate buffer versus ammonium sulfate buffer) on the drug loading was studied. Ammonium sulfate provided higher drug loading efficiencies. As DOTAP liposome showed higher cell cytotoxicity compared with liposomes made of other lipids, DOTAP (cationic lipid) based liposomal formulations were selected to further incorporate different ceramides, such as C_6-Ceramide, C_8-Ceramide and C_8-Glucosylceramide. These ceramides were incorporated at 8% (molar).

5.3.3 Characterization

5.3.3.1 Encapsulation efficiency measurement

The amount of DOX encapsulated in the liposomes was determined using column separation method according to Wang and coworkers (41). Sephadex G75 was utilized to separate the free and encapsulated DOX. 0.5 ml of the liposome sample was added to the column, eluted with 20 mM HEPES buffer (pH 7.0) and 1.5 ml fractions were collected. The samples were then solubilized in 1% (w/v) Triton X-100 to break the liposome bilayer and release the encapsulated DOX. The concentration of liposomal DOX in each fraction was measured fluorometrically at 480 nm (excitation) and 590 nm (emission) using a microplate reader

(Fluostar, BMG labtechnologies, Germany). The DOX concentration in each fraction was plotted versus elution volumes. The first peak (fractions 2-6) reflects the liposomal drug, and the second peak (fractions 7-16) reflects the free drug. The DOX content in each peak was combined to quantify the encapsulated and free drug fractions in the liposome formulation. The recovery was calculated as:

$$\text{Recovery (\%)} = \text{amount of liposomal drug/ total amount of drug} \times 100$$

5.3.3.2 Particle size and zeta potential determination of liposomal formulations

Particle size and zeta potential of different formulations were determined based on dynamic light scattering (DLS) and electrophoretic light scattering (ELS), respectively, using a Nicomp Model 380/ZLS particle sizer (PSS, Santa Barbara, CA).

5.3.4 *In vitro* release

The release profile of DOX from liposome formulations was determined by dialysis. Phosphate buffered saline (PBS) pH 7.4, 250 ml, in a conical flask was used as a receptor phase. Dialysis tubing (12,000 to 14,000 Daltons molecular weight cut off), 30 mm ×25 mm release area, pre-soaked in buffer solution for 30 minutes, was used. 1 ml of the formulation or DOX solution (0.15 mg/ml of DOX) was placed in the dialysis tubing (42). All flasks were incubated at 37°C in a rotary shaker set at 150 rpm. Samples (1 ml) were collected at different time intervals and the sample volumes were replenished with fresh buffer immediately. The concentration of DOX in the receptor buffer (dialysate) was analyzed fluorometrically at 480 nm (excitation) and 590 nm (emission). The cumulative amount of DOX released versus time was plotted.

5.3.5 Cell cytoxicity assay

In vitro cytotoxicity was determined by MTT (3-[4, 5-dimethylthiazol-2-yl]-2, 5-diphenyl tetrazolium bromide) assay (43). The B16BL6 cells were grown in Dulbecco's Modified Eagle's Medium (DMEM) supplemented with 10% fetal bovine serum (FBS), 100 U/ml penicillin, and 100 μg/ml streptomycin at 37°C in a humidified atmosphere containing 5% CO_2. The B16BL6 cells were seeded in 96-well plates containing 100 μl of medium in each well. The cell density in the wells was 8×10^3 cells/well. Serial DOX formulations diluted in DMEM medium were added to each well 16 h after seedling. The cells received treatments of various formulations for 48 h prior to MTT assay. Then, MTT reagent was added to the culture medium at a final concentration of 0.5 mg/ml and the cells were incubated at 37°C for an additional 4 hours. Finally, the medium was discarded and 100 μl dimethylsulfoxid (DMSO) was added to each well to solubilize the dyes remaining in the plates. The absorbance was measured using a microplate reader (Fluostar, BMG labtechnologies, Germany) at 540 nm. Cell cytoxicity was expressed as a percentage of the untreated control cells (100%).

5.3.6 Statistical analysis

The release data was subjected to diffusion kinetics analysis. The multiple comparisons of cytotoxicity data were subjected to one-way analysis of variance (ANOVA) to determine the statistical levels of significance. $P < 0.05$ was considered to be statistically significant.

5.4 Results and discussion

5.4.1 Formulation optimization

Amphipathic anthracyclines usually have a low and variable oil/water partition coefficient. This makes it difficult for them to be encapsulated into the aqueous phase of

liposome. A transmembrane ammonium sulfate gradient (also called active loading) in and out of liposomes produced efficient and stable entrapment of amphipathic weak bases (39). Formulations were optimized through different parameters summarized in Table 5.1 A&B. As shown in Figure 5.2a, liposomes with ammonium sulfate buffer inside and citrate buffer outside demonstrated significantly higher encapsulation efficiency than the one with ammonium sulfate buffer both in- and out- of the liposome structure. Mostly drug was not entrapped in liposome without a pH gradient as indicated by a noticeable peak (second) in Figure 5.2a. This confirms that a differential pH gradient is critical for doxorubicin loading into the aqueous phase of liposome. The DOX active loading mechanism is dependent on the base exchange with ammonium ions.

To obtain liposomes with desirable encapsulation efficiency, two doxorubicin concentrations (0.3 mg/ml, 0.6 mg/ml in 20mM HEPES, pH 7.0) were studied. Encapsulation efficiency was a function of DOX concentrations (Figure 5.2b). Encapsulation efficiency decreased with increased DOX concentration. The encapsulation efficiency was above 90% for 0.3mg/ml DOX, but was below 60% at 0.6 mg/ml with a noticeable presence of free drug (second peak). This indicated that the encapsulation process is already saturated at 0.3 mg/ml DOX as indicated by more than 90% drug loading efficiency. Adding more DOX only led to more free DOX, resulting in significantly decreased encapsulation efficiency. The addition of cholesterol can provide rigidity to the lipid bilayer, which could improve the *in vitro* and *in vivo* stability of liposomes. Therefore, liposomes with different concentrations of cholesterol (20% and 40%) were formulated. The data (Figure 5.2c) showed that liposomes with 40% cholesterol had better encapsulation efficiency than those with 20% cholesterol (91.9%, 79.2% respectively). Also, it was difficult to prepare stable liposomes without cholesterol using 100 nm film

extrusion filter device. In addition, the encapsulated DOX leaked out over time (data not shown). Therefore, cholesterol helped retain the encapsulated drug within the liposomes. Cholesterol plays an important role in obtaining high drug loading efficiency due to increased rigidity of the liposome bilayer.

Liposomes were prepared with various charged lipids and were evaluated for particle size and encapsulation efficiency. As shown in Table 5.2 and Figure 5.2d, there is no significant difference in particle size or encapsulation efficiency with different lipids, except DSPC exhibited slightly lower encapsulation efficiency (81.0%). Usually formulations had a particle size of around 150 nm and encapsulation efficiency was approximately 90%. Addition of DSPE to DSPC at a molar ratio of 1 to 4 increased DOX loading from 81.0% to 91.6%. The particle size of all formulations was in the range of 120-190 nm with a narrow particle size distribution (polydispersity index is < 0.2). Different levels of PEG in the formulation produced no significantly different recovery (Figure 5.2e).

Three different short-chain ceramides (C_6-Cer, C_8-Cer, C_8-GlcCer) with varied carbon lengths and glucosyl modification were employed in the fabrication of DOTAP liposomes. As shown in Table 5.2, the particle size was similar in liposomes with or without ceramides, ranging from 145 to 185 nm. Thus, the addition of ceramide had no effect on particle size. Also, all of these formulations had high encapsulation efficiency, indicating that ceramide could be successfully incorporated into liposomes without compromising drug loading.

5.4.2 Release profiles

Drug release studies play an important role in determining the therapeutic activity and toxicity of liposomal drug delivery systems in cancer treatment (44). After liposomes have localized to tumors, the drug must be released and become bioavailable in order to exert its

biological effects (45). The release profiles of DOX from different drug-loaded liposomes are shown in Figure 5.3. The DOX Solution (control) reached 100% release within 6 hours, which confirmd that the dialysis membrane did not restrict diffusion of the released DOX. Compared with free DOX, liposome formulations exhibited significantly slower release because of additional time needed for the release of drug from the liposome lipid bilayer. In addition, as shown in Figure 5.3a, the formulation with 20% cholesterol exhibited faster release than the one with 40% cholesterol. The amounts released after 24 hours were 68% and 52%, respectively. The introduction of cholesterol decreased the flexibility of the lipid bilayer, leading to slower release of DOX. This data is consistent with the encapsulation efficiency results. The release of DOX from the liposomes with different amounts of PEG and ceramides was also investigated (Figure 5.3 b&c). Interestingly, there is no significant difference in release profiles among the formulations with varied PEG concentrations and ceramide types, but all of these formulations released slower than free DOX. The release of DOX after 24h for different liposomes was around 50%. Therefore, incorporating PEG and ceramide exerted negligible effect on particle size, drug loading efficiency, and DOX release.

5.4.3 Cell cytotoxicity

Doxorubicin is an anthraquinone anticancer drug that is commonly used for treatment of human malignancies, including various tumors such as the breast (46), ovary (47) and melanoma (48, 49). Compared with systemic application of free doxorubicin, liposomal doxorubicin exhibits significant advantages, such as reduced toxicities and therapeutic efficacies (50). Improved drug loading for liposomes resulted in high doxorubicin encapsulation efficiency and increased the therapeutic index of doxorubicin (51). Liposomes with various lipids were formulated to evaluate the influence of lipid charge and composition on cytotoxicity toward

melanoma cell line B16BL6 at a fixed DOX concentration. Empty liposomes with different lipids had a negligible cytotoxic effect on B16BL6 cells (data not shown). As shown in Figure 5.4, DOX incorporated DOTAP liposomes exhibited significantly higher anti-tumor activity followed by DPPC, a combination of DSPC and DSPE, and DSPC ($P < 0.05$). The cell cytotoxicity due to DOTAP, DPPC, DSPC & DSPE, and DSPC treatments was 12.7%, 64.2%, 69.3% and 86.9% respectively. The positive charge on the surface of the DOTAP liposome may increase DOX uptake through the inseration of the liposome with the negatively charged cell membrane (52). However, without DOTAP, the liposomes were difficult to be taken up less by melanoma cells, leading to a compromised cytotoxic effect. In addition, the formulation with the combination of DSPE and DSPC had greater cytotoxicity than the one with DSPC alone. This is probably related to the increased DOX EE (91.57% versus 80.98%).

Pegylated liposome slows recognition by opsonins and reduces clearance by the RES, resulting in prolonged circulation times. PEG-liposome-encapsulated doxorubicin (Gaelyx and Doxil) is in clinical use for the treatment of various types of neoplasms (55, 56). Innovations such as covalent attachment of tumor-specific antibodies or ligands will further enhance drug targeting and therapeutic value (57, 58). Therefore, to investigate the effect of DSPE-mPEG (2000) concentration on cell cytotoxicity, we formulated DOTAP liposomes with different amounts of DSPE-mPEG (2000) and compared their cytotoxicity in melanoma cell line B16BL6. As shown in Figure 5.5, there was no significant difference among the three groups. Only 10% DSPE-mPEG (2000) showed slightly decreased cytotoxicity in melanoma cell line, it can be explained by the shield effect because of hydrophilicity of PEG.

Ceramide is one of many sphingolipid metabolites known to have biological activity, serving as a lipid-derived second messenger that modulates the induction of cell differentiation,

cell cycle arrest, and apoptosis (59, 60). It has been reported that short-chain sphingolipids, C6-ceramide in the tumor cell membrane enhances cellular DOX uptake (61). To deliver DOX and Ceramide simultaneously, liposome carrying various ceramides (C6-Cer, C8-Cer and C8-GlcCer) in the lipid bilayer and DOX in the aqueous phase were developed and their cytotoxicities were tested in Melanoma B16BL6 cells. As shown in Figure 5.6, liposome with DOTAP/C8-Cer exhibited the highest cytotoxicity on B16BL6 cells, followed by DOTAP/C8-GlcCer, DOTAP/C6-Cer DOTAP and finally DOX solution. The cell viabilities due to C8-Cer, C8-GlcCer, C6-Cer, DOTAP and DOX were 2.29, 5.93, 12.1, 12.7 and 20.2, respectively. Thus, the antitumor activity of DOTAP/ C8-Cer is 5-fold higher than DOTAP liposomes and 9-fold higher than DOX solution (control). DOTAP/C8-GlcCer liposome also exhibited significantly enhanced cytotoxicity compared to DOTAP liposome and control. There is no statistically significant difference in the cytotoxicity of DOTAP/C6-Cer and DOTAP liposomes. However, these have a much higher cytotoxicity than free drug. Empty liposome has not significant cytotoxicity on cells at the equivalent concentration of drug-loaded liposome (data not shown). The results demonstrated that the liposome delivery system significantly enhanced the delivery of DOX to cells. More importantly, co-delivery of ceramide and DOX was more cytotoxic in melanoma cells than DOX alone. The enhanced cytotoxic effect of DOTAP liposomes could be explained by two possible reasons. One is the increased cytotoxicity and cell apoptosis of ceramides in combination with other anticancer drugs through the PI3K/Akt pathway, which is deregulated in most melanoma cells (62, 63). The other one is that ceramide could adjust the packing of the lipid bilayer and enhance the permeation and uptake of DOX through cells (61).

5.5 Conclusion

We developed a formulation for simultaneous delivery of doxorubicin and a ceramide. The liposomes were prepared at a 5:1 molar ratio of lipid to drug, with a narrow particle size distribution, high encapsulation efficiency and desirable DOX release kinetics. The final optimum liposome had 10:10:1:2:2 molar ratio for lipid/ cholesterol/DSPE-mPEG(2000)/ Ceramide/DOX. They exhibited a higher cytotoxic effect on melanoma cell line B16BL6 than free DOX or liposomes with no ceramide. Therefore, this formulation appears to be a promising delivery system in the treatment of melanoma.

5.6 References

1. Gniadecka M, Philipsen PA, Sigurdsson S, et al. Melanom diagnosis by Raman spectroscopy and neural networks: structure alterations in proteins and lipids in intact cancer tissue. J Invest Dermatol. 2004; 122(2):443-9.
2. Siegel R, Naishadham D, Jemal A. Cancer statistics, 2012. CA Cancer J Clin. 2012; 62(1):10-29.
3. Gray-Schopfer V, Wellbrock C, Marais R. Melanoma biology and new targeted therapy. Nature. 2007; 445:851–857.
4. Ahmed MD, Henry MD. What Is the Role of Chemotherapy in the Treatment of Melanoma? Current Treatment Options in Oncology; 2014, 15:321–335.
5. Matos AM, Francisco AP. Targets, structures, and recent approaches in malignant melanoma chemotherapy. Chem Med Chem. 2013; 8(11):1751-65.
6. Arienti C, Zoli W, Pignatta S, et al. Efficacy of different sequences of radio- and chemotherapy in experimental models of human melanoma. J Cell Physiol. 2014; 229(10):1548-56.

7. Hao MZ, Zhou WY, Du XL, et al. Novel anti-melanoma treatment: focus on immunotherapy. Chin J Cancer 2014; 33(9):458-65.

8. Qu X, Felder MA, Perez Horta Z, et al. Antitumor effects of anti-CD40/CpG immunotherapy combined with gemcitabine or 5-fluorouracil chemotherapy in the B16 melanoma model. Int Immunopharmacol. 2013; 17(4):1141.

9. Queirolo P, Marincola F, Spagnolo F. Electrochemotherapy for the management of melanoma skin metastasis: a review of the literature and possible combinations with immunotherapy. Arch Dermatol Res. 2014; 306(6):521-6.

10. Kudriavtsev DV, Kudriavtseva GT, Mardynskiĭ IuS. Adjuvant chemotherapy as a component of complex treatment for skin melanoma. Vopr Onkol. 2008; 54(2):170-7.

11. Luke JJ, Schwartz GK. Chemotherapy in the management of advanced cutaneous malignant melanoma. Clin Dermatol. 2013; 31(3):290-7.

12. Szwed M, Laroche-Clary A, Robert J, Jozwiak Z. Induction of apoptosis by doxorubicin-transferrin conjugate compared to free doxorubicin in the human leukemiacell lines. Chem Biol Interact. 2014; 220C:140-148.

13. Nomura H, Kawakami H, Usui H, et al. Information provided by pharmacists regarding the effective timing of the coadministration of first-generation serotonin receptor antagonists and dexamethasone for chemotherapy-induced nausea and vomiting in patients receiving Doxorubicin and cyclophosphamide chemotherapy for breast cancer - the second report. Gan To Kagaku Ryoho. 2014; 41(9):1129-33.

14. Rocconi RP, Straughn JM Jr, Leath CA III, et al. Pegylated lipo- somal doxorubicin consolidation therapy after platinum/ paclitaxel-based chemotherapy for suboptimally

debulked, advanced-stage epithelial ovarian cancer patients. Oncologist. 2006; 11: 336-341.

15. Petznek H, Kleiter M, Tichy A, et al. Murine xenograft model demonstrates significant radio-sensitising effect of liposomal doxorubicin in a combination therapy for Feline Injection Site Sarcoma. Res Vet Sci. 2014: S0034-5288(14)00209-4.

16. Young CW and Raymond V. Clinical assessment of the structure-activity relationship of anthracyclines and related synthetic derivatives. Cancer Treat Rep.1986; 70:51-63.

17. Wadler S and Yang P. Reversal of doxorubicin resistance by hydrophobic, but not hydrophilic, forskolins. Mol Pharmacol. 1991, 40: 960-964.

18. Hershman DL, McBride RB, Eisenberger A, et al. Doxorubicin, cardiac risk factors, and cardiac toxicity in elderly patients with diffuse B-cell non-Hodgkin's lymphoma. J Clin Oncol. 2008; 26(19):3159-65.

19. Speelmans G, Staffhorst RW, Kruijff B, Wolf FA. Transport studies of doxorubicin in model membranes indicate a difference in passive diffusion across and binding at the outer and inner leaflets of the plasma membrane. Biochemistry. 1994; 33(46):13761-8.

20. Zheng L, Gou M, Zhou S, et al. Antitumor activity of monomethoxy poly (ethylene glycol)-poly (ε-caprolactone) micelle-encapsulated doxorubicinagainst mouse melanoma. Oncol Rep. 2011; 25(6):1557-64.

21. Jones AK, Bejugam NK, Nettey H, et al. Spray-dried doxorubicin albumin microparticulate systems for treatment of multidrug resistant melanomas. J Drug Target. 2011; 19(6):427-33.

22. Smylie MG, Wong R, Mihalcioiu C, et al. A phase II, open label, monotherapy study of liposomal doxorubicin in patients with metastatic malignant melanoma. Invest New Drugs. 2007; 25(2):155-9.

23. Gabizon A. Pegylated liposomal doxorubicin: meta- morphosis of an old drug into a new form of chemo- therapy. Cancer Invest. 2001; 19: 424-36.

24. Maeda H, SawaT, KonnoT. Mechanism of tumor- targeted delivery of macromolecular drugs, including the EPR effect in solid tumor and clinical overview of the prototype polymeric drug SMANCS. J Control Release. 2001; 74: 47-61.

25. Safra T, Muggia F, Jeffers S, et al. Pegylated liposomal doxorubicin(Doxil): reduced clinical cardiotoxicity inpatients reaching or exceeding cumulative doses of 500mg/m2.Ann Oncol.2000; 11:1029-33.

26. Bendle M, Pealing J, Papanastasopoulos P, Bower M. Liposomal anthracycline chemotherapy and the risk of second malignancies in patients with Kaposi's sarcoma (KS). Cancer Chemother Pharmacol. 2014; 74(3):611-5.

27. Leonard RC, Williams S, Tulpule A, et al. Improving the therapeutic index of anthracycline chemotherapy: focus on liposomal doxorubicin (Myocet). Breast. 2009; 18(4):218-24.

28. Burenjargal M, Lee YS, Yoo JM, et al. Arch Pharm Res. Endogenous sphingolipid metabolites related to the growth in Sphingomonas chungbukensis. 2007; 30(3):317-22.

29. Hannun YA. Functions of ceramide in coordinating cellular responses to stress. Science (Wash DC). 1996; 274: 1855-1859.

30. Kolesnick RN, Kronke M. Regulation of ceramide production and apoptosis. Annu Rev Physiol.1998; 60: 643-665.

31. Radin NS. Killing cancer cells by poly-drug elevation of ceramide levels: a hypothesis whose time has come? Eur J Biochem. 2001; 268: 193-204.

32. Johns DG, Charpie JR, Webb RC. Is ceramide signaling a target for vascular therapeutic intervention? Curr Pharm Des. 1998; 4: 481-488.

33. Kolesnick RN, Kronke M. Regulation of ceramide production and apoptosis. Annu Rev Physiol. 1998; 60: 643 - 65.

34. Shabbits JA, Mayer LD. Intracellular delivery of ceramide lipids via liposomes enhances apoptosis in vitro. Biochim Biophys Acta. 2003; 1612:98 -106.

35. Shabbits JA, Mayer LD. High ceramide content liposomes with in vivo antitumor activity. Anticancer Res. 2003; 23: 3663 -9.

36. Stover T, Kester M. Liposomal delivery enhances short-chain ceramide-induced apoptosis of breast cancer cells. J Pharmacol Exp Ther. 2003; 307(2):468-75.

37. Tran MA, Smith CD, Kester M, Robertson GP. Combing nanoliposomal ceramide with sorafenib synergistically inhibits melanoma and breast cancer cell survival to decrease tumor development. Clin Cancer Res. 2008; 14(11): 3571-81.

38. Veldman RJ, Koning GA, van Hell A, et al. Coformulated N-octanoyl glucosylceramide improves cellular delivery and cytotoxicity of liposomal doxorubicin. J Pharmacol Exp Ther. 2005; 315(2):704-10.

39. Haran G, Cohen R, Bar LK, Barenholz Y. Transmembrane ammonium sulfate gradients in liposomes produce efficient and stable entrapment of amphipathic weak bases. Biochim Biophys Acta. 1993; 1151(2):201-15.

40. Johnston MJ, Edwards K, Karlsson G, Cullis PR. Influence of drug-to lipid ration on drug release properties and liposome integrity in liposomal doxorubicin formulations. J Liposome Res. 2008; 18(2):145-57.

41. Wang Y, Chen L, Ding Y, Yan W. Oxidized phospholipid based pH sensitive micelles for delivery of anthracyclines to resistant leukemia cells in vitro. Int J Pharm. 2012; 422(1-2):409-17.

42. Wang Y, Ding Y, et al. Bioactive lipids-based pH sensitive micelles for co-delivery of doxorubicin and ceramide to overcome multidrug resistance in leukemia. Pharm Res.2013; 30(11):2902-16.43.

43. Sudimack JJ, Guo W, Tjarks W, Lee RJ. A novel pH sensitive liposome formulation containing oleyl alcohol. Biochim Biophys Acta. 2002; 1564(1):31-7.

44. Allen TM, Mehra T, Hansen C, Chin YC. Stealth liposomes: an improved sustained release system for 1-beta-D-arabinofuranosylcytosine. Cancer Res. 1992; 52(9):2431-9.

45. Charrois GJ, Allen TM. Drug release rate influences the pharmacokinetics, biodistribution, therapeutic activity, and toxicity of pegylatedliposomal doxorubicin formulations in murine breast cancer. Biochim Biophys Acta. 2004; 1663(1-2):167-77.

46. Zheng RR, Hu W, Sui CG, et al. Effects of doxorubicin and gemcitabine on the induction of apoptosis in breast cancer cells. Oncol Rep. 2014 Sep 24.

47. Shavit L, Lifschitz MD, Gabizon A, et al. Pegylated liposomal doxorubicin and renal thrombotic micro-angiopathy: an under-recognized complication of prolonged treatment for ovarian cancer. Kidney Int. 2014; 85: 213.

48. Zhao JY, Ma XL, Li ZM, et al. Down-regulation of MFG-E8 by RNA interference combined with doxorubicin triggers melanoma destruction. Clin Exp Med. 2014 Mar 12.

49. Mittal A, Tabasum S, Singh RP. Berberine in combination with doxorubicin suppresses growth of murine melanoma B16F10 cells in culture and xenograft. Phytomedicine. 2014; 21(3):340-7.

50. Gabizon A, Shmeeda H, Grenader T. Pharmacological basis of pegylated liposomal doxorubicin: impact on cancer therapy. Eur J Pharm Sci.2012; 45: 388–398.

51. Ke X, Bei JH, Zhang Y, Li J. In vitro and in vivo evaluation of sanguinarine liposomes prepared by a remote loading method with three different ammonium salts. Pharmazie. 2011; 66(4):258-63.

52. Felgner PL, Gadek TR, Holm M, et al. Lipofection: a highly efficient, lipid-mediated DNA-transfection procedure. Proc Natl Acad Sci. 1987; 84(21):7413-7.

53. Cabanes A, Tzemach D, Goren D, et al. Comparative study of the antitumor activity of free doxorubicin and polyethylene glycol- coated liposomal doxorubicin in a mouse lymphoma model. Clin Cancer Res. 1998; 4: 499–505.

54. Maeda H, Bharate GY, Daruwalla J. Polymeric drugs for efficient tumor- targeted drug delivery based on EPR-effect. Eur J Pharm Biopharm. 2009: 71, 409–419.

55. Barenholz Y. Doxil–the first FDA-approved nano-drug: lessons learned. J Control Release. 2012; 160:117–134.

56. La-BeckNM, Zamboni BA, Gabizon A. Factors affecting the pharmacokinetics of pegylated liposomal doxorubicin in patients. Cancer Chemother Pharmacol. 2012; 69: 43–50

57. Molavi O, Xiong XB, Douglas D, et al. Anti-CD30 antibody conjugated liposomal doxorubicin with significantly improved therapeutic efficacy againstanaplastic large cell lymphoma. Biomaterials. 2013; 34(34):8718-25.

58. Lowery A, Onishko H, Hallahan DE, Han Z. Tumor-targeted delivery of liposome-encapsultated doxorubicin by use of a peptide that selectively binds toirradiated tumors. J Control Release. 2011; 150(1):117-24.

59. Yu T, Li J, Sun H. C6 ceramide potentiates curcumin-induced cell death and apoptosis in melanoma cell lines in vitro. Cancer Chemother Pharmacol. 2010; 66(5):999-1003.

60. Stover TC, Sharma A, Robertson GP, Kester M. Systemic delivery of liposomal short-chain ceramide limits solid tumor growth in murine models of breast adenocarcinoma. Clin Cancer Res. 2005; 11(9): 3465-74.

61. Lummel M, Blitterswijk WJ, Vink SR, et al. Enriching lipid nanovesicles with short chain glucosylceramide improves doxorubicin delivery and efficacy in solid tumors. FASEB J. 2011; 25(1):280-9.

62. Han WS, Yoo JY, Youn SW, et al. Effects of C2-ceramide on the Malme-3M melanoma cell line. J Dermatol Sci. 2002; 30(1):10-9.

63. Shabbits JA, Mayer LD. Intracellular delivery of ceramide lipids via liposomes enhances apoptosis in vitro. Biochim Biophys Acta. 2003; 1612(1):98-106.

Table 5.1A: Liposome formulation with various PEG, cholesterol concentrations and lipids							
Ingredient	**F1**	**F2**	**F3**	**F4**	**F5**	**F6**	**F7**
DOX	8	8	8	8	8	8	8
Cholesterol	40	40	40	20	40	40	40
DSPE-mPEG (2000)	2	4	10	4	4	4	4
DOTAP	50	48	42	68	-	-	-
DPPC	-	-	-	-	48	-	
DSPC	-	-	-	-	-	48	-
DSPC and DSPE (Mole 4:1)	-	-	-	-	-	-	48

Table 5.1B: Liposome formulations with various ceramides			
Ingredient	**F8**	**F9**	**F10**
DOX	8	8	8
Cholesterol	40	40	40
DSPE-mPEG (2000)	4	4	4
DOTAP	40	40	40
C_6-Ceramide	8	-	-
C_8-Ceramide	-	8	-
C_8-GlucosylCeramide	-	-	8

Table 5.2 Particle Diameter, PI, Zeta Potential, Recovery and Drug Loading of Different Liposomes					
Formulation	Particle Diameter (nm)	Polydispersity Index (PI)	Zeta Potential (mv)	Recovery (%)	Drug Loading (%)
DOTAP-2% PEG	171.1±9.0	0.123±0.07	41.7±5.2	90.4±1.8	12.7±0.22
DOTAP-4% PEG	174.8±15.1	0.101±0.08	39.2±2.5	91.9±2.1	12.8±0.31
DOTAP-10% PEG	120.4±12.7	0.113±0.12	32.9±5.9	91.2±2.4	12.8±0.27
DOTAP-20% Chol	169.3±21.6	0.111±0.10	35.8±2.5	79.2±2.9	11.2±0.45
DPPC	160.2±9.9	0.111±0.10	15.9±5.9	90.1±3.1	12.1±0.30
DSPC	171.6±15.4	0.069±0.05	11.5±3.7	81.0±2.1	10.4±0.19
DSPC & DSPE	160.0±11.4	0.092±0.09	12.7±2.1	91.6±1.2	11.6±0.11
DOTAP-C_6-Cer	148.2±10.2	0.131±0.02	40.8±2.9	92.9±1.1	12.9±0.21
DOTAP-C_8-Cer	169.3±17.5	0.114±0.04	41.2±3.9	90.2±1.7	12.5±0.15
DOTAP-C_8-GlcCer	181.4±9.9	0.062±0.01	35.6±2.5	92.8±1.4	12.9±0.14

Note: All data were presented as Mean ± SD (n=4); all formulations contain 4% PEG, 40% cholesterol unless labeled.

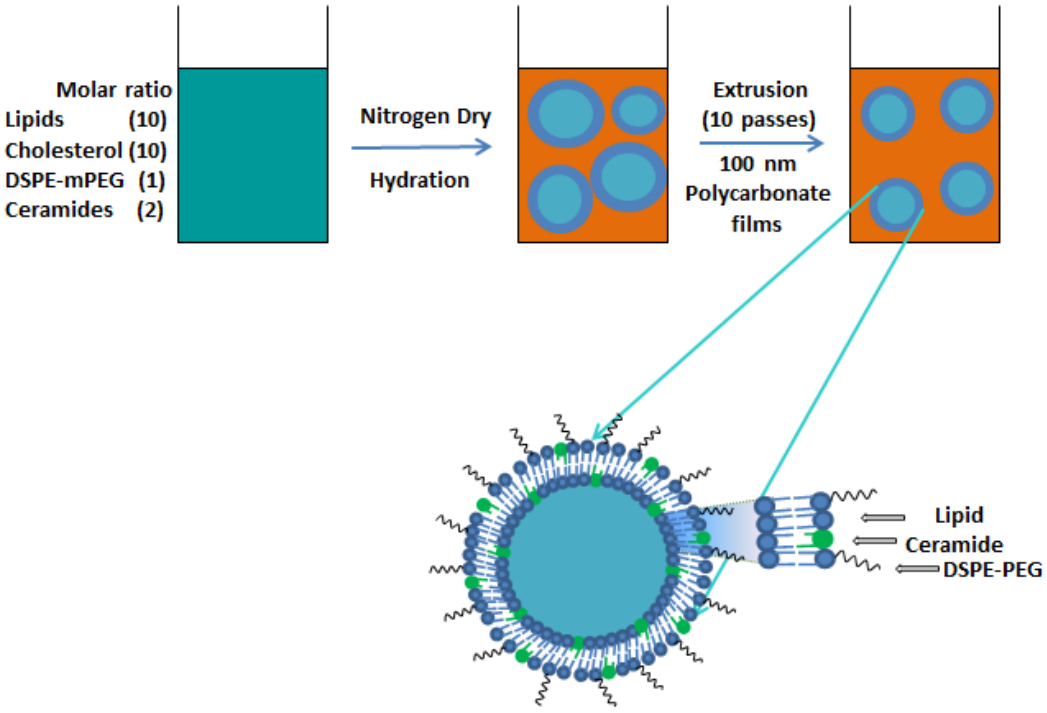

Figure 5.1 Schematic representation of empty liposome modified with DSPE-mPEG (2000) and ceramide.

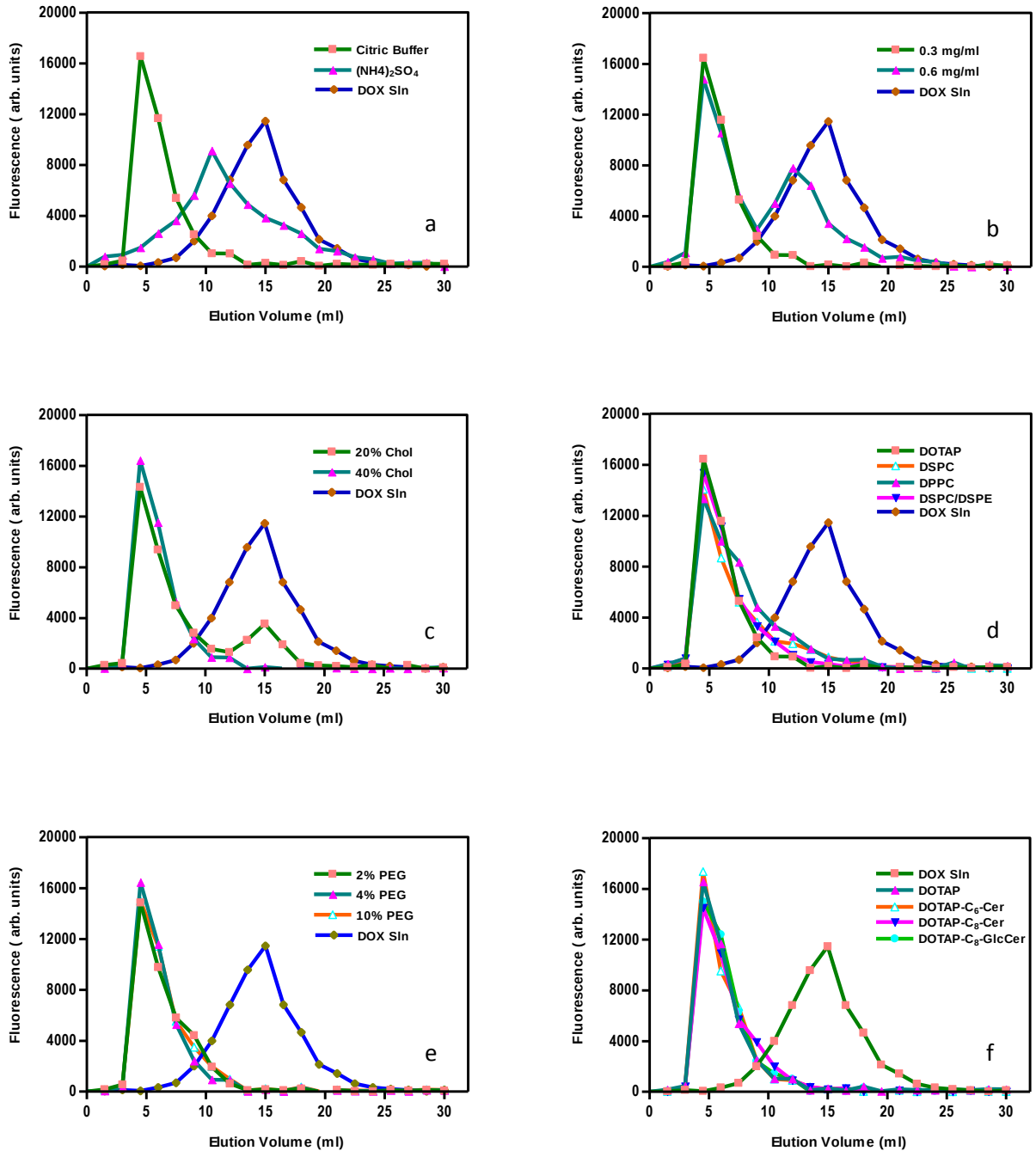

Figure 5.2 The elution profile of DOX encapsulated liposome with 20 nM HEPES buffer under different conditions: (a) different buffer systems; (b) different DOX concentrations; (c) different cholesterol concentrations; (d) different lipids; (e) varied PEG concentrations; (f) different ceramides.

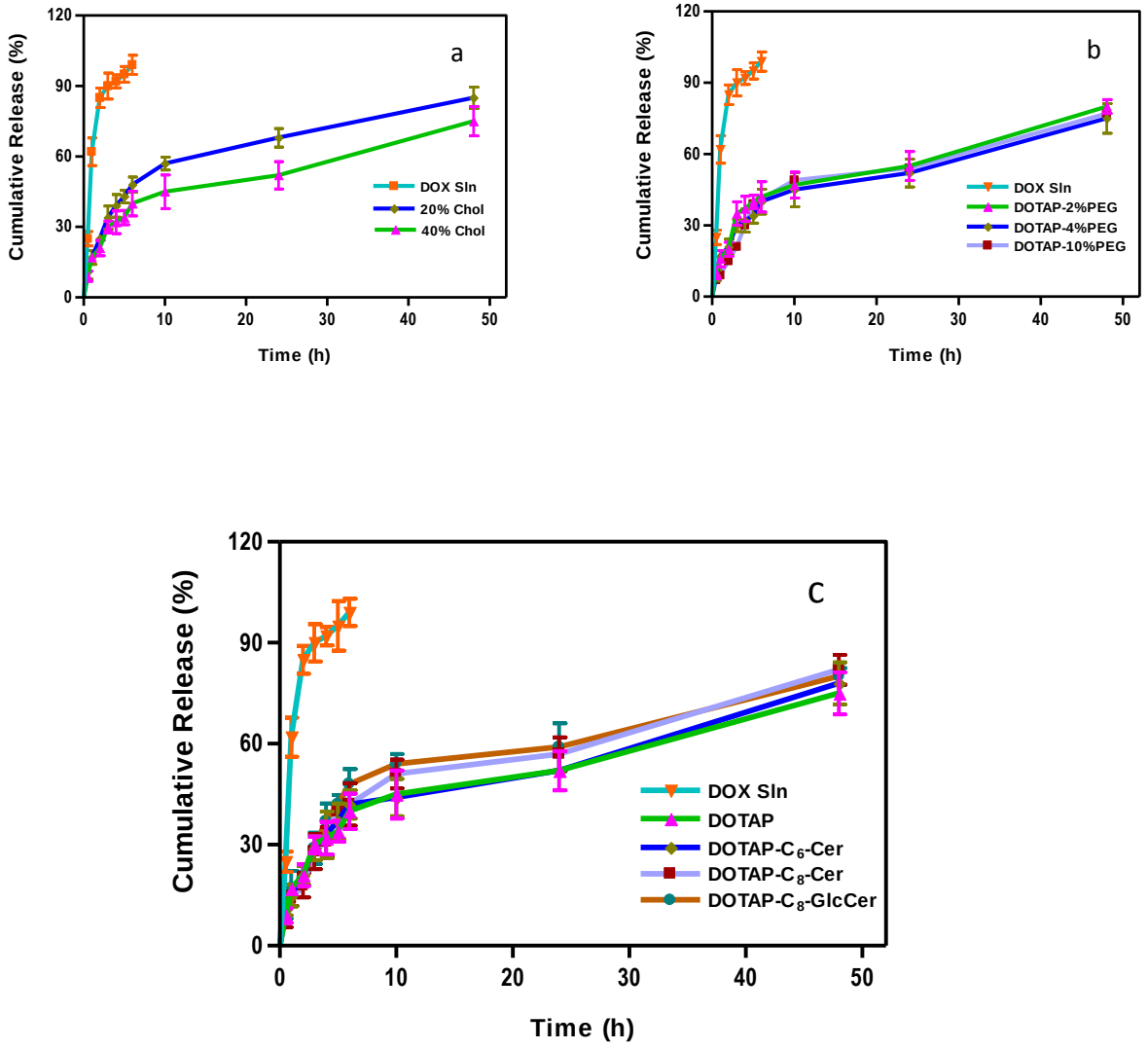

Figure 5.3 *In vitro* release profiles of DOX encapsulated liposome with different cholesterol concentrations (a), different DSPE-mPEG concentrations (b), and various ceramides (c). Formulations contained 4% (molar) PEG and 40% (molar) cholesterol unless otherwise labeled. All data were presented as Mean ± SD (n=4).

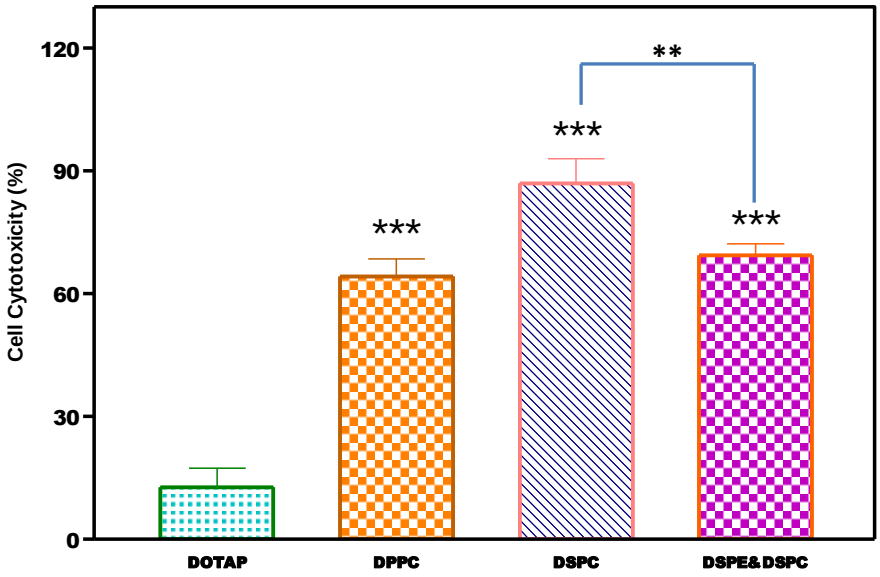

Figure 5.4 *In vitro* cytotoxicity of formulations containing various lipids in B16BL6 cell line, with 0.5 μg/ml DOX. ***p<0.001, compared to DOTAP liposome, ** p<0.01 between two groups.

Note: In combination of DSPE DSPC formulation, the molar ratio of DSPE to DSPC is 1:4. All data were presented as Mean ± SD (n=4).

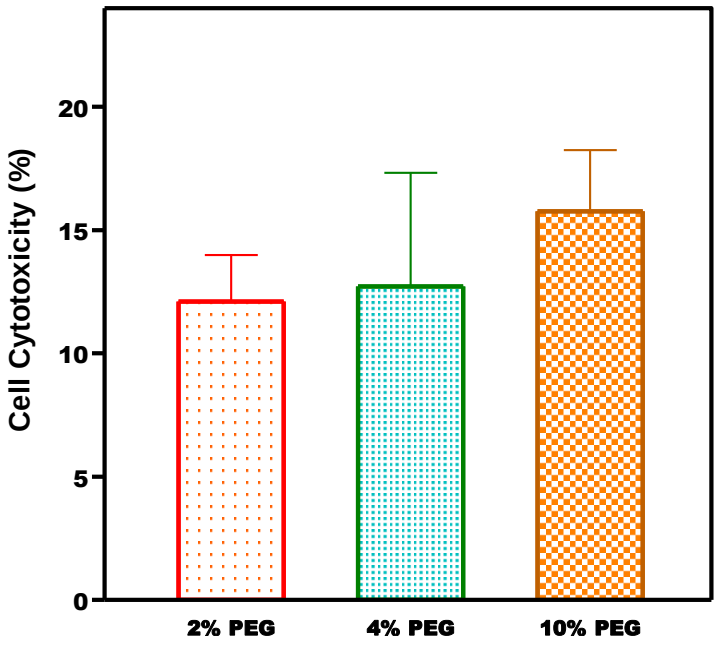

Figure 5.5 *In vitro* cytotoxicity of formulations containing different amounts of PEG in B16BL6 cell line with 0.5µg/ml DOX. All data were presented as Mean ± SD (n=4).

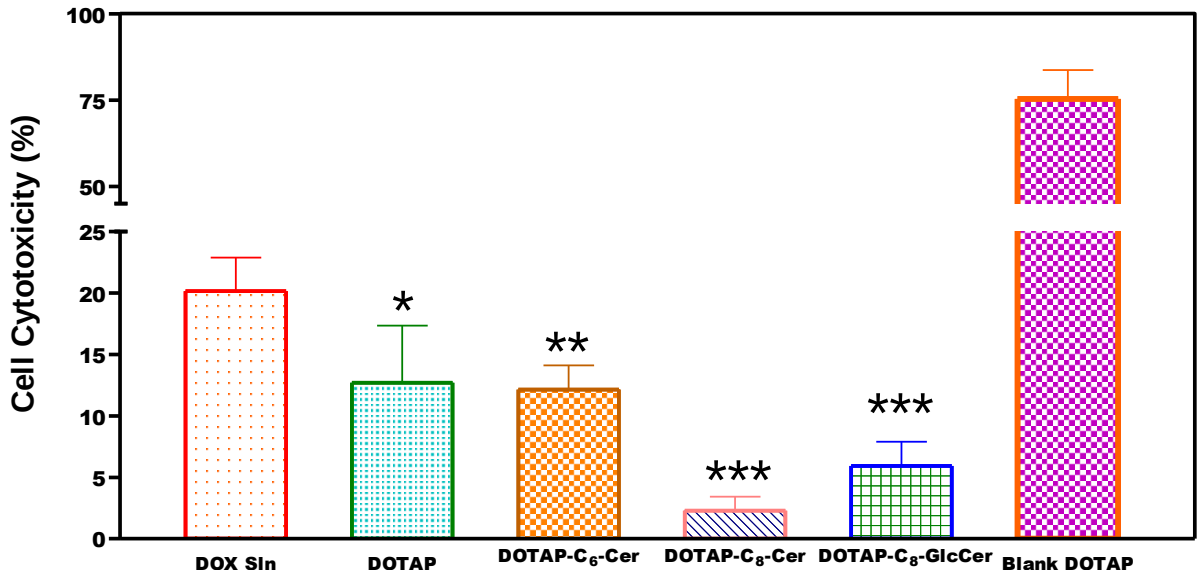

Figure 5.6 *In vitro* cytotoxicity of formulations containing different ceramides in B16BL6 melanoma cell line with 0.5μg/ml DOX. *p<0.05 as compared to free DOX, **p<0.01, compared to free DOX. ***p<0.001 as compared to free DOX. All data were presented as Mean ± SD (n=4).

6. Summary and Future Work

There are several methods for cancer treatment including radiotherapy, chemotherapy, immunotherapy, and different combinations of these. Chemo-immunotherapy, the combination of chemotherapy and immunotherapy, is popular with promising outcomes. Chemotherapy is still the conventional therapy for cancer treatment, but it is usually associated with several side effects and the development of multidrug resistance. Immunotherapy is receiving more attention since immune system plays an important role in killing cancer cells. The combination of these two methods is reported to be very effective, even synergistic inhibitory effects for cancer treatment.

Nanoparticles based delivery system provides a promising approach for chemo-immunotherapy, as cytotoxic drugs and immune stimulators could be loaded into the same delivery system simultaneously. More importantly, nanoparticles have various merits. They can encapsulate wide ranges of drugs, especially poorly water-soluble drugs which usually have low bioavailability. They could also significantly enhance cell uptake either through passive targeting or active ligand targeting and alleviating adverse side effects.

This dissertation developed different lipid based delivery systems, such as micelles, liposomes and microemulsions, for tumor treatment. We designed and developed a novel micellar formulation using a single oxidized phospholipid, PazPC, for delivery of anthracycline anticancer drugs, DOX and IDA. We investigated the conditions of ion-pair complex formation. Subsequent micelle preparations were optimized and *in vitro* drug release studies under different

pH values were investigated. Finally, we determined cell uptake and cytotoxicity of a micellar drug formulation in sensitive and drug resistance leukemia cell lines. The drug loaded micelles significantly enhanced drug uptake and exhibited higher cytotoxicity for both sensitive and resistant leukemia cells in comparison to free drugs. Therefore, an oxidized phospholipid-based micelle system could be a promising carrier that may improve the therapeutic outcomes of cancer treatment.

We prepared lipid-coated nanoparticles including a calcium phosphate core and lipid shell for simultaneous delivery of zoledronic acid and poly (I:C). The LCP were fully characterized for mean diameter size, zeta potential, efficiency in loading zoledronic acid, cytotoxic effect in a B16BL6 melanoma cell line *in vitro*, and antitumor effect in B16BL6 melanoma-bearing mice. It had a narrow particle size distribution and high loading efficiency for poly (I:C) and zoledronic acid, with good stability. In addition, codelivery of zoledronic acid and poly (I:C) offered superior antitumor activity in both *in vitro* and *in vivo* studies. Furthermore, codelivery of zoledronic acid and poly (I:C) by LCP had higher cytotoxicity than delivering poly (I:C) alone by LCP ($P < 0.05$), indicating a synergism between zoledronic acid and poly (I:C).

Microemulsions were fabricated for enhanced transdermal delivery of genistein, which is poorly water soluble. Various factors affecting the emulsion formation and skin permeation and deposition of genistein from the microemulsion, such as type of surfactant, oil, and water content, were optimized using pseudo-ternary phase diagrams. The water content in the formulation played an important role in the microemulsion stability, droplet size, transdermal flux. The oleic acid based microemulsions with 20% water exhibited 40 fold higher flux than the control (genistein aqueous suspension). The optimized formulation consisted of 2% genistein, 18% oleic acid, 60% cremophor EL/ethanol (5:11) and 20% water. It exhibited a small particle

size and the highest skin permeation rate. This formulation significantly increased skin permeation and deposition compared with microemulsion made with other components or both aqueous base and emulsion base controls.

Finally, a liposomal system co-delivering doxorubicin (DOX) and ceramide were developed and optimized for different types of ceramides (C_6-ceramide, C_8-ceramide and C_8-glucosylceramide) and lipids (DOTAP, DPPC, DSPE and DSPC). Liposomes were prepared by dry film hydration and extrusion with subsequent remote loading of DOX. Cytotoxic effect on B16BL6 melanoma cell lines was measured by MTT assay. The optimized liposome formulation provided a mean diameter of 150 nm, a narrow size distribution (poly-dispersity index of 0.09), positive zeta potential (+34mv) and 92% DOX encapsulation efficiency. The final optimized liposome has 10:10:1:2:2 molar ratio for lipid/ cholesterol/ PEG2000-DSPE/ Ceramide/ DOX. Co-delivery of DOX and C_8-ceramide with DOTAP lipids based liposome demonstrated a 9 fold higher cytotoxicity compared to DOX alone. Therefore, this formulation could be a promising delivery system for anthracycline anticancer drugs to improve the treatment of melanoma.

Future work is directed to explore the mechanism of enhanced cytotoxic effects for these delivery systems and the application of delivering two or more agents in cancer treatment.

1. Investigation of the mechanism of synergistic cytotoxic effects of PIC and ZOL in melanoma cells. Pegylation of LCP nanoparticle and targeting ligand for systematic delivery can be attempted and the changes of tumor micro-environment induced by nanoparticles will be investigated. This will give guidance on developing a more potent system.

2. For genistien microemulsions, in order to determine the correlation between skin deposition and anti-cancer activity of genistein, the efficacy of the formulations is to be tested in tumor-bearing mice and mice with photo-damaged skin. Skin deposition of genistein will be

determined. The levels of hydrogen peroxide and the lipid peroxidation product, malondialdehyde (MDA) in mice skin will also be studied.

3. For co-delivery of doxorubicin and ceramide by liposome, the efficacy of the formulation will be conducted in tumor-bearing mice. More importantly, cell signaling pathways for the synergistim between ceramide and doxorubicin will be explored to further understand the potentials of nanoparticle delivering two agents simultaneously.

Appendix: Journal Publications and Conference Presentations

Journal Publications

1. Wang Y, Ding Y, Liu Z, Liu X, **Chen L**, Yan W. Bioactive lipids-based pH sensitive micelles for co-delivery of doxorubicin and ceramide to overcome multidrug resistance in leukemia. Pharm Res. 2013; 30(11): 2902-16.
2. **Chen L**, Ding Y, Wang Y, Liu X, Babu RJ, Ravis WR, Yan W. Co-delivery of Zoledronic Acid and Double-strand RNA from Core-shell Nanoparticles. Int J Nanomedicine. 2013; 8:137-45.
3. Wang Y, **Chen L**, Ding Y, Yan W. Oxidized phospholipid based pH sensitive micelles for delivery of anthracyclines to resistant leukemia cells in vitro. Int J Pharm. 2012; 422(1-2):409-17.
4. **Chen L**, Ravis WR, Babu RJ. Topical Delivery of Genistein Nanoemulsion for UV Induced Skin Damage.(Manuscript in preparation for submission to Biomedical Nanotechnology)
5. **Chen L**, Ravis WR, Babu RJ. Co-delivery of Doxorubicin and Ceramide as a Nanoparticle Based System for the Treatment of Melanoma (In preparation for submission to Int. J. Nanomedicine)
6. **Chen L**, Ravis WR, Babu RJ. High performance liquid chromatography (HPLC) assay method for analysis of Genistein and Tetrahydrocumin in the nanoemulsion formulation (In preparation for submission to Biomedical Chromatography)

Book Chapters

1. Babu RJ, **Chen L**, Kanikkannan N. Fatty alcohols, fatty acids and fatty acid esters, In Percutaneous Penetration Enhancers, Volume 3. Dragicevic-Curic,N. and Maibach, H.I., Eds., Springer Science, Palo Alto, CA. (In Press)
2. Babu RJ, **Chen L**. Pyrrolidones, In Percutaneous Penetration Enhancers, Volume 3. Dragicevic-Curic, N and Maibach, H.I., Eds., Springer Science, Palo Alto, CA. (In Press)

Conference Presentation

1. **Chen L**, Ravis WR, Babu RJ, Formulation of Genistein Nanoemulsions for Enhanced Cytotoxicity in Melanoma Treatment. Annual National Meeting of American Association of Pharmaceutical scientists (AAPS). #M1133, 2014.
2. **Chen L**, Ravis WR, Babu RJ. Co-delivery of Doxorubicin and Ceramide as a Nanoparticle Based System for the Treatment of Melanoma. Annual National Meeting of American Association of Pharmaceutical scientists (AAPS). #M1134, 2014.
3. Porter H, **Chen L**, Kurapati S, Mulabagal V, Babu RJ. Stability and Degradation Profiles of Betamethasone Diporpionate in Topical Nanoparticle Formulation. Annual National Meeting of American Association of Pharmaceutical scientists (AAPS). #M1092, 2014.
4. **Chen L**, Babu RJ, Ravis WR. Formulation of Genistein Nanoemulsions for Enhanced Transdermal Delivery, In Vitro. Annual National Meeting of American Association of Pharmaceutical Scientists (AAPS). #T2245, 2013.
5. **Chen L**, Babu RJ, Ravis WR, Yan W. Co-delivery of Zoledronic Acid and Double-strand RNA from Core-shell Nanoparticles. Annual National Meeting of American Association of Pharmaceutical Scientists (AAPS). #T3195, 2012.

6. **Chen L**, Ravis WR, Babu RJ. Stability and Degradation Profiles of Genistein Topical Nano-emulsions. Annual National Meeting of American Association of Pharmaceutical Scientists (AAPS), #R6071, 2012.
7. **Chen L**, Babu RJ, Ravis WR, Yan W. Co-delivery of Zoledronic Acid and Double-strand RNA from Core-shell Nanoparticles. Annual Regional Meeting of Graduate Association of Students of pharmacy (GRASP), #F5, 2012.
8. **Chen L**, Babu RJ, Ravis WR, Yan W. Co-delivery of Zoledronic Acid and Double-strand RNA from Core-shell Nanoparticles. Auburn University Research Week, 2013.
9. **Chen L**, Babu RJ, Ravis WR. Yan W. Co-delivery of Zoledronic Acid and Double-strand RNA from Core-shell Nanoparticles. Annual Regional Meeting of Graduate Association of Students of pharmacy (GRASP), #F5, 2012.
10. **Chen L**, Ravis WR, Babu RJ. Formulation of Genistein Nanoemulsions for Enhanced Transdermal Delivery, In Vitro, Graduate Students Council, Auburn University, 2014.
11. **Chen L**, Ravis WR, Babu RJ. Formulation of Genistein Nanoemulsions for Enhanced Transdermal Delivery, In Vitro, Harrison School of Pharmacy, Auburn University, 2014.
12. Duran SH, Ravis WR, Passler T, Bayne J, Lin YJ, **Chen L**. Pharmacokinetics of Intravenous and oral Flunxin in Alpacas, Auburn University Research Week, 2013.
13. Wang Y, **Chen L**, Yan W. Bioactive lipids-based pH Sensitive Micelles for Delivery of Doxorubicin: in vitro and in vivo Studies in Leukemia. Annual National Meeting of American Association of Pharmaceutical Scientists (AAPS), 2011.